

**Development of a new database for thermodynamic modelling
of the system $\text{Na}_2\text{O-K}_2\text{O-Al}_2\text{O}_3\text{-SiO}_2$**

Von der Fakultät für Georessourcen und Materialtechnik
der Rheinisch -Westfälischen Technischen Hochschule Aachen

zur Erlangung des akademischen Grades eines
Doktors der Naturwissenschaften

genehmigte Dissertation

vorgelegt von **Magister in Chemie**

Elena Yazhenskikh

aus Scherkali, Russland

Berichter: Univ.-Prof. Jochen M. Schneider, Ph. D.
Prof. Dr.rer.nat. Klaus Hilpert

Tag der mündlichen Prüfung: 26. April 2005

Diese Dissertation ist auf den Internetseiten der Hochschulbibliothek online verfügbar

"It is a capital mistake to theorise before one has data.
Insensibly one begins to twist facts to suit theories, instead of theories to suit facts"
Sir Arthur Conan Doyle (1859-1930)

Zusammenfassung

Komplexe silikatische Oxid-Systeme sind in Wissenschaft und Industrie von großer Bedeutung. Bei der Stromerzeugung aus Kohle sind alkalihaltige Systeme von Interesse, da während der Verbrennung korrosive Alkaliverbindungen freigesetzt werden.

Thermodynamische Modellrechnungen erlauben die Beschreibung der Systeme und die Voraussage thermodynamischer Eigenschaften auch in Bereichen, in denen experimentelle Untersuchungen nicht oder nur sehr schwer möglich sind. Voraussetzung für Modellrechnungen sind geeignete Datenbanken und Modelle für Lösungsphasen.

Das Ziel der vorliegenden Arbeit war die Entwicklung einer neuen Datenbank für das quaternäre Oxid-System $\text{Na}_2\text{O}-\text{K}_2\text{O}-\text{SiO}_2-\text{Al}_2\text{O}_3$. Dieses System dient als Basis-System zur Beschreibung oxidischer Schmelzen und kann mit weiteren schlackerelevanten Oxiden wie z.B. Fe_2O_3 und den Erdalkalioxiden MgO und CaO erweitert werden.

Zur Beschreibung von Lösungsphasen wurde das Assoziat-Modell ausgewählt. Es wurden Startparameter für die Lösungsphase definiert und mittels einer Optimierungsroutine verbessert, um die Phasengleichgewichte im betrachteten System optimal zu beschreiben. Die anzupassenden Lösungsparameter sind die Bildungsenthalpie und -entropie von Lösungskomponenten und Wechselwirkungsparameter zwischen den Lösungskomponenten, die die Abweichung vom idealen Verhalten der Lösung beschreiben. Als Basis für die Optimierung wurden verfügbare experimentelle Daten, z.B. Phasendiagramme und Aktivitäten, verwendet.

Die neu erhaltene Datenbank ist mit der FACT Datenbank, aus der die Daten für die reinen festen, flüssigen und gasförmigen Phasen stammen, voll kompatibel. Dies ermöglicht die gleichzeitige Verwendung beider Datenbanken in einer Modellrechnung.

Die Gleichgewichtsrechnungen wurden für die binären Systeme $\text{Me}_2\text{O}-\text{SiO}_2$, $\text{Me}_2\text{O}-\text{Al}_2\text{O}_3$ (mit $\text{Me} = \text{Na}, \text{K}$) und $\text{SiO}_2-\text{Al}_2\text{O}_3$ und die ternären Systeme $\text{K}_2\text{O}-\text{Na}_2\text{O}-\text{SiO}_2$ und $\text{Na}_2\text{O}-\text{SiO}_2-\text{Al}_2\text{O}_3$ durchgeführt. Die gerechneten Phasendiagramme zeigen jeweils eine sehr gute Übereinstimmung mit den verfügbaren experimentellen Daten. Im Gegensatz zu den bisher verfügbaren Datenbanken, die vor allem in Bereichen hoher Alkalikonzentrationen Lücken aufweisen, erlaubt die neue Datenbank die Beschreibung der Systeme im gesamten Konzentrationsbereich. Die Untersuchungen zeigen, daß das Assoziat-Modell nicht nur für flüssige sondern auch für feste Lösungen zu geeigneten Lösungen führt. Dampfdrücke der Alkalien über der quaternären Schmelze und Aktivitäten der Alkalioxide in dieser Schmelze werden deutlich besser berechnet als mit den alten Datenbanken. Die Abweichungen zwischen den experimentellen und den mit der alten Datenbank berechneten Werten von

teilweise über zwei Größenordnungen konnten durch die neue Datenbank auf unter eine Größenordnung gesenkt werden.

Die Untersuchungen zeigen deutlich, daß die neue Datenbank mit dem verwendeten erweiterten Assoziat-Modell für die Beschreibung komplexer Oxid-Systeme geeignet ist. Durch Einbeziehung komplexer Wechselwirkungen kann die Datenbank für die Berechnung technisch relevanter Multikomponentensysteme erweitert werden.

Abstract

Complex oxide systems containing silica and alumina (so-called slag) are important in many fields of science and industry. One of the main problems in coal combustion processes is the alkali release. This alkali release leads to an alkali concentration in the flue gas significantly higher than the specifications of the gas turbine manufacture`s. Molten coal ash slag containing high concentration of SiO_2 , Al_2O_3 , Fe_2O_3 and alkali and other alkaline-earth oxides has a high potential for alkali retention depending on the alkali oxide activity in the slag.

Compared to experimental methods thermodynamic equilibrium modelling is able to generate results within less time at lower costs. In order to perform calculations concerning systems which have a complicated structure and strong interactions between the constituents an adequate thermodynamic model and assessed thermodynamic data are needed. The accuracy of the calculation depends on the reliability of the database and adaptability of the model.

The goal of the present work is the development of a new database optimised for the basic quaternary oxide system containing the main slag components SiO_2 and Al_2O_3 and the alkali oxides Na_2O and K_2O . This system can be considered as a basis for the future addition of further slag-relevant oxides such as Fe_2O_3 and the alkaline earth oxides CaO and MgO .

This complex oxide system was investigated with respect to the thermodynamic description of the liquid solution (slag). The available thermodynamic data were collected, analysed and modified for the purpose of improving the solution database. The associate solution model was adapted to the accepted database FACT.

The associate species approach was applied to represent the phase relations in the binary systems $\text{Me}_2\text{O-SiO}_2$, $\text{Me}_2\text{O-Al}_2\text{O}_3$ ($\text{Me}=\text{Na}, \text{K}$) and $\text{SiO}_2\text{-Al}_2\text{O}_3$ and in the ternary systems $\text{K}_2\text{O-Na}_2\text{O-SiO}_2$ and $\text{Na}_2\text{O-Al}_2\text{O}_3\text{-SiO}_2$. The phase equilibria calculated using the associate model with the new optimised slag solution data show good agreement with the experimental points. In the literature, the binary systems $\text{Me}_2\text{O-SiO}_2$ and $\text{Me}_2\text{O-Al}_2\text{O}_3$ ($\text{Me}=\text{Na}, \text{K}$) were not investigated regarding their phase diagrams in the composition range near the pure alkali oxide. In contrast to the old database, the new dataset allows the description of the whole composition range of the binary systems.

The investigations performed show that the associate species approach cannot only be used for the representation of liquid solutions but also for the representation of solid solutions (nepheline and carnegieite) without taking into account the structure of the solid solution.

The comparison of measured partial pressures of potassium over the liquid phase and of potassium oxide activities in the quaternary $\text{Na}_2\text{O-K}_2\text{O-SiO}_2\text{-Al}_2\text{O}_3$ melt with calculated values show relatively good agreement although these data have not yet been taken into account for the optimisation.

The associate species model can therefore be applied to describe and predict the thermodynamic properties of the considered system (phase diagram and activity data) and extended to multicomponent systems taking into account “multicomponent” interactions as well.

Contents

1. Introduction and aims.....	1
2. Thermodynamic modelling of the oxide systems	3
2.1. Gibbs energy of a solution.	3
2.1.1. Polynomial expressions for the excess Gibbs energy.....	5
2.2. Solution models for slags	7
2.2.1. Modified quasichemical model	8
2.2.2. Ideal mixing of complex components	13
2.2.3. Modified associate species model	15
2.3. Thermodynamic calculations: basic principles and application.....	18
2.3.1. Thermodynamic data	18
2.3.2. Calculation program: ChemSage.....	19
2.3.3. Calculation program: FactSage	22
2.3.4. Parameter optimisation	23
3. Review of literature data	27
3.1. Binary systems	27
3.1.1. Na ₂ O-SiO ₂	27
3.1.2. K ₂ O-SiO ₂	32
3.1.3. Al ₂ O ₃ -SiO ₂	33
3.1.4. Na ₂ O-Al ₂ O ₃	36
3.1.5. K ₂ O-Al ₂ O ₃	39
3.2. Ternary systems.....	42
3.2.1. K ₂ O-Na ₂ O-SiO ₂	42
3.2.2. Na ₂ O-Al ₂ O ₃ -SiO ₂	44
4. Optimisation routine	53
5. Results.....	57
5.1. Binary systems	57
5.1.1. Na ₂ O-SiO ₂	57
5.1.2. K ₂ O-SiO ₂	64
5.1.3. Al ₂ O ₃ -SiO ₂	68

5.1.4. $\text{Na}_2\text{O}-\text{Al}_2\text{O}_3$	71
5.1.5. $\text{K}_2\text{O}-\text{Al}_2\text{O}_3$	75
5.2. Ternary systems.....	79
5.2.1. $\text{Na}_2\text{O}-\text{K}_2\text{O}-\text{SiO}_2$	79
5.2.2. $\text{Na}_2\text{O}-\text{Al}_2\text{O}_3-\text{SiO}_2$	83
5.2.3. Application of the associate species model to calculate K_2O activities	87
6. Discussion	89
7. Summary and conclusions	93
8. Acknowledgements.....	97
9. References	99
10. Appendix.....	105
11. List of figures.....	109
12. List of tables.....	113

1. Introduction and aims

The limited fossil fuel resources and the necessity of reducing CO₂ emissions require an increase of the efficiency of power plants by using combined cycle power systems. Up to now efficiencies in excess of 50 per cent are only achievable by using ash-free fuels such as natural gas or oil, in gas and steam power plants. However, coal constitutes 80 per cent of the world's total fossil fuel resources. Therefore, coal-fired systems with high efficiency have to be developed.

Pressured pulverised coal combustion (PPCC)¹ is a potential concept for realising these objectives. In this concept the gas burner of a conventional combined cycle is replaced by a coal burner. The direct use of the hot flue gas for driving a gas turbine requires hot gas refinement to prevent corrosion of the turbine blading.

One of the main problems is the alkali release during the coal combustion process. The alkali metals are mainly bound in the mineral matter of the coal as salts and silicates. The alkali release leads to an alkali concentration in the flue gas significantly higher than the specifications of the gas turbine manufacture's.

Molten coal ash slags contain high concentrations of SiO₂, Al₂O₃, Fe₂O₃ as well as alkali and alkaline-earth oxides. They have a high potential for alkali retention depending on the alkali oxide activity in the slag.

Two possible strategies have been proposed to remove the alkalis: (1) optimising the alkali retention potential of the coal ash slag in the combustion chamber and the liquid slag separators and (2) separate alkali removal with solid aluminosilicate sorbents (getters) at temperatures above 1350 °C. Therefore, the alkali partial pressure over coal ash slag should be determined in order to get information about the retention potential of the slag. Investigations should show whether the alkali partial pressure over the slag is generally low enough in the case of thermodynamic equilibrium. In the case of too high alkali partial pressures a separate alkali removal is needed.

Measurements on complex and reactive systems such as slags at high temperature are difficult and not practical for the whole range of composition and temperature of technological interest. Compared to experimental methods, thermodynamic equilibrium modelling is able to generate results within shorter time at less expense while allowing free variation of parameters such as temperature and chemical composition of the system. Moreover, the thermodynamic properties cannot only be calculated in the temperature and composition ranges of the experimental data on which the data assessments were based, but may be used for extrapolations into extended regions as well.

However, investigations have shown² that the available thermochemical databases are not sufficient to model the complete coal ash slag and gas system. Therefore, a new database is necessary optimised for the system considered here.

The aim of the present work was the development of a new database optimised for the basic quaternary oxide system, containing the main slag components SiO_2 and Al_2O_3 and the alkali oxides Na_2O and K_2O . This system can be considered as the basis for the future addition of further slag-relevant oxides such as Fe_2O_3 and the alkaline earth oxides CaO and MgO .

A necessary prerequisite was a critical review of the literature with respect to the data available for the system under consideration. The data had to be scrutinised with respect to their relevance and consistency. For concentration ranges where experimental data points are missing appropriate assumptions concerning the phase relations had to be made.

A main task of the present work was the thermodynamic description of the liquid slag using an appropriate solution model for the purpose of successful realisation of calculations and a more adequate description of the thermodynamic properties of the complex oxide system. However, it should be noted that a prime requirement for the new liquid dataset was its consistency with data already available for the solid phases.

2. Thermodynamic modelling of the oxide systems

2.1. Gibbs energy of a solution.

Solution models permit the interpolation and extrapolation of thermodynamic data and the prediction of the thermodynamic properties of multicomponent mixtures. Coupling of evaluated solution databases for metals, slags etc. with general Gibbs energy minimisation programs allows the calculation of equilibrium states in multiphase industrial systems. In order to be useful in interpolations, extrapolations and predictions, it is essential that the solution model correctly represents the thermodynamic properties and structure of the solution.

The simplest case of a solution is a simple substitutional solution. In a binary system the substitutional solution model assumes that atoms or molecules of components 1 and 2 are very similar so that there will be a very small change in bonding energy or volume upon mixing. For the same reasons, the atoms or molecules will be randomly distributed over the lattice sites. In the case of a liquid solution, the “lattice sites” can be considered as the instantaneous atomic positions. The Gibbs energy for a solution can in general be written by the equation:

$$G = \sum x_i G_i^0 + G^m, \quad (1)$$

where G_i^0 is the Gibbs energy value for the pure component i of the solution, x_i is the mole fraction. The term G^m describes the solution behaviour. This is called Gibbs energy of mixing or “Gibbs energy of solution” because it represents the effect of forming a solution from a mechanical mixture. For a binary system the reference (i.e. the mechanical mixture) is represented by a straight line in the molar Gibbs energy diagram, in a ternary system it is a plane, etc. The simplest model for the mixing of atoms in a solution is based on the assumption of random mixing and simple pairwise interactions between atoms of different kinds. (A solution with only the entropy contribution to the Gibbs energy of mixing is regarded as an ideal solution.) For that general case the Gibbs energy is given as

$$G^m = -TS_m^{ideal} + G^{ex}. \quad (2)$$

The expression for the ideal (or so called “Bragg-Williams”) entropy of mixing S_m^{ideal} can be derived from Boltzmann’s relation

$$S_m^{ideal} = -R \sum x_i \ln x_i. \quad (3)$$

The term $-TS_m^{ideal}$ is important in all solutions, not only ideal ones, and gives the Gibbs energy its characteristic shape of a “hanging rope” for a binary system and a “canopy” for a ternary.

It is usual to summarise all other contributions to the Gibbs energy in a term called the excess Gibbs energy G^{ex} . This may be defined relative to an ideal solution

$$G = \sum x_i G_i^0 + RT \sum x_i \ln x_i + G^{ex}. \quad (4)$$

The excess quantities represent the deviation from ideal behaviour and are thus subject to study and modelling.

For any solution one can see that the excess Gibbs energy must approach zero for the pure components. A convenient way to describe the composition dependence in a binary system is to introduce the product $x_1 x_2$, which goes to zero for pure component 1 as well as for pure component 2. Then the excess Gibbs energy can be written as

$$G^{ex} = \alpha x_1 x_2. \quad (5)$$

The parameter α may be assigned as a representation of the interaction between the components 1 and 2. For the so-called **regular** solution α is constant, independent of composition and temperature. Several liquid and solid solutions conform approximately to regular solution behaviour, particularly if G^{ex} is small. To understand this behaviour it is assumed that the atoms or molecules of components 1 and 2 are similar in size and electronic structure so that they form a nearly random substitutional solution. The configurational entropy of mixing will be nearly ideal. It is assumed that the bond energies ϵ_{11} , ϵ_{22} , ϵ_{12} of the nearest neighbour pairs are independent of temperature and composition, and that the average nearest neighbour coordination number z is constant. The enthalpy of mixing is considered as resulting mainly from the change in the total energy of nearest neighbour bonds. There are $\frac{N^0 z}{2}$ pair bonds in one mole solution, where N^0 is Avogadro's number. Since the distribution is random, the probabilities that a given bond is a 1-1, a 2-2 or a 1-2 bond are x_1^2 , x_2^2 , and $2x_1 x_2$, respectively. The molar energy of mixing is then equal to the sum of the energies of the pair bonds in one mole solution less that of the energy of the 1-1 bonds in x_1 mole of pure component 1 and the energy of the 2-2 bonds in x_2 mole of pure component 2:

$$\begin{aligned} \Delta H^{mix} &= \frac{N^0 z}{2} (x_1^2 \epsilon_{11} + x_2^2 \epsilon_{22} + 2x_1 x_2 \epsilon_{12} - x_1 \epsilon_{11} - x_2 \epsilon_{22}) = \\ &= (N^0 z) \left(\epsilon_{12} - \frac{(\epsilon_{11} + \epsilon_{22})}{2} \right) x_1 x_2 = C_1 x_1 x_2 \end{aligned} \quad (6)$$

where C_1 is constant. A similar consideration is valid with respect to vibrational entropies of the nearest neighbour pair bonds. Replacing ϵ_{ij} with σ_{ij} gives the nonconfigurational entropy term $S^{nonconfig} = C_2 x_1 x_2$, where C_2 is constant. Then Eq.(5) results in $\alpha = (C_1 - C_2 T)$.

Simple nonpolar molecular solutions and simple ionic solutions often exhibit approximately regular behaviour. In such solutions with Van der Waals or Coulomb forces, the assumption of the additivity of pair bonds is quite realistic.

The partial values are connected with the integral thermodynamic solution functions by the defining equation for chemical potentials introduced by J.W.Gibbs as $\mu_i = \frac{\partial G}{\partial n_i}$. In

order to describe the real solution, the chemical activity a_i of a component in the solution is introduced by the expression:

$$G_i = G_i^0 + RT \ln a_i = G_i^0 + RT \ln x_i + RT \ln f_i, \quad (7)$$

where $a_i = x_i f_i$ and f_i is denoted as the activity coefficient of the component i . G_i^0 is the Gibbs energy of component i in the reference state. It is common to choose as the reference state the pure component i at the same temperature and pressure as well as the state under consideration. The activity is defined from the difference between the component energy in the pure state and in the solution:

$$a_i = e^{\frac{G_i - G_i^0}{RT}} \quad (8)$$

and the activity coefficient is obtained from

$$RT \ln f_i = G_i^{\text{ex}} = \frac{\partial G^{\text{ex}}}{\partial n_i} = \left(1 + \frac{\partial}{\partial x_i} - \sum_{j \neq i} x_j \frac{\partial}{\partial x_j}\right) G^{\text{ex}}. \quad (9)$$

For a regular solution the activity coefficients can be written as

$$\begin{aligned} RT \ln f_1 &= x_2^2 \alpha \\ RT \ln f_2 &= x_1^2 \alpha \end{aligned} \quad (10)$$

A fundamental problem with the regular solution theory arises from the assumption of random mixing. If 1-2 bonds are relatively stronger than 1-1 and 2-2 bonds, then there will be a tendency for the number of the 1-2 bonds to be greater than that in a random mixture, since such nonrandomness will decrease the Gibbs energy. Similarly, if 1-2 bonds are relatively weaker, then the number of the 1-2 bonds will be less than that in a random distribution. In either case, the configurational entropy is no longer ideal. However, such non-ideal entropical contributions can all be subsumed in the above-mentioned parameter C_2 .

2.1.1. Polynomial expressions for the excess Gibbs energy

In the general case, the α parameter from Eq.(5) is a function of temperature and composition. It has been found that the excess properties of simple binary substitutional solutions can often be represented quite adequately by expanding the enthalpy and excess entropy as polynomials in the component mole fractions:

$$G^{\text{ex}} = \alpha x_1 x_2, \text{ with } \alpha = {}^0L_{12} + {}^1L_{12}(x_1 - x_2) + {}^2L_{12}(x_1 - x_2)^2 + \dots, \quad (11)$$

where ${}^kL_{12}$ are empirical coefficients which are (usually linear) functions of temperature. If the series is truncated after the first term, then the solution is regular. The polynomial representation can be considered to be an empirical extension of regular solution theory, and the fundamental assumptions of the polynomial model are the same as those of the regular solution model, namely a substitutional solution with close to random mixing.

The power series Eq.(11) was introduced by Redlich and Kister³ for organic liquids and is now called the Redlich-Kister polynomial. The excess Gibbs energy in a multi-component system is then represented in the form

$$G^{ex} = \sum_{i < j} \sum x_i x_j \sum_{v=0}^{n_{ij}} L_{ij}^{(v)} (x_i - x_j)^v \quad (12)$$

where $L_{ij}^{(v)}$ is the interaction coefficient between corresponding i-th and j-th constituents,

$$L_{ij}^{(v)} = A_{ij}^{(v)} + B_{ij}^{(v)}T + C_{ij}^{(v)}T \ln T + D_{ij}^{(v)}T^2 + \dots \quad (13)$$

A fundamental weakness of the interaction parameter formalism is the use of the ideal configurational entropy term. For example, a solution of Al and O in molten Fe is treated as a randomly mixed solution, whereas in reality the formation of “complexes” such as AlO is expected due to the strong attractive interaction between Al and O. Neither the temperature dependence nor the composition dependence of such entropic contribution to G^{ex} can be represented simply by the use of a very negative ε_{AlO} . Rather, complex formation should be taken into account.

On the other hand, positive values of the regular solution parameter result in a tendency to demix. A miscibility gap will be formed if the temperature is lowered and the excess term becomes more important than the contributinal term.

Liquids are not in every case completely soluble in each other. As a result the liquid separates out as two phases, a condition which is referred to as liquid immiscibility. In the phase diagram it is depicted as a miscibility gap, as a field where two liquids with different compositions are in equilibrium with each other. The microstructure of the melt undergoes a change. In some instances, the second liquid phase separates out as discrete droplets dispersed in a matrix of the first phase. In other cases, the boundaries between the phases will be diffuse and both phases may be continuous. The reason for the separation of a liquid into two phases may be found by considering the thermodynamics of a non-ideal solution. In such solutions, the attractions between like and unlike atoms are not equal. If the forces of attraction between like atoms are greater than those between unlike atoms, there is a tendency towards clustering of like atoms or a demixing of the solution to form two phases.

Liquid-liquid separation has important applications in the field of ceramics. In the area of glass-ceramics (sometimes called recrystallised glasses), nucleation of the crystalline phases may occur at the energetically favourable interface between the liquid phases. Thus, liquid-liquid separation provides an effective means of nucleating the crystallisation process within a glass.

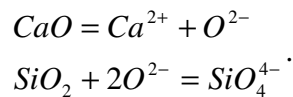
2.2. Solution models for slags

Slags are formed when metals are extracted from ores which contain some gangue minerals such as SiO_2 and Al_2O_3 . They consist of those gangue minerals and fluxes added to improve their separation from crude metals by lowering their melting temperatures and viscosities. The typical industrial slags encountered in various metallurgical processes consist of SiO_2 , Al_2O_3 , FeO , CaO , MgO and others such as MnO , P_2O_5 , CaF_2 and etc. Since silica is always present in any ore, slags are essentially silicate melts accompanied by various oxides and in some cases sulphide or halide. Slags are also formed on refining of crude metals. In this case, oxidised impurities of the crude metals are major constituents, for example MnO , SiO_2 and FeO in steelmaking slags. Thus, the generation of slags cannot be avoided in metal production, because the original ores are impure.

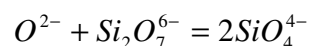
The most important property of a slag is its separability from the metal. For this purpose, the composition of a slag is controlled to ensure low viscosity and low density. Another important function is to adsorb impurities in the metal. Slags also can protect the metal from being contaminated by the environment and reduce excessive heat loss from the metal. For these reasons, slag control is very important in metallurgical processes.

Molten slags are usually ionic conductors, they consist of cations such as Ca^{2+} , Mg^{2+} , Fe^{2+} , and anions such as O^{2-} , SiO_4^{4-} , PO_4^{3-} . Silicon is coordinated by four O^{2-} to form SiO_4^{4-} with a tetrahedral structure. Depending on the SiO_2 content, a number of SiO_4^{2-} units are connected as chains or rings, in what is called a network structure, to form a large polymerised ion. As the size of silicate ion clusters is increased, the slag viscosity also increases. The addition of CaF_2 to silicate melts is considered to make them less viscous by breaking the network.

Oxides are classified into donors and acceptors of an oxide ion, O^{2-} , as can be described by reaction equations:



Donors and acceptors are called basic oxides and acidic oxides, respectively. In slag melts, acidic oxides exist as complex ions having various coordination numbers for oxygen, such as SiO_4^{4-} or $\text{Si}_2\text{O}_7^{6-}$ (SiO_2), PO_4^{3-} (P_2O_5), AlO_4^{5-} (Al_2O_3), FeO_4^{5-} (Fe_2O_3), TiO_4^{4-} (TiO_2). Neutral oxides behave as amphoteric oxides depending on the presence of other oxides. For instance, Al_2O_3 can be stable in the slag as Al^{3+} or as AlO_4^{5-} . When CaO is added to a silicate slag, the bond connecting an oxygen atom to two silicon atoms is broken to form a smaller unit as SiO_4^{4-} in equation,



and the slag becomes more fluid.

Complex silicate solutions, particularly the general amorphous slag and glass systems, are important to both established and developing technologies. The formation and function of slags are important in common metallurgical processes, such as the production of iron, steel, copper, aluminium etc, and in glass processing. High-temperature investigations of such complex, reactive phases are difficult and not practical for the whole range of the compositions and temperatures of technological interest. Modelling high-temperature mixing solutions of complex oxides, using standard non-ideal solution model techniques, cannot correctly represent their properties.

The chemical thermodynamics of oxide melts, slags and glasses are difficult because of strong interaction between constituents, particularly with SiO_2 . There are at the same time strong attractive forces between the basic constituents, e.g. CaO and SiO_2 , leading to large negative deviations from ideality and subtle repulsive forces leading to miscibility gaps in regions of high SiO_2 concentration. Thus, unlike many metallic alloys, simple solution models do not reproduce the thermodynamic properties and phase relations in most oxide liquid systems. They have very specific short-range/cluster periodicity that is a function of composition. There are two successful approaches for modelling thermodynamic behaviour and, thus, phase relations of complex oxide systems. These approaches are the modified quasi-chemical model of Pelton and Blander⁴ and the so-called associate species model introduced for slags by Hastie and Bonnell^{5, 6} and further developed by Besmann, Spear, and Allendorf^{7, 8}. These models will be considered in detail.

2.2.1. Modified quasichemical model

When dealing with systems containing a liquid phase which exhibits strong structural “ordering” about a certain composition, the enthalpy of mixing tends to exhibit a negative, “V”-shaped peak near the composition of maximum ordering, while the entropy of mixing tends to have the shape of the letter “m” with a minimum near this composition as shown in **Fig. 1**.

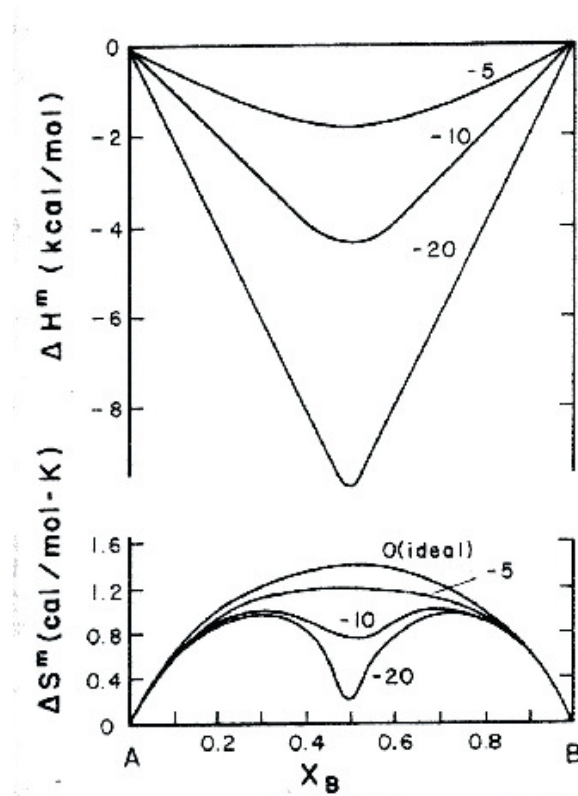


Fig. 1. Enthalpy and entropy of mixing of a binary system for different degrees of ordering at about $x_a=x_b=0.5$. Curves are calculated⁴ from the modified quasichemical theory at $T=1000\text{ }^{\circ}\text{C}$ with $z=2$ for a constant values of ω (kcal) and $\eta=0$

In binary silicate systems MeO-SiO_2 ($\text{Me}=\text{Ca, Mg, Pb, Fe, Mn, etc}$) ordering is observed at a mole fraction of SiO_2 , $x_{\text{SiO}_2} \approx 1/3$. This corresponds to the composition Me_2SiO_4 and this ordering is generally attributed to the formation of orthosilicate ions. To represent the thermodynamic properties of ordered systems a set of equations based on a physical model accounting for the ordering is required, which gives the characteristic shapes of the ΔH and ΔS functions.

In the case of molten silicate systems, many physical models (“polymeric” or “sublattice”) have been proposed, but almost all of these models are very detailed and too complex for practical purposes. In accordance with the quasichemical approach, a set of equations is required which takes ordering into account in a general way and for which only a small set of coefficients is needed. It is also advisable to have a formalism that is as simple and as general as possible. For instance, the formalism used for ordered liquids should also be applicable to unordered liquids (such as CaO-MgO). Thus one could describe the multicomponent system CaO-MgO-SiO_2 by one set of equations. It would be desirable to have a single formalism applicable to a variety of ordered systems such as alloys, halides and slags. A modification of the quasichemical theory of Guggenheim for short-range ordering introduced by Pelton and Blander⁴ meets the above requirements.

In a binary system with components “1” and “2” particles are mixed substitutionally on a quasi-lattice. The relative amounts of the three types of nearest neighbour pairs (namely, 1-1, 1-2, 2-2 pairs) are determined by the energy change associated with the formation of two 1-2 pairs from a 1-1 and 2-2 pair according to:

$$[1-1]+[2-2]=2 [1-2] \quad (14)$$

If this energy change is zero, then the solution is an ideal mixture. If this energy change becomes more and more negative, the formation of the 1-2 pairs is favoured. As a result, the entropy and enthalpy functions take on the characteristic shapes shown in **Fig. 1**. However, the simple quasichemical equations cannot be used for silicate melts where the minimum in enthalpies and entropies of mixing of a binary system is not at a mole fraction of 0.5 and where the energy change for reaction Eq.(14) depends on the local environment of the bonds involved. Then the basic quasichemical theory is modified in order to provide an expression for the entropy and enthalpy of a highly ordered system with minima in entropy and enthalpy at any desired composition. As a further modification, the energy change for reaction Eq.(14) is introduced as a function of composition with adjustable coefficients. Finally, the theory is extended to ternary and multicomponent systems.

In a binary silicate melt such as MeO-SiO₂, Me and Si particles defined as “1” and “2” are mixed in a cationic quasi-lattice. The tendency to ordering through the preferential formation of pairs 1-2 (Me-Si) could be identified with the formation of orthosilicate ions and that of the resultant creation of second-nearest-neighbour Me-Si pairs. The completely ordered solution is considered to consist of only Me²⁺ cations and SiO₄⁴⁻ anions.

This model is not intended as a detailed theory of silicate structure but rather as a mathematical formalism which has the advantages of simplicity and generality that permits this approach to be used for interpolation and extrapolation in the unmeasured regions⁴.

There are three types of nearest-neighbour pairs (namely, 1-1, 2-2, 1-2) with “pair bond energies” ε_{ij} in a binary system with components “1” and “2” mixed substitutionally on a quasi-lattice with a constant coordination number z . The total number of such pairs per mole solution is $N^0 z/2$, where N^0 is the Avogadro constant. The pairs 1-2 are formed from pairs 1-1 and 2-2 according to reaction Eq.(14). The enthalpy change for this process is $(2\varepsilon_{12} - \varepsilon_{11} - \varepsilon_{22})$. Multiplying the latter by $N^0 z/2$, a molar enthalpy change, ω , can be defined as

$$\omega = \frac{N^0 z}{2} (2\varepsilon_{12} - \varepsilon_{11} - \varepsilon_{22}). \quad (15)$$

In the same way, a molar non-configurational entropy change, η is defined as

$$\eta = \frac{N^0 z}{2} (2\sigma_{12} - \sigma_{11} - \sigma_{22}), \quad (16)$$

where σ_{ij} is the “non-configurational entropy of the pair bond”.

Let n_{11} , n_{22} and n_{12} be the number of moles of each type of pair in solution. The fraction of pairs which are i - j pairs is defined as:

$$x_{ij} = \frac{n_{ij}}{n_{11} + n_{22} + n_{12}}. \quad (17)$$

When components “1” and “2” are mixed, 1-2 pairs are formed at the expense of 1-1 and 2-2 pairs. In the model, the enthalpy of mixing is then given by summing the pair bond energies:

$$\Delta H = \frac{x_{12}}{2} \omega. \quad (18)$$

The total molar entropy of the solution is given as:

$$S^E = -\frac{Rz}{2} \left(x_{11} \ln \frac{x_{11}}{x_1^2} + x_{22} \ln \frac{x_{22}}{x_2^2} + x_{12} \ln \frac{x_{12}}{2x_1x_2} \right) + \frac{x_{12}}{2} \eta, \quad (19)$$

where x_1 and x_2 are mole fractions of the particles 1 and 2.

The equilibrium concentrations of the various pairs are given by minimising the Gibbs energy at constant composition:

$$\frac{d(\Delta H - T\Delta S)}{dx_{12}} = 0. \quad (20)$$

and therefore:

$$\frac{x_{12}^2}{x_{11}x_{22}} = 4e^{\frac{2(\omega - \eta T)}{zRT}}. \quad (21)$$

Eq. (21) is similar to an equilibrium constant for reaction Eq.(14). That is the reason why the model is called “quasichemical”.

If $\omega=0$ and $\eta=0$, then $\Delta H=0$ and $S^E=0$ and the solution is ideal. If values ω and η are small then $x_{12} \approx 2x_1x_2$. From Eq.(18) $\Delta H \approx x_{12}\omega$ then results. In this case, the solution is regular. If $(\omega - T\eta)$ is made progressively more negative, ΔH assumes a negative peaked form as shown in **Fig. 1** and ΔS assumes the m-shaped form of **Fig. 1**.

Two points must be noted: (1) the model is exact in one dimension ($z=2$) with no approximations, and (2) for highly-ordered systems, the correct entropy expression is given by the model only when $z=2$.

The next modification to the model concerns the composition of maximum ordering. As presented above, the model always gives maximum ordering at $x_1=x_2=1/2$. To make the model general, one must be able to choose a composition which is observed in the system. For example, in the binary system MeO-SiO₂ this composition is observed near $x_{\text{MeO}}=2/3$.

The simplest way is to replace the mole fractions x_1 and x_2 in the preceding equations by “equivalent fractions” y_1 and y_2 defined by:

$$y_1 = \frac{b_1 x_1}{b_1 x_1 + b_2 x_2} \text{ and } y_2 = \frac{b_2 x_2}{b_1 x_1 + b_2 x_2}, \quad (22)$$

where b_1 and b_2 are numbers chosen such that $y_1 = y_2 = 1/2$ at the composition of maximum ordering. This can be achieved by choosing b_1 and b_2 such that $\frac{b_1}{b_1 + b_2} = \frac{1}{3}$.

The molar enthalpy of mixing and molar excess entropy (per mole of components “1” and “2”) become:

$$\Delta H = (b_1 x_1 + b_2 x_2) \frac{x_{12}}{2} \omega \quad (23)$$

$$S^E = -\frac{Rz}{2} (b_1 x_1 + b_2 x_2) \left(x_{11} \ln \frac{x_{11}}{y_1^2} + x_{22} \ln \frac{x_{22}}{y_2^2} + x_{12} \ln \frac{x_{12}}{2y_1 y_2} \right) + (b_1 x_1 + b_2 x_2) \frac{x_{12}}{2} \eta \quad (24)$$

The constant values of ω and η are sufficient to represent the main features of the curves of ΔH and ΔS for ordered systems, but for a quantitative representation of the thermodynamic properties of real systems it is necessary to introduce a composition dependence of ω and η , which can be expressed in the form of the simple polynomial:

$$\omega = \omega_0 + \omega_1 y_2 + \omega_2 y_2^2 + \omega_3 y_2^3 + \dots \quad (25)$$

and

$$\eta = \eta_0 + \eta_1 y_2 + \eta_2 y_2^2 + \eta_3 y_2^3 + \dots \quad (26)$$

where the temperature- and composition-independent coefficients ω_i and η_i are empirically chosen to give the best representation of the available experimental data for a system. These coefficients can be obtained by computer optimising.

The modified quasichemical equations can be extended to multicomponent systems. For a ternary system with mole fractions x_1, x_2, x_3 , the equivalent fraction may be defined as:

$$y_1 = \frac{b_1 x_1}{b_1 x_1 + b_2 x_2 + b_3 x_3}. \quad (27)$$

The functions $\omega_{12}, \omega_{23}, \omega_{31}$ and $\eta_{12}, \eta_{23}, \eta_{31}$ are the molar enthalpy and non-configurational entropy changes for the pair exchange reaction:



The ternary enthalpy and excess entropy are then given by extension of Eqs.(18) and (19):

$$\Delta H = (b_1x_1 + b_2x_2 + b_3x_3) \frac{(x_{12}\omega_{12} + x_{23}\omega_{23} + x_{31}\omega_{31})}{2} \quad (29)$$

$$S^E = -\frac{Rz}{2}(b_1x_1 + b_2x_2 + b_3x_3) \times \left(x_{11} \ln \frac{x_{11}}{y_1^2} + x_{22} \ln \frac{x_{22}}{y_2^2} + x_{33} \ln \frac{x_{33}}{y_3^2} + x_{12} \ln \frac{x_{12}}{2y_1y_2} + \right. \\ \left. + x_{23} \ln \frac{x_{23}}{2y_2y_3} + x_{31} \ln \frac{x_{31}}{2y_3y_1} \right) + \quad (30) \\ + (b_1x_1 + b_2x_2 + b_3x_3) \frac{(x_{12}\eta_{12} + x_{23}\eta_{23} + x_{31}\eta_{31})}{2}$$

where x_i is overall mole fractions of the component oxides, x_{ij} – mole fraction of pair bonds, y_i - equivalent fractions (weighted mole fractions). The equations similar to Eq.(21) for three different pairs are derived by minimising the total Gibbs energy at constant compositions:

$$\frac{x_{ij}^2}{x_{ii}x_{jj}} = 4e^{-\frac{(\omega_{ij}-\eta_{ij}T)}{zRT}} \quad (31)$$

The functions ω_{ij} (pair enthalpy change) and η_{ij} (pair entropy change) are the polynomial expansions in the three binary subsystems. In order to estimate the thermodynamic properties of the ternary from the binary data, it is necessary to approximate ω_{ij} and η_{ij} in the ternary system from their values in the binaries. There are two methods: the “symmetrical approximation” which assumes that ω_{ij} and η_{ij} are constant along the lines of constant molar ratio y_i/y_j , and the “asymmetrical approximation”, in which ω_{12} and ω_{31} (and η_{12} and η_{31}) are constant at constant y_1 , while ω_{23} (and η_{23}) is constant at constant y_2/y_3 ratio. These two methods are also called the Kohler and Toop interpolations respectively.

The properties of ternary phases may be approximated from the assessed parameters of the binary subsystems. If experimental ternary data are available, then the approximations may be refined by the addition to the Gibbs energy expression of “ternary terms” such as $\Phi_{ijk}x_1^i x_2^j x_3^k$, where i, j, k are all positive non-zero integers and where Φ_{ijk} are the adjustable ternary parameters. Ideally, these parameters should be small if not zero.

2.2.2. Ideal mixing of complex components

The second appropriate approach for slag systems is the modified associate species model. This is based on the original associate species model that was first applied for complex oxide solutions by Hastie, Bonnell and co-workers (Ref.^{5,6}) in the 1980s in order to obtain vapour pressure data for slag systems. This was a predictive method for conditions of temperature, pressure, and gaseous atmosphere for which only limited experimental data exist.

As indicated above, slag systems are characterised by strong acid-base chemical interactions leading to negative deviations in thermodynamic activities which are much larger than those predicted by the ideal or regular solution models.

Such models are generally satisfactory only for systems where the thermodynamic mixing interactions behave smoothly over the entire composition range. For acid-base inorganic systems, particularly those containing alkali oxides, the ratio of formal concentration to thermodynamic activity can, however, vary over the range $\sim 1\text{-}10^{10}$. Rapid change in activity can occur over narrow concentration ranges. Within the framework of the IMCC (ideal mixing of complex components) model it is attempted to avoid these difficulties by considering that the strong acid-base interactions result in the formation of liquid complexes with well-known stoichiometries and Gibbs energies of formation. These complexes are regarded as explicit components of the liquid. However, they are not necessarily independent molecular or ionic species like gas species, but serve to represent the local associative order.

In most cases, the additional liquid complex components are derived as neutral, stable, thermodynamically defined species with compositions that relate to the congruently melting solid compounds of a system. The standard Gibbs energy of formation $\Delta_f G(T)$ as a function of temperature can often be derived from the melting data of the solid compounds. In a few cases, namely in complex aluminosilicate systems, liquid constituents which have no known corresponding pure solid phases were included in the model database. The presence of such liquid species in the model is required to account for the additional associative order present in highly complex solutions. The contribution of strong attractive interaction is thus contained in the $\Delta_f G(T)$ function of the complex components, which then mix ideally according to Raoult's law.

Gibbs energy of formation of each species $\Delta_f G(T)$ in such database functions is defined as

$$\Delta_f G(T) = a + bT + cT \ln T + dT^2 + eT^3 + \frac{f}{T} \text{ (J/mol)}, \quad (32)$$

where a-f are fitted coefficients. The calculated concentration of each individual solution species is then taken as an activity. This is the key assumption in the model. The complex oxide solutions are thus represented by an ideal solution of end-member species *and* model species. The solution Gibbs energy of an ideal solution is defined as

$$G = \sum_i x_i G_i = \sum_i x_i (G_i^0 + RT \ln x_i) \quad (33)$$

The equilibrium composition with respect to these components can be calculated by minimising the total system free energy in the same way as for an ideal gas.

The solution modelling approach using an IMCC approximation has the following basic features:

- Selection of known solid and liquid components from available phase diagrams and thermodynamic tables, where possible.
- Assignment of hypothetical components (solution species) where required by mismatch with experimental activity data.
- Assessment of $\Delta_f G(T)$ of the model species from experimental data.
- Estimation of $\Delta_f G(T)$ for liquids of known congruently melting solids where necessary.
- Assumption that $\Delta_f G(T)$ for glass and liquid are identical at least within experimental error.
- Free Gibbs energy minimisation to determine equilibrium composition and hence activities.

The Na₂O-SiO₂ slag is considered as an example. Then, the overall mole fractions of the system components Na₂O and SiO₂ are known. From these the equilibrium mole fraction of Na₂O, SiO₂ and chosen Na_xSi_yO_z liquid species are calculated. Since the solution is considered as ideal, the activities of the species are equal to their calculated mole fractions. The physical interactions among the complex species are considered negligible compared with the strong chemical interactions leading to their formation.

The advantages of this approach:

- It accurately represents the thermodynamic behaviour of complex systems over wide ranges of composition and temperature.
- It correctly predicts the activities of the components in metastable equilibrium glass phases.
- It allows a logical estimate of unknown thermodynamic values.
- It is relatively easy for nonspecialists in thermochemistry to understand and use.

A general weakness of this model consists in its apparent inapplicability to systems exhibiting positive deviations from Raoult's law, i.e. systems having a liquid miscibility gap. Bonnell and Hastie^{5,6} did not consider this aspect in detail since the systems studied by them only cover compositions which exhibit large negative deviation from ideality.

2.2.3. Modified associate species model

As shown above, the ideal mixing of associate species (including the pure end members) provides a good representation of the solution energies for liquids in which the end-

member components exhibit attractive forces. The modification to the associate species model is the incorporation of positive interaction energies in a solution. With these parameters, it is possible to accurately represent reported immiscibility in a solution phase (e.g. liquid-liquid immiscibility common in many SiO₂-containing systems). The results are simple equations for Gibbs energies which can be extrapolated and interpolated to unstudied temperature and composition ranges. The Gibbs energy of the binary associate species solution can be written as the equation:

$$G = \sum_i x_i G_i^0 + RT \sum_i x_i \ln x_i + G^{ex,bin} \quad (34)$$

where the excess Gibbs energy is expressed by the Redlich-Kister polynomial (Eqs.12, 13). If necessary, ternary excess terms can be considered.

$$G^{ex,tern} = \sum_i \sum_j \sum_k x_i x_j x_k L_{ijk}^{(T)} \quad (35)$$

$$L_{ijk} = x_i L_i(T) + x_j L_j(T) + x_k L_k(T)$$

Like the IMCC, the associate species solution model uses intermediate "chemical species" with their corresponding thermodynamic data to represent the negative non-ideal mixing of the end-member components in a system, i.e., the heat of mixing or attractive forces/ordering between constituents⁷. For example, liquid NaAlO₂(liq) and Na₂Al₄O₇(liq) species mix with the end-member Na₂O(liq) and Al₂O₃(liq) to represent the liquid phase in the Na₂O-Al₂O₃ binary system⁸. Although NaAlO₂(liq) and Na₂Al₄O₇(liq) may not exist as chemical entities that can be isolated and characterised, these species in the model can accurately represent the negative interaction energies that occur between Na₂O and Al₂O₃ in an oxide liquid solution. The negative energies of interactions, which occur between basic oxide and SiO₂ at specific compositions in this liquid silicate slag, can also be represented accurately. It should be noted that in the approach taken by Spear, Besmann and Allendorf^{7,8,9} all liquid associate species have formulas that contain two non-oxygen atoms per mole to allow equal weighting of each species with regard to its contribution to the ideal mixing entropy. Thus, the Na₂Al₄O₇(liq) species noted above is actually Na_{2/3}Al_{4/3}O_{7/3}(liq) or Na₂Al₄O₇·1/3(liq)⁷.

This choice was adopted during the optimisation process when phase-diagram information was mathematically compared with thermodynamic data to obtain internally consistent sets of data for a given chemical system. It was found that for all systems (aluminates, borates, silicates, aluminosilicates, etc.) the thermochemical data can be more easily optimised when liquid associate species contain two non-oxygen atoms per species rather than one atom. As noted, this assumption is suitable for the ideal mixing energy of the solution phase, but the implications of its use are not yet fully understood. However, for very stable liquid associate species, no ideal mixing energy (ideal mixing entropy) exists at the composition of that associate because a single associate species makes up the entire liquid solution at that composition.

Complex, multicomponent system models are built up in a manner similar to that used by Pelton and Blander⁴. Binary and ternary constituent systems are modelled so that they accurately represent the experimentally determined phase equilibria and other thermodynamic properties. The various associates of these binary and ternary systems can then be included in a single solution for many constituent oxides, allowing equilibria to be easily computed and chemical activities to be derived. Where liquid immiscibilities exist in the binary and ternary systems, such that some interaction terms are necessary to accommodate repulsive energetic relationships, these can also be represented by the introduction of additional interaction terms, i.e. in the form of Redlich-Kister polynomials. Unlike the modified quasi-chemical model, these interaction terms do not require more than two terms of an expansion, which include temperature dependences. Fitting the phase diagram can often be accomplished “manually” (i.e., by trial and error), preventing the need for sophisticated optimisation routines.

2.3. Thermodynamic calculations: basic principles and application

Computerised thermochemical data and the associated software for the calculation of chemical equilibria can be powerful tools in studying the chemistry of materials at high temperatures. Reliable thermodynamic data, which are retrieved and manipulated by computer programs, enable scientists and engineers to analyse chemical reactions and complex equilibria of metal production, electronic and ceramic materials development, alloy design, coating technology, process analysis, nuclear waste disposal and so on. Thermodynamic calculations are especially useful in the case of describing reactions and processes which are difficult to realise owing to high temperature, pressure or long time before reaching the equilibrium state.

Such calculations require the following conditions:

- State-of-the-art computer software;
- Self-consistent, critically assessed thermodynamic data.

2.3.1. Thermodynamic data

As stated above, one of the main parts of the thermodynamic calculations is the so-called thermodynamic database, which must contain all available thermodynamic data about condensed, liquid and gaseous phases. For the present purposes, the databases FACT and SGTE (Scientific Group Thermodata Europe), and as well as the application-oriented database developed by Besmann, Spear, Allendorf^{7,8,9} are available.

FACT^{10, 11, 12} was chosen as the reference database because it contains the most complete data set regarding complex oxide systems. For the general description of a chemical system two types of data are needed: compound (i.e. pure substances) and real solution data.

Compound data are for inorganic stoichiometric pure solid, liquid and gaseous species such as SiO₂(s), K₂O(liq), Na(g). Allotropes (for example graphite C(s1) and diamond C(s2)) and isomers (for example ethylene C₂H₄O(liq1) and acetylene C₂H₄O(liq2)) are also included. Data on non-integer stoichiometric compounds, such as FeO_x (x = 0.947), can also be stored. Depending on the type of phase (solid, liquid, gas) and data availability, the stored properties include:

- $\Delta H(\text{formation}, 298.15\text{K}, 1\text{bar})$,
- standard entropy $S(298.15\text{K}, 1\text{bar})$,
- heat capacity as function of temperature $C_p(T) = A + BT + CT \ln T + DT^2$,
- magnetic coefficients (Curie or Neel temperature and magnetic moment if applicable),

- molar volumes (298.15K, 1bar) coupled with expansivities and compressibilities as functions of temperature (when avoidable).

The thermodynamic functions are derived according to equations:

$$H = \Delta H_{298} + \int_{298}^T c_p dT, \quad \text{with } c_p = a + bT + cT^2 + dT^3$$

$$S = S_{298} + \int_{298}^T \frac{c_p}{T} dT \quad (36)$$

Dilute aqueous solution data (Henrian activity coefficients) and non-ideal gas properties (using T_{crit} , P_{crit} , V_{crit} , the acentric factor (ω) and the dipole moment) are also stored in the compound databases.

Solution data are for solid and liquid alloys, concentrated aqueous solutions, ceramics, salts, matters, **slags** etc. The data are stored in the form of Gibbs energy functions for the phase constituents and parameters for the excess Gibbs energy of mixing between the phase constituents. There are 14 different solution models including simple polynomial models such as the Redlich-Kister or the Legendre polynomial combined with different higher order extrapolations (Muggianu, Kohler, Toop), the quasichemical model and sublattice models.

The FACT solution database for slags provides critically evaluated thermodynamic data for the molten oxide phase containing the primary slag constituents Al_2O_3 , CaO , FeO , Fe_2O_3 , K_2O , Na_2O , SiO_2 and so on. Many solid solutions (ceramics) of these components are also stored: monoxide, perovskite, spinels, pseudobrookite, melilite, olivine, wollastonite etc.

The complete dataset of thermodynamic information for a system containing SiO_2 , Al_2O_3 , B_2O_3 , CaO , FeO , Na_2O , K_2O , SnO_2 , MgO was refined and tested by Besmann, Spear, Allendorf^{7, 8, 9} to give reasonable thermodynamic and phase diagram information. The complex liquid solution was described using the modified associate species model. The database included the formation energy data of the associate species and interaction parameter to represent the excess Gibbs energy of the solution.

The SGTE database at present contains only data for pure substances, i.e. compounds, for the solid and sometimes also liquid state. For the present system data, are contained for the compounds in the complex system $\text{SiO}_2\text{-Al}_2\text{O}_3\text{-Na}_2\text{O-K}_2\text{O}$.

2.3.2. Calculation program: ChemSage

One of the most widespread computer programs for chemical equilibrium calculations is SOLGASMIX¹³. To make the use of the Gibbs energy minimisation routine of SOLGASMIX more user-friendly an extensive library of subroutines with the most frequently

utilised models for non-ideal integral molar Gibbs energies has been added. This augmented program was given the name ChemSage¹³.

ChemSage was originally designed to perform three types of thermochemical calculations in multicomponent systems involving phases with non-ideal mixing properties, i.e. thermodynamic functions, chemical and phase equilibria and steady-state conditions for the simulation of simple multistage chemical reactors. Later a module for the generation of phase diagrams using the zero phase fraction line principle¹⁴ was added.

Many thermodynamic properties of solutions can be derived from the Gibbs energy by taking into account the appropriate temperature and composition derivatives. In the routines for thermodynamic function calculations, the following quantities are calculated with respect to a chosen reference state: integral and partial values of heat capacity, enthalpy, total or excess entropy, and total and excess Gibbs energy for single mixture phases and heat capacity, enthalpy, entropy and Gibbs energy for stoichiometric condensed phases.

The phase equilibrium routines enable a user to predict the chemical equilibrium state of a system which has been uniquely defined with respect to T, pressure (or volume), and total amounts and/or equilibrium activities for independent system components. A calculation can also be controlled by the change of an extensive property of the system, e.g. enthalpy, to calculate an adiabatic flame temperature, or volume, to calculate a vapour pressure, or by a target phase, e.g. to calculate the liquidus temperature for a given input composition.

The total Gibbs energy of a system, which has to be minimised for a given temperature, pressure and composition to establish equilibrium, is often represented as

$$G = \sum_i n_i \mu_i \quad (37)$$

where n is the amount, μ is the chemical potential, and the sum extends over all chemically distinct entities (or species) of the system. Eq.(37) can be misinterpreted because it is easy to confuse the chemical potential of a species with that of an independent system component. The alternative expression,

$$G = \sum_{\varphi} N^{\varphi} G_m^{\varphi} \quad (38)$$

where φ is a phase index and where N^{φ} is the amount and G_m^{φ} is the integral molar Gibbs energy of phase φ , provides a better picture, as there are phases of a certain total amount and internal composition which coexist at equilibrium. The minimisation of G in equation (38) at constant temperature and pressure is reached with constraints imposed by the mass balance equations. In terms of l independent system components, these may be written as

$$\sum_{\varphi} \sum_i n_i^{\varphi} a_{ij}^{\varphi} = b_j \quad (j=1,2,...l), \quad (39)$$

where n_i^φ is the amount of the i -th constituent of phase φ , a_{ij}^φ is a coefficient of the stoichiometry matrix composed of the constituents of phase φ , and b_j is the total amount of the j -th system component. At equilibrium, the following simple linear relation holds:

$$G = \sum_j b_j \mu_j \quad (40)$$

Here, the chemical potential of the independent system components can be replaced by the Lagrangian multiplier that satisfies the minimum condition of equation (38) under the constraints of equation (39).

In the equilibrium calculations, integral and partial molar Gibbs energy expressions are required. Generally, the integral expression can be written as

$$G_m = G_m^0 + G_m^{id} + G_m^{ex} + G_m^p + G_m^{mo}, \quad (41)$$

where G_m^0 and G_m^{id} are the Gibbs energy contributions from pure phase components and from the ideal entropy term with respect to these components, respectively. The excess Gibbs energy contribution G_m^{ex} is often small or even negligible if proper phase components, and thus a proper ideal state, have been chosen. However, the effects like immiscibility or chemical ordering cannot be modelled without G_m^{ex} , which therefore can be called the chemical interaction term. The Gibbs energy contributions from changes in molar volumes, G_m^p , and magnetic ordering, G_m^{mo} , are of a non-chemical nature and can normally be neglected (G_m^p) or are not applicable (G_m^{mo}).

Explicit magnetic contributions to the integral molar Gibbs energy have been included in ChemSage according to the formalism proposed by Inden and modified by Hillert and Jarl. Its mathematical form is given by

$$G_m^{mo} = RTf(\tau)\ln(\beta + 1), \quad (42)$$

where the function $f(\tau)$ changes coefficients when the reduced Curie temperature ($\tau = T/T_c$) is equal to unity, and where β denotes the average magnetic moment per atom. The Curie temperature and the magnetic moment are composition-dependent according to a relationship based on a linear contribution from the pure phase components and an additional composition-dependent part of the form of a Redlich-Kister polynomial.

The minimisation algorithm is completely independent of the solution models, and the convergence criteria are the same for ideal or non-ideal systems.

The shape of the Gibbs energy surface and the existence and uniqueness of the minimum are important considerations. For systems containing ideal fluid and solid phases it can be established that the Gibbs energy surface is convex and does not have local minima and that a computed equilibrium composition corresponds to a global minimum. For non-

ideal systems, however, uniqueness cannot be guaranteed. The most common case for a false solution occurs when a stable mixture phase may have a region of demixing. In order to avoid confusion two copies of the mixture have to be entered and ChemSage will automatically find both stable mixtures at equilibrium or the composition of the one with the lowest Gibbs energy.

It must be pointed out that the computational efficiency and convergence reliability have recently been improved by a routine which provides close starting estimates of the equilibrium mole numbers¹³. By selecting the most stable species as system components and by keeping track of the rank of the stoichiometry matrix, this routine makes it possible to calculate equilibria in systems where the number of dominant compounds is less than the number of elements, and also equilibria where the number of system components changes during the course of a calculation. A system with the composition of a stable multicomponent stoichiometric solid phase is considered as an example. Below the temperature at which this solid melts or sublimates, it is the only equilibrium phase in a constant pressure and temperature calculation and, hence, only one chemical potential is defined. An appended Gibbs energy minimisation for every mixture phase, assuming that their compositions are equal to the solid, is then applied to calculate the remaining phase-dependent chemical potentials¹³.

Different solution models are available in ChemSage. The chemical interactions of the models may be grouped into three classes, namely, those *with explicit equations for G_m* Eq.(41) models(Ideal Mixing, Redlich-Kister-Miggiannu polynomial, Redlich-Kister-Miggiannu polynomial for pseudobinary phase, general polynomial Kohler-Toop formalism, multisublattice formalism etc.); those *with explicit equations for chemical potential* (unified interaction parameter formalism based on Wagner, Pitzer formalism for aqueous solution), and those *with implicit formalisms* (Gaye-Kapoor-Frohberg cell formalism, modified quasichemical formalism).

The model based on the Redlich-Kister-Miggiannu polynomial can be applied as example of the analytical expression of the Gibbs energy of simple substitutional or associate solutions. For a phase described by this model (without ternary terms), one may write the Redlich-Kister polynomial as shown by Eqs.(12, 13) .

The Gaye model and the quasichemical model are treated in ChemSage by a special numerical routine that performs phase-internal minimisations. The calculated equilibrium values, the distributions of “cells” for the Gaye model and the fraction of different types of bonds for the quasichemical model can be related to partial excess Gibbs energies of the phase constituents.

2.3.3. Calculation program: FactSage

FactSage is an amalgamation of the powerful thermochemical modules of ChemSage and the user-friendly windows-oriented FACT-Win.

FactSage consists of a suite of modules which allow thermodynamic calculations to be performed for different kinds of chemical systems. The most important modules are *Equilib* and *Phase Diagram*.

The *Equilib* module is the Gibbs energy minimisation workhorse of FactSage. It calculates the concentration of the chemical species when specified elements or compounds react or partially react to *reach a state of chemical equilibrium*. *Equilib* uses the Gibbs energy minimisation algorithm and thermochemical functions of ChemSage and offers great flexibility in the way the calculations may be performed. For example, the following are allowed: a choice of unit (K, °C, F, bar, atm, psi, J, cal, BTU, kwh, wt%,...); dormant phases in equilibrium; equilibria constrained with respect to T, P, V, H, S, G, U or A or their changes; user-specified product-activities (the reactant amounts are then computed); user specified compound and solution data.

Phase Diagram is a generalised module that permits unitary, binary, ternary and multicomponent phase diagram sections to be calculated, plotted and edited where the axes can be various combinations of T, P, V, composition, activities, chemical potential etc. The resulting phase diagram is plotted by the *Figure* module. It is possible to calculate and plot: classical unitary temperature versus pressure, binary temperature versus composition, ternary isothermal isobaric Gibbs triangle phase diagrams; two-dimensional sections of a multicomponent system where the axes are various combinations of T, P, V, composition, activities, chemical potential etc. The phase diagram sections that may be calculated are based on the theory of zero phase fraction line mapping.

A user may create and edit his own private database using the *Compound* and *Solution* modules of the FactSage program. This feature was used so that the modified associate species model database by Spear, Besmann, Allendorf^{7, 8, 9} can be employed for FactSage calculations.

2.3.4. Parameter optimisation

One of the major capabilities of ChemSage permits the optimisation of standard and excess Gibbs functions using experimental information. The optimisation routine of ChemSage is reported in Ref.¹⁵. Parameters for all available solution models in ChemSage can be simultaneously adjusted.

A Bayesian algorithm is employed in the improvement of thermodynamic parameters because of its advantages over conventional least squares algorithms.

In Bayesian estimation methods, the objective function $E(p)$, which is to be optimised with respect to the vector of model parameter p , consists of two parts: (1) the difference between predicted and experimental data and (2) the difference between estimated and a

priori parameters, where the latter result from independent measurements or theoretical considerations, i.e.

$$E(p) = [f(p) - y]^T \frac{1}{C_y} [f(p) - y] + [p - p^0]^T \frac{1}{C_{p^0}} [p - p^0], \quad (43)$$

where p^0 , y and $f(p)$ denote vectors of *a priori* parameters, experimental data and corresponding calculated values, respectively. C_y and C_{p^0} are covariance matrices of experimental function values y and *a priori* parameters p^0 , respectively, which for the first iteration have to be provided by the user. The inverse of C equals the weighting matrix. The user can therefore weight the two parts of the objective function differently depending on whether he places more confidence in the experimental data or the original model properties. For example, it is often advantageous to use parameters derived from calorimetric measurements (e.g. enthalpies of formation of compounds) as *a priori* information. When a subsequent optimisation with regard to, for example, phase equilibrium data is performed, the Bayesian algorithm allows these parameters to be adjusted within their experimental uncertainty, thus ensuring that physically reasonable values are considered during optimisation.

The Bayesian method is known to improve the convergence of the iterative process. “Oscillation” of parameters, i.e. changes by several orders of magnitude from one iteration to another, can be stopped when small *a priori* uncertainties are selected. Moreover, parameters of different orders of magnitude (e.g., from 10^{-3} to 10^8) can be adjusted simultaneously.

A special feature of the ChemSage optimiser is that adjustable parameters can be coupled to each other, e.g. H^E and S^E for linear free enthalpy relationships resulting in a “common vanishing temperature” for G^E .

The vector of calculated values $f(p)$ is provided by the phase equilibrium module of ChemSage. For each set of experimental data points, an appropriate calculation, corresponding to the type of experiment performed, has to be specified. These calculations may include:

- Simple equilibrium calculations, where temperature, pressure or volume, and total composition of the system may be specified to calculate compositions and stabilities of phases, activities of components or the total volume.
- Extensive-property calculations, where e.g. heat capacity c_p of phases and ΔG , ΔH and ΔV of formation reactions may be calculated, when the temperature and pressure of the reactants are known.
- Formation or precipitation phase target calculations, which can be utilised when phase boundary data are available.

The PARAMETER OPTIMISATION module is used for the assessment of Gibbs energy coefficients from experimental thermodynamic data to obtain an improved database. Such data can include

- phase diagram information, e.g. temperature and possibly pressure as well as amount and composition of the phases at equilibrium,
- calorimetric information, e.g. enthalpies of formation or phase transformation, enthalpy of solution or mixing, heat content and heat capacity measurements,
- Gibbs energy information, e.g. activities from vapour pressure or EMF (electromotive force) measurements,
- volume data, e.g. from dilatometry.

All such measurements contain information that finally leads to Gibbs energy functions of all phases in a system, with temperature and possible composition and/or total pressure dependence as needed. An assessment usually combines all known Gibbs energy data compiled in a preliminary thermochemical set with the set of known experimental information. The user has to determine which of the known parameters should remain untouched and which need refinement in the optimisation, which new parameters have to be introduced, especially when assessing data for non-ideal solution phases.

In general a three step procedure has to be performed:

- (1) Setting up a thermochemical datafile
- (2) Setting up an experimental datafile
- (3) Executing the assessment interactively.

(1) First, it is necessary to set up a thermochemical datafile with a suitable choice of T and, where applicable, composition dependence of the Gibbs energies of all phases of the system. The setting up of the data is carried out in accordance with the data format of the different Gibbs energy models and by using the data input module. In the extreme case all parameters in this file might have the value 0. This provides an empty model into which the user has to “bring” the information contained in the experimental data. In fact, a file with all parameters equal to zero contains the names of the system components, molar masses, phase and species names, stoichiometric coefficients and Gibbs energy model names used for the non-ideal solutions.

(2) Next, the available experimental data need to be prepared in a form suitable for the PARAMETER OPTIMISATION module. Essentially, each experiment is the inverse of a normal ChemSage calculation. So normal ChemSage commands are used to define a particular “experimental (point)”. Therefore it is necessary that the

thermochemical datafile - although (partially) “empty” with respect to the actual Gibbs energy parameters - is available since phase and species names, and possibly molar masses, are needed to define an equilibrium calculation.

- (3) Finally, the assessment is carried out interactively by selecting the experimental data to be used, by entering initial estimates of the parameters that are to be optimised and by giving standard deviations for the parameters to be used in the Bayesian algorithm that is employed in ChemSage. The user can also specify the number of iterations which the algorithm is to carry out. After execution of the optimisation the user can inspect the agreement obtained between calculation and experiment in a result table. This table shows the most recent set of Gibbs energy parameters, some statistical output and all experiments together with the appropriate calculated values. In order to carry out test calculations after assessment it is useful to employ other modules of ChemSage or (after data export) FactSage, especially to depict the phase diagram based on the new parameters.

The entire optimiser module has been integrated into FactSage under the name of OptiSage. All interactive actions etc. discussed for ChemSage can now be performed in the user-friendly windows-based environment of FactSage. However, this feature was not available in time to be used for the present work.

3. Review of literature data

The considered system consists of sodium, potassium, aluminium, and silicon oxide as important slag components. The phase equilibria data were collected and used for optimisation in order to describe and predict the thermodynamic properties of the liquid slag.

3.1. Binary systems

3.1.1. $\text{Na}_2\text{O}-\text{SiO}_2$

The first system contains sodium oxide and silicon oxide. The phase equilibria in the composition range between sodium metasilicate Na_2SiO_3 and silica were studied by Morey and Bowen¹⁶. The liquidus curve of the $\text{Na}_2\text{O}-\text{SiO}_2$ system was determined by the quenching method. The temperature-composition diagram is presented in Fig. 2.

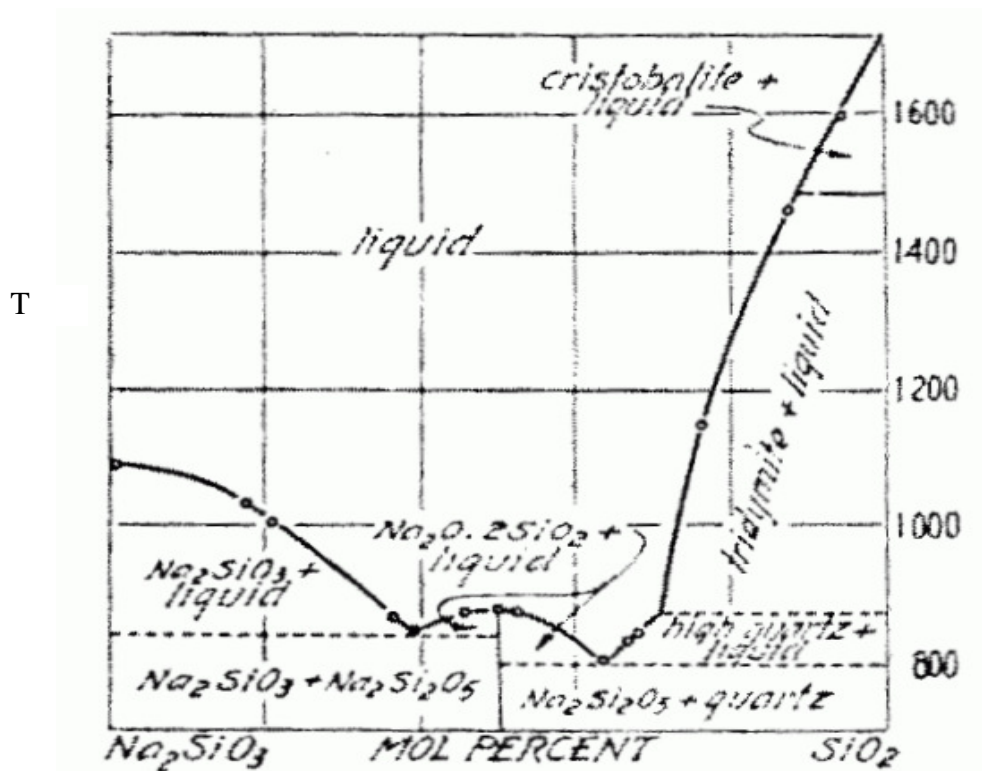


Fig. 2. Temperature composition diagram of the binary system $\text{Na}_2\text{SiO}_3\text{-SiO}_2$ according to Morey, Bowen¹⁶

The melting point of sodium metasilicate was found at 1086 °C. The eutectic between metasilicate (Na_2SiO_3) and disilicate ($\text{Na}_2\text{Si}_2\text{O}_5$) was located by extrapolation of the metasilicate and disilicate curves. The eutectic temperature determined is 840 °C and composition is 37.5 mole percent SiO_2 in term of $\text{Na}_2\text{SiO}_3\text{-SiO}_2$. Sodium disilicate $\text{Na}_2\text{Si}_2\text{O}_5$ has a congruent melting point at 874 °C. The liquidus curve is unusually flat, especially on the side toward Na_2SiO_3 . A present excess of 4.3 mole percent silica leads to a decrease of the

melting point of only 2.5 °C. A further addition of SiO₂ results in a more rapid decrease of the melting point, until the disilicate-quartz eutectic is reached. The mixture with 63.56 mole percent SiO₂ melts at 802.7 °C, and the primary phase is Na₂Si₂O₅. A mixture containing 66.73 percent SiO₂ melts at 827 °C, and high-quartz is the primary phase. The temperature of the eutectic was determined by holding these two mixtures at successively increasing temperatures until the first indication of glass formation was observed, and both mixtures gave the same temperature of 793 °C. If the eutectic temperature is known, extrapolation of the two liquidus curves becomes a more reliable method of locating the eutectic composition, which is estimated as 35 mole percent Na₂Si₂O₅ and 65 percent SiO₂.

Addition of Na₂O to silica produced a rapid decrease of the melting point, and there is no limited miscibility. Addition of 4.07 mole percent Na₂O, giving a mixture containing 5.12 mole percent Na₂SiO₃ and 94.88 mole percent SiO₂, decreases the melting point from 1710 °C, the melting point of cristobalite, to 1598 °C, with cristobalite as solid phase. A mixture containing 68 mole percent SiO₂ was crystallised by annealing at 750 °C for three days. It was most difficult to determine this point. Both crystal and glass were heated together at constant temperature for 14 hours in each run. A shorter time was not sufficient to dissolve the quartz above the liquidus or to form crystals in the glass below the liquidus.

The Na₂O-SiO₂ system was revised afterwards by Kracek^{17,18} in a more extensive composition range from orthosilicate Na₄SiO₄ to silica.

The preparations were made from selected pure quartz as source of SiO₂ and from especially pure Na₂CO₃. The materials were mixed in the required proportions by weight, placed in a platinum crucible and heated at 700 °C to hold in the major portion of the CO₂ present before noticeable quantities of liquid were formed. After this initial sintering the temperature was slowly raised until the mixture became completely fluid. The final melting was always done in a large platinum crucible to avoid contamination of silica. In order to make homogeneous preparations it was necessary to raise the temperature to the point at which rapid diffusion of the constituents took place in the mixture. It was reasonable to heat no higher than was essential, because at high temperature both the soda and silica are somewhat volatile. After heating of the molten preparation at a selected temperature for the required time the glass was cooled, weighed, powdered and examined under the microscope for homogeneity. Finally, most of the preparations were crystallised. This is not essential except with mixtures from which quartz separates as the primary phase, or in which quartz forms one of the eutectic components. Quartz is a very reluctant crystalliser and, when once obtained, disappears from the melt very slowly. All the other crystalline phases occurring in this system grow with sufficient rapidity to insuring equilibrium is achieved in a relatively short time.

The various equilibrium temperatures were established by the method of quenching for most of the diagram shown in **Fig. 3**. In the orthosilicate region, where it is difficult to freeze the equilibrium, the method of heating curves was used.

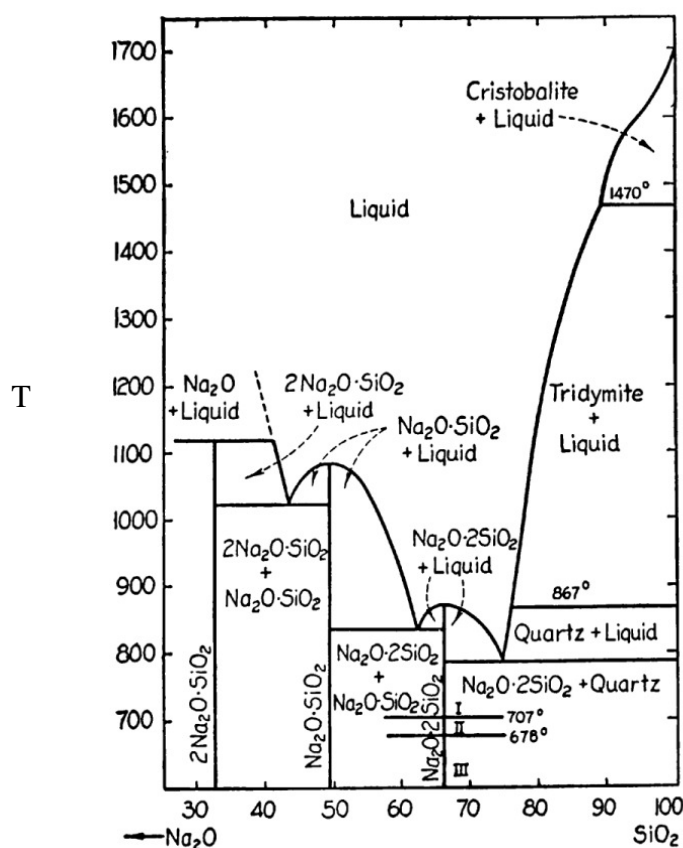


Fig. 3. Equilibrium phase diagram of the binary system $\text{Na}_2\text{O-SiO}_2$ (after Kracek^{17,18})

Silica crystallises from sodium silicate preparations in three modifications. Quartz transforms to tridymite at 870 °C, and tridymite goes into cristobalite at 1470 °C. The high temperature modification cristobalite melts at 1713 °C. The cristobalite liquidus descends from the melting point to the inversion point (1470 ± 10 °C) between cristobalite and tridymite, located at 88.7 mass percent SiO_2 .

The tridymite-liquid line descends smoothly from this point. At 75.5 mass percent SiO_2 it meets the liquidus curve of quartz. The liquidus curve of quartz extends over a short range of temperature only, namely from 870 to 793 °C, ending at the disilicate-quartz eutectic. It should be noted that only the high modification of quartz (so-called α -quartz or high quartz), which is stable above 573 °C, is the modification encountered in the liquid.

The location of the eutectic between high quartz and sodium disilicate was estimated by determining the temperatures at which the disilicate disappeared from a preparation previously crystallised at a temperature below that of the eutectics. The eutectic was obtained roughly within the temperature interval from about 788 to nearly 800 °C. To verify the location of this eutectic, crystalline preparations of 74.8 and 76 percent SiO_2 were heated

completely at various temperatures and quenched as reported in Ref.¹⁸. When the mixture was exposed for two days at 786 °C, the preparations remained powdery. At 788 °C they sintered to porous lumps, with little or even no glass at all evident under the microscope. At 790 °C there was a great deal of glass, in which quartz crystals and larger eroded quartz grains with very little remnants of sodium disilicate crystals were imbedded. The eutectic temperature is accordingly 789 °C at 73.9 mass percent SiO₂. The temperature is in agreement with that determined by Morey and Bowen¹⁶ (73.4 mass percent SiO₂ at 793 °C).

The measurements of thermal arrests in the sodium disilicate region, carried out by Kracek^{17,18}, showed that Na₂Si₂O₅ has three crystalline modifications with inversions located at atmospheric pressure at average temperatures of 678 and 707 °C as depicted in **Fig. 3**. At temperatures above 706 °C, Na₂Si₂O₅ takes up excess of Na₂O, and above 768 °C - excess SiO₂ into solid solution. The melting point of Na₂O-2SiO₂ (sodium disilicate) is determined as 874 °C

The metastable eutectic between tridymite and sodium disilicate is at 74.6 mass percent SiO₂ and 782 °C.

The field of sodium disilicate extends from the quartz-disilicate eutectic to the metasilicate-disilicate eutectic, which is located at 62.1 mass percent SiO₂ and 846 °C. That is in agreement with data (840 °C, 60.8 mass percent silica) from Morey, Bowen¹⁶. The revised values¹⁷ are 837 °C and 62.1±0.2 mass percent silica as eutectic temperature and composition, respectively.

Sodium metasilicate Na₂O-SiO₂ (Na₂SiO₃) melts at 1088 °C. This value was determined by use of the heating curve method on a preparation which contained a slight excess of SiO₂. On the orthosilicate side, the liquidus curve of the sodium metasilicate ends at the sodium orthosilicate - metasilicate eutectic at 43.1 mass percent SiO₂ and 1022 °C.

The compound Na₄SiO₄, sodium orthosilicate, melts incongruently with decomposition into liquid and crystals of Na₂O. It was extremely difficult to remove CO₂ from preparations in this region. Further, since the orthosilicate crystallises readily, good quenches were not obtained, and the extremely hygroscopic nature of the quenched samples made the microscopic examination so difficult that no reliable information could be obtained regarding the presence of Na₂O crystals and their properties. The method of heating curves, which is used for the samples in this region, did not give reliable data either. The Na₂O-rich liquids are very mobile. There is reason to doubt the correctness of the interpretation of the results.

The alkali part of the phase diagram needs further study in order to obtain more reliable data concerning phase relations.

The compound Na₄SiO₄ melts peritectically at 1118 °C according to data from Refs.^{17,18}. It forms an eutectic at 40.7 mass percent silica and at 1022 °C. Since the accepted

melting point of Na_2O is $1132\text{ }^\circ\text{C}$ ¹⁹ and since no compounds with a composition between Na_2O and Na_4SiO_4 have been reported, the peritectic melting of sodium orthosilicate seems to be unlikely. In fact, D`Ans and Loeffler²⁰ (also later Loeffler²¹) reported that Na_4SiO_4 melts congruently at $1078\text{ }^\circ\text{C}$. They also reported another compound, $\text{Na}_6\text{Si}_2\text{O}_7$, with a congruent melting point of $1115\text{ }^\circ\text{C}$ and two eutectics: between Na_4SiO_4 and $\text{Na}_6\text{Si}_2\text{O}_7$ at $962\text{ }^\circ\text{C}$ and 36.5 mole percent silica and between $\text{Na}_6\text{Si}_2\text{O}_7$ and metasilicate Na_2SiO_3 at $1015\text{ }^\circ\text{C}$ and 45.5 mol% SiO_2 .

Another compound $\text{Na}_2\text{Si}_3\text{O}_7$ was reported by Williamson and Glasser²² to exist in the binary system $\text{Na}_2\text{O}-\text{SiO}_2$. XRD showed that the correct stoichiometry seems to be $\text{Na}_6\text{Si}_8\text{O}_{19}$. They reported that this compound melts incongruently at $808\pm 2\text{ }^\circ\text{C}$ to quartz and liquid and decomposes below $700\text{ }^\circ\text{C}$ to quartz and $\text{Na}_2\text{Si}_2\text{O}_5$. A part of the phase diagram of the system $\text{Na}_2\text{O}-\text{SiO}_2$ is given in **Fig. 4** according to Williamson and Glasser²².

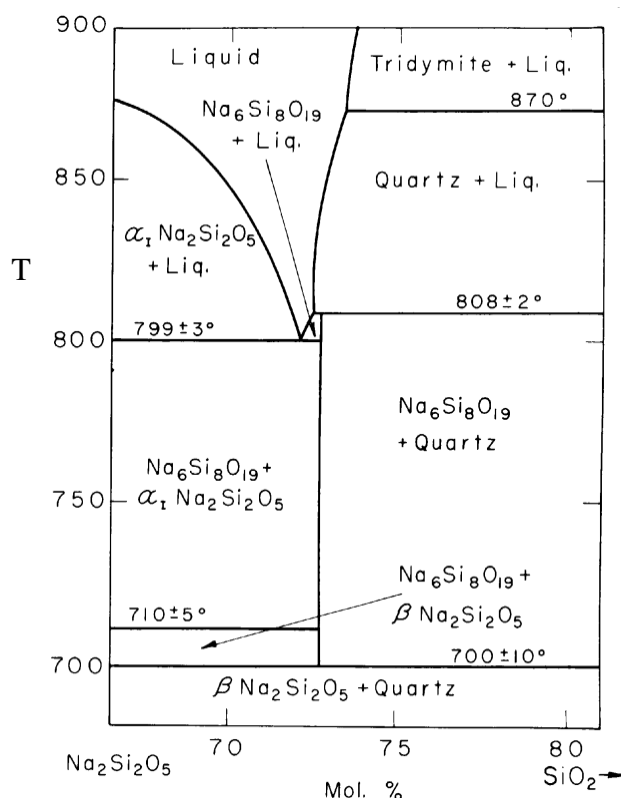


Fig. 4. Part of the equilibrium phase diagram of the system $\text{Na}_2\text{Si}_2\text{O}_5$ - SiO_2 , showing a stability field of $\text{Na}_6\text{Si}_8\text{O}_{19}$

However, Kracek¹⁷ on the one hand and D`Ans and Loeffler²⁰ on the other hand reported eutectic at $789\text{ }^\circ\text{C}$ and $799\text{ }^\circ\text{C}$, correspondingly, at a SiO_2 concentration higher than that of $\text{Na}_6\text{Si}_8\text{O}_{19}$. However, this is inconsistent with the incongruent melting of $\text{Na}_6\text{Si}_8\text{O}_{19}$ to liquid and quartz. Therefore $\text{Na}_6\text{Si}_8\text{O}_{19}$ can be assumed to melt incongruently at $809\text{ }^\circ\text{C}$ as reported in Ref.²², but to liquid and $\text{Na}_2\text{Si}_2\text{O}_5$.

3.1.2. K₂O-SiO₂

The K_2O - SiO_2 system is like the Na_2O -containing system in many respects.

The phase relations of the K_2O - SiO_2 system were studied by Kracek²³ (1937) by the method of quenching. All the mixtures were freshly prepared, crystallised dry, and the liquidus was determined on the crystallised material at once to avoid the disturbing effects produced by the absorption of moisture. For this reason the use of hydrothermal methods of crystallisation was avoided.

The tetrasilicate $\text{K}_2\text{Si}_4\text{O}_9$ was found to crystallise in the dry way with some reluctance at 680 to 700 °C. On the other hand, quartz crystals have never been obtained in this system by dry crystallisation, and accordingly the silica liquidus at temperatures below 870 °C is determined for tridymite instead of quartz as the primary phase. The preparations in this system, particularly those which are richer in K_2O than the disilicate, are very hygroscopic. This was taken into special consideration, since moisture in the glasses tends to produce excessively large crystals upon devitrification, and thus to introduce inhomogeneity into the preparations.

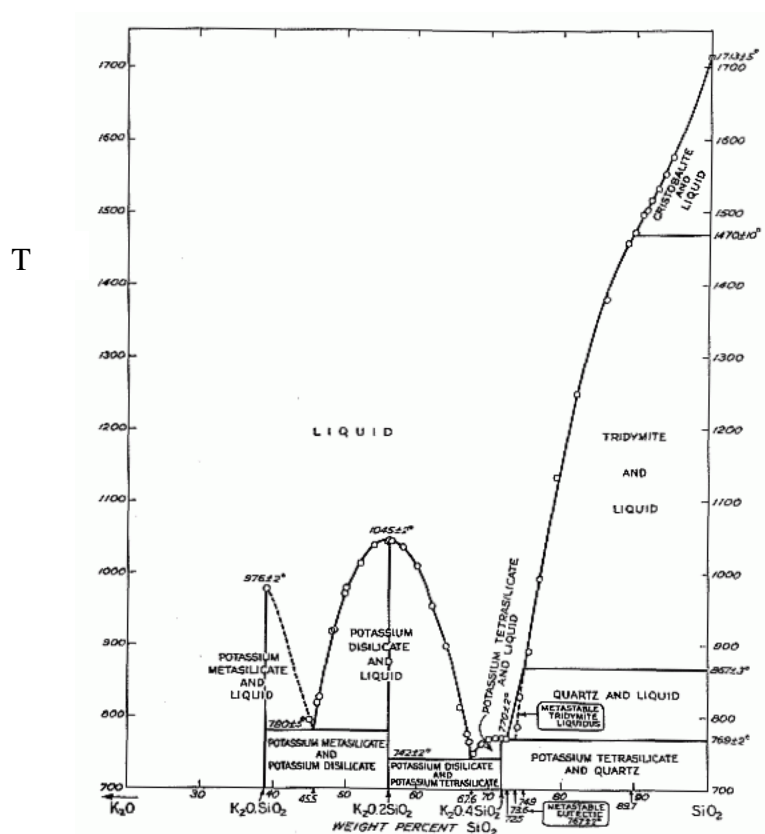


Fig. 5. Experimental phase diagram for $\text{K}_2\text{O-SiO}_2$ system reproduced from Ref.²³

The experimental phase diagram of the K_2O - SiO_2 system is shown in **Fig. 5**. No solid solutions were found in the system, and the solid potassium silicates were treated as stoichiometric compounds. There are three potassium silicates: metasilicate K_2SiO_3 , disilicate

$\text{K}_2\text{Si}_2\text{O}_5$ and $\text{K}_2\text{Si}_4\text{O}_9$, which melt at 976 °C, 1045 °C, and 770 °C, respectively. The reversible inversions for disilicate and tetrasilicate were observed. From the thermal measurements²³ the equilibrium inversion temperatures were detected to be 594 ± 2 °C for $\text{K}_2\text{Si}_2\text{O}_5$ and 592 ± 2 °C for $\text{K}_2\text{Si}_4\text{O}_9$.

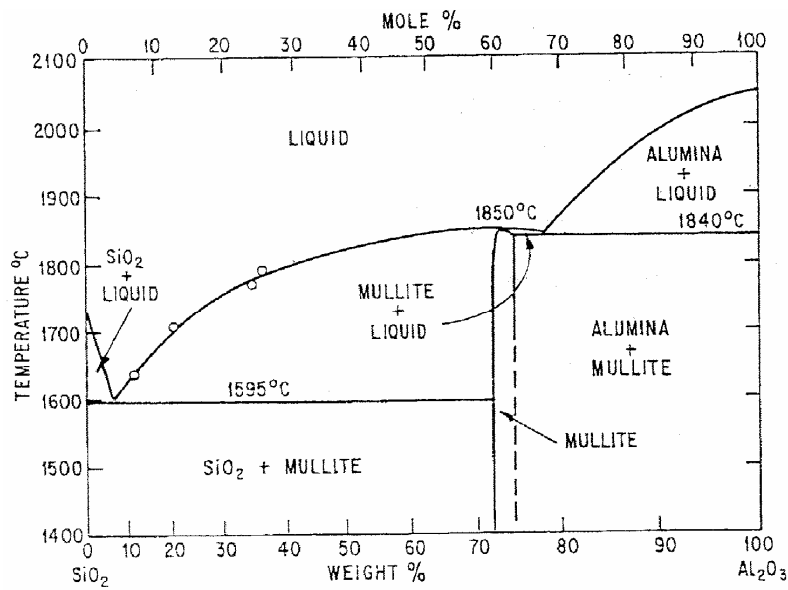
A noticeable feature of this diagram is the slightly flattened shape of the silica curve at high SiO_2 content. This results from the tendency to liquid immiscibility and this is expected to result in a metastable liquid-liquid miscibility gap at low temperatures. However, experimental evidence of metastable phase separation was not obtained in the K_2O - SiO_2 system. It is possible that the critical point of the miscibility gap lies below the glass transition temperature and phase separation is not observed due to kinetic reasons.

3.1.3. Al_2O_3 - SiO_2

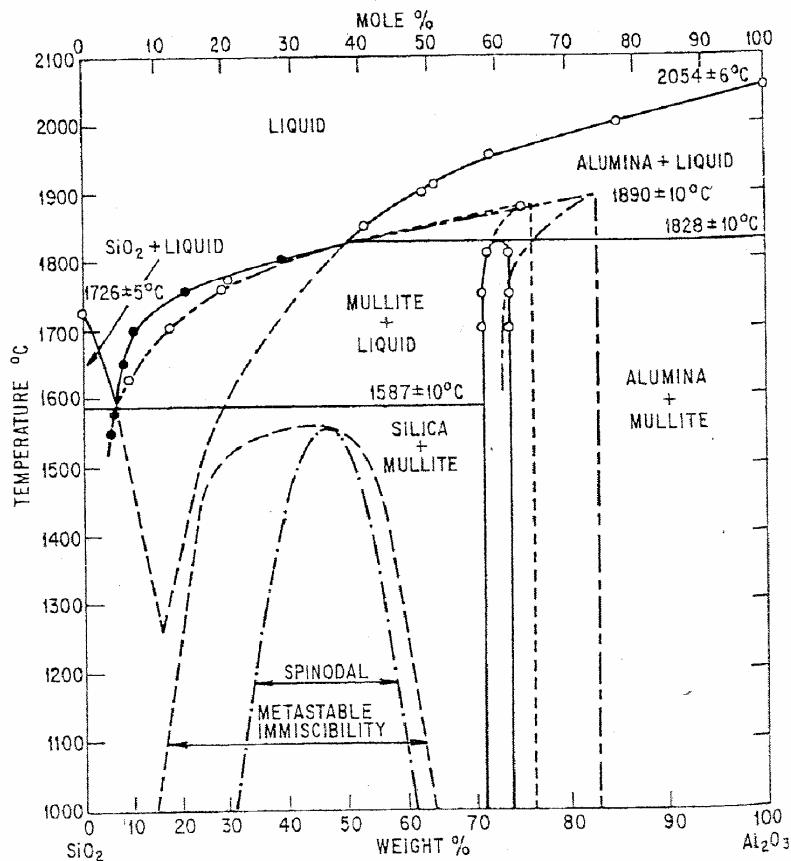
Alumina and silica are components of many commercial ceramics, important minerals and metallurgical slags, and their phase diagram is therefore one of the most important. There is some disagreement in regard to phase boundaries and mullite compound in different investigations. Experimental difficulties due to high temperatures, volatility of silica, and slow reaction rates in solids seem to lead to different experimental results and interpretations. **Fig. 6** shows this discrepancy very clearly.

Aramaki and Roy²⁴ studied the mullite region with samples of mixed alumina and silica powders heated to the desired temperature and quenched to room temperature. Their preparations were sealed in Pt-Rh containers to prevent loss of silica. Phases were identified by optical microscopy.

Aksay and Pask²⁵ deduced a quite different equilibrium diagram from an electron microprobe study of reaction zones in diffusion couples between sapphire and aluminosilicate glass. Concentration profiles in quenched couples and the concentration of alumina at phase interfaces were measured by the microprobe. They also encapsulated the samples to prevent silica loss. These authors found that mullite did not grow on the sapphire interface at a temperature of 1853 °C and above, but a coherent layer of mullite grew below 1800 °C. Mullite crystals were found close to the interface at temperature 1853 °C and above. It was assumed that these crystals grew from the melt on cooling because the composition and morphology were the same as for crystals grown at a distance from the interface. Taking into account the morphology and the composition of the mullite growing at the interface and the position of the liquidus curves, Aksay and Pask concluded that mullite melts incongruently at 1828 ± 10 °C with peritectic at 52.3 mass percent Al_2O_3 . The equilibrium solid reaction limits were found to be almost identical with those of Aramaki and Roy, ranging from 70.5 to 74 mass percent alumina.



(1)



(2)

Fig. 6. Comparison of the experimental phase diagrams for the Al_2O_3 - SiO_2 system. Reproduced from: (1) Aramaki and Roy²⁴ and (2) Aksay and Pask²⁵, modified by Risbud and Pask²⁶

Aksay and Pask studied the effect of the cooling rate as well. The precipitation of alumina was cooling-rate dependent. Alumina-fused silica diffusion couples formed mullite and glass when they were rapidly cooled. They formed alumina and glass when they were slowly cooled. All three phases were formed at intermediate cooling rates. Similar results were observed with a 78 to 80 mass percent alumina-containing melt. The mullite formed from the high alumina silicate melts is a metastable mullite with alumina contents of 83.2 mass percent. Aksay and Pask found that the melting point of hot-pressed mullite (71.8 mass percent of alumina) was 1880 °C, in contrast to the peritectic temperature of 1828 °C. This and other metastable regions in the phase diagram are shown by dashed lines in **Fig. 6(2)**.

The diagram proposed by Staronka²⁷ agrees with data obtained by Aramaki and Roy²⁴.

The eutectic equilibrium close to silica is observed at 9 mass percent alumina and 1595 °C as detected by Aramaki and Roy²⁴, which is in good agreement with data from Ref.²⁵ (1587 °C). The eutectic temperature of 1546 °C given by Staronka seems to be lower.

Klug et al.²⁸ studied the alumina-silica phase relations by optical microscopy, image analysis, X-ray diffraction and electron microprobe. The samples obtained by the sol-gel method were annealed in oxygen and quenched. The phase diagram deduced from their measurements is shown in **Fig. 7**.

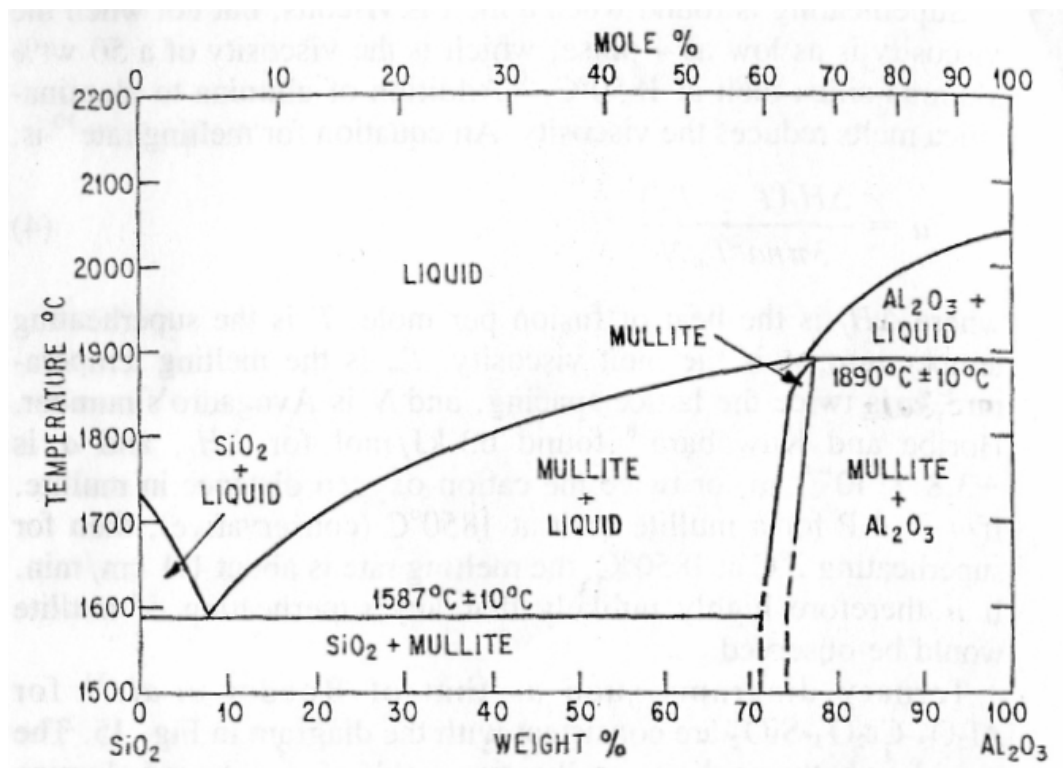


Fig. 7. Composite alumina - silica phase diagram. Reproduced from Klug et al²⁸

The phase diagram in the composition range from 0 to 70 wt% alumina was taken from Aramaki and Roy, except for the eutectic temperature of 1587 °C from Aksay and Pask. The melting point of mullite incongruent is obtained at a temperature of 1890±10 °C and a composition of 77.15 wt% alumina.

The mullite is considered to exist as a solution phase with variable compositions. Single crystals of mullite grown by Welch²⁹ from slowly cooled melts had an analysed composition of 77.2 wt% alumina, which was considered to be the composition of mullite in equilibrium with alumina and liquid at the peritectic decomposition temperature. This composition of the crystals is very close to that with the value of 77.15 wt% alumina found in Ref.²⁸.

A melting point of 1880 °C for a sample with 71.8 wt % alumina was found by Aksay and Pask²⁵. This sample contained no second-phase (alumina), and the mullite composition was 76.8 wt% alumina. They supposed the mullite was overheated due to slow alumina nucleation. They proposed a solid solution range of mullite from 70.5 to 74 wt% Al₂O₃, and suggested that all mullite compositions above 74 wt% are metastable.

The peritectic composition between 76.5 and 77.0 wt% at 1880 °C was determined by Klug²⁸.

A thermodynamic study of the mullite solid solution region was performed by Shornikov³⁰ using a mass spectrometric technique. The Gibbs energy of formation of mullite was determined on the basis of data on the partial pressures of molecular vapour species over a variety of subsolidus regions of the Al₂O₃-SiO₂ system in the temperature interval from 1403 to 1907 °C. Shornikov³⁰ defined mullite as a stoichiometric compound (in contrast to the results reported in Refs.^{28,29} where mullite was considered as a phase) with 71.8±0.08 wt% alumina, which corresponds to the formula of stoichiometric mullite 3Al₂O₃·2SiO₂. A combination of the determined enthalpy and entropy of the formation of mullite (12.93±0.95 kJ/mol and 11.64±0.46 J/(mol K), respectively) and the thermodynamic properties of aluminosilicate melts determined previously were used to calculate the enthalpy of congruent melting of mullite, which is equal to 74.84±1.63 kJ/mol.

3.1.4. Na₂O-Al₂O₃

The Na₂O-Al₂O₃ system is of interest due to the high ionic conductivity of the well-known refractory phase, which is called beta alumina (β-Al₂O₃)³¹. The crystal structure of β-alumina is quite unusual and results in extreme mobility of the sodium ion. β-Alumina has the empirical formula Na₂O·11Al₂O₃ and in Ref.³² it was first believed to be an isomorph of Al₂O₃, since the presence of soda in the first specimens was either undetected or ignored. It is known today that the sodium ion in β-alumina can be replaced by many different ions using ion exchange from molten salts.

In this binary system there is another compound with the empirical formula $\text{Na}_2\text{O} \cdot 5\text{Al}_2\text{O}_3$ as well, designated as β'' -alumina, since it has a similar structure to β -alumina. This led to some confusion in the literature, when the different compounds were attributed to the same compound. Scholder and Mansman³³ reported that β -alumina did not exist at all. They were misled by their method of preparation, since the reaction between Na_2CO_3 and Al_2O_3 only leads to β'' -alumina and not to β -alumina below 1100 °C. The formation of β -alumina requires higher temperatures up to about 1500 °C. β'' -Alumina was reported and named by Yamaguchi³⁴. It has the formula $\text{Na}_2\text{O} \cdot 7\text{Al}_2\text{O}_3$ and appears to be very similar to β -alumina. There are no other literature references confirming the existence of this compound and it is probably β -alumina as well.

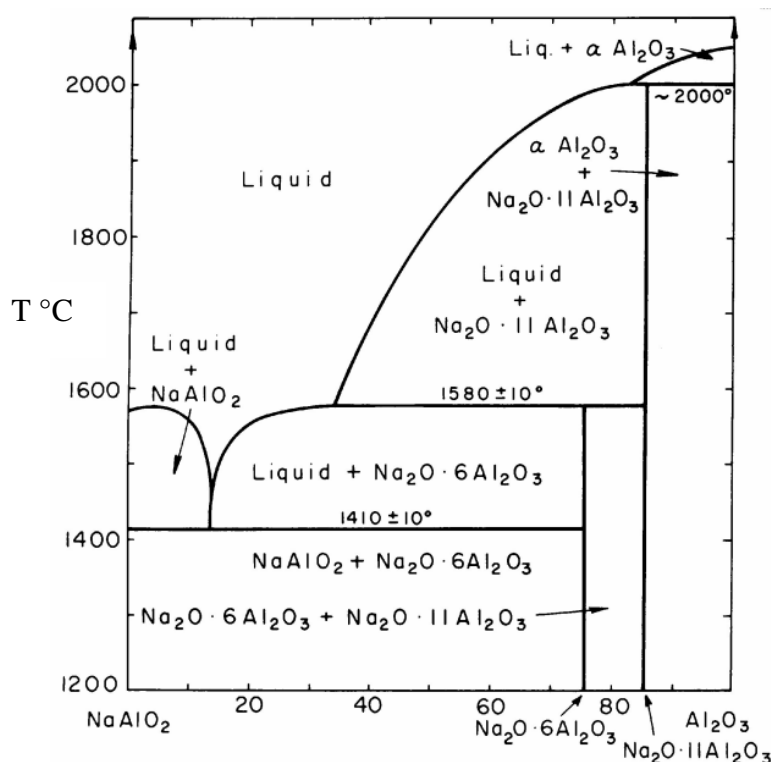


Fig. 8. Phase diagram for the NaAlO_2 - Al_2O_3 system reproduced from Rolin and Thanh³⁵

The phase diagram for the binary system Na_2O - Al_2O_3 was proposed by Rolin and Thanh³⁵. Then it was critically analysed by DeVrie and Roth³⁶ and modified by Weber and Venero³⁷. The diagram shown in **Fig. 8** was derived by Rolin and Thanh³⁵ from cooling curve data. The compound NaAlO_2 was reported to melt at 1582 °C. Rolin and Thanh also observed thermal arrests at 2003 °C, 1582 °C, and 1412 °C. These arrests were attributed to the incongruent melting of β -alumina, which they defined as $\text{NaAl}_{11}\text{O}_{17}$, the incongruent melting of β'' -alumina (defined as $\text{Na}_2\text{Al}_{12}\text{O}_{19}$ or $\text{Na}_2\text{O} \cdot 6\text{Al}_2\text{O}_3$), and the eutectic of β'' -alumina and NaAlO_2 , respectively. DeVrie and Roth³⁶ attributed the thermal effect at 1412 °C to a phase transformation of NaAlO_2 and proposed that an eutectic region occurs at 1582 °C.

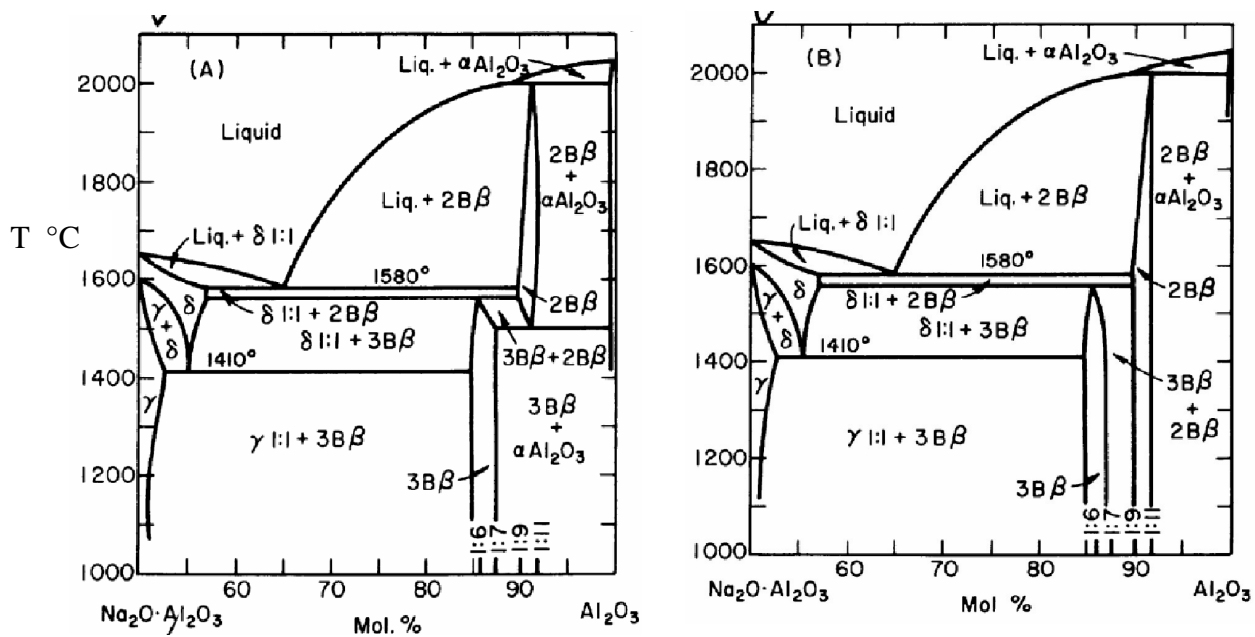


Fig. 9. $\text{NaAlO}_2\text{-Al}_2\text{O}_3$ phase diagrams proposed by DeVries and Roth³⁶

The phase diagrams revised by DeVrie and Roth³⁶ are presented in **Fig. 9**. They considered the cited literature data which result in the existence of at least two β -alumina-like phases. One can be represented as $\text{Na}_2\text{O} \cdot 11\text{Al}_2\text{O}_3$ (possibly 1:9) and the composition of the other lies in the range of 1:5 to 1:7. They are structurally characterised as consisting of 2- and 3-spinel blocks per unit cell, respectively. Each phase can exist over a composition range, but neither the extent of nonstoichiometry nor the extent of coexistence of the two type phases is known to date.

Fig. 9 shows two variants of the phase diagram. Variant A is the case when 2-blocks of β -alumina ($2B\beta$) are considered to be metastable below about 1500 °C. The other variant B is the case when $2B\beta$ is stable at all temperatures up to the incongruent melting point. In both cases an attempt was made to incorporate the cooling curve data of Rolin near the 1:1 region by assuming the existence of a new polymorph δ -phase which is stable at high temperature and over a rather broad composition range. At high alumina content this diagram (variant B) is not very different from that reported by Rolin and Thanh, except the nonstoichiometry indication of both phases.

The authors³⁶ concluded that β -alumina melts incongruently and that both phases β - and β'' -alumina are nonstoichiometric. The eutectic between β -alumina and NaAlO_2 is placed at about 1580 °C. The heat effect at 1410 °C is likely to be explained by a phase change in NaAlO_2 .

Ray and Subbarao³⁸ reported β'' -alumina decomposition at 1450 °C. This temperature differs from that reported by Rolin and Thanh³⁵ (1580 °C).

The eutectic temperature was obtained by Dzierich and Weber³⁹ as equal to 1595 °C. Weber and Venero³⁷ revised this temperature later and found that it has a value of 1585 °C. They also proposed a liquid composition of 65 mole % Al_2O_3 and a melting point of NaAlO_2 of 1867 °C, which is much higher than the values of 1582 °C and 1650 °C reported earlier by Rolin and Thanh³⁵ and Matignon⁴⁰, respectively, but this is in agreement with the value of 1850 °C previously estimated by Schairer and Bowen⁴¹. Losses of Na_2O due to volatilisation may be responsible for the lower reported values.

The data on β -alumina were revised by Kumer³¹ in terms of formation, stability, crystal structure and conductivity of the β -alumina. Three important points concerning the diagram are the follows:

- (1) The existence of a eutectic melt at 1585 °C between β -alumina and sodium aluminate that was confirmed in Ref. ³⁷
- (2) A higher soda content than that for the stoichiometry of β -alumina in the equilibrium diagram.
- (3) A lack of β'' -alumina having the formula $\text{Na}_2\text{O} \cdot 5\text{Al}_2\text{O}_3$ above 1585 °C.

The homogeneity range of β -alumina (nominally $\text{Na}_2\text{O} \cdot 11\text{Al}_2\text{O}_3$ for a perfect crystal structure) and β'' -alumina (nominally $\text{Na}_2\text{O} \cdot 6\text{Al}_2\text{O}_3$) was found by Jakob⁴² using electron probe microanalysis at 900 °C. The content of alumina varies from $\text{Na}_2\text{O} \cdot 8.1\text{Al}_2\text{O}_3$ to $\text{Na}_2\text{O} \cdot 9.5\text{Al}_2\text{O}_3$ in the former, and from $\text{Na}_2\text{O} \cdot 5.3\text{Al}_2\text{O}_3$ to $\text{Na}_2\text{O} \cdot 6.5\text{Al}_2\text{O}_3$ in the latter investigations.

3.1.5. $\text{K}_2\text{O}-\text{Al}_2\text{O}_3$

For the $\text{K}_2\text{O}-\text{Al}_2\text{O}_3$ system the phase diagrams were investigated only in the composition range from 0.5 to 1 mole percent Al_2O_3 , i.e. from pure KAlO_2 to Al_2O_3 . A phase diagram published by Roth⁴³ is shown in **Fig. 10**. The first melting of a sample held in an open crucible was found at 1910 °C, which was interpreted as an eutectic temperature. The eutectic composition was not determined exactly, but was estimated to be about 73 mole % Al_2O_3 . Samples of KAlO_2 heated in sealed Mo tubes were still solid at 2250 °C. However, an internal pressure increase caused tube rupture at nearly 2260 °C. This temperature was taken as an estimated melting point.

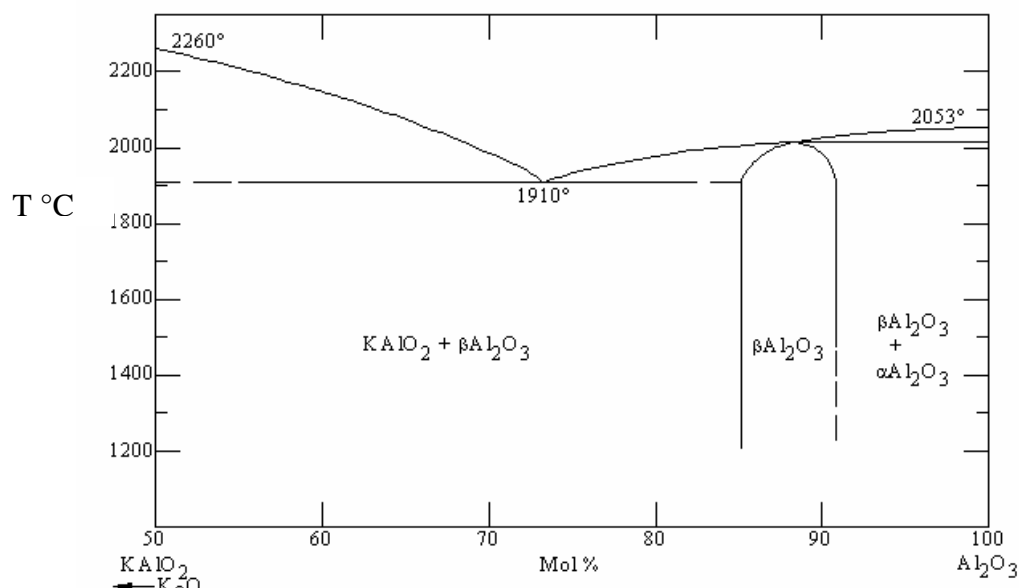


Fig. 10. Phase diagram of the system $K_2O-Al_2O_3$ according to Roth⁴³

The β -alumina phase was reported on the basis of thermogravimetric studies to have a range of stoichiometry from about $K_2O \cdot 5.7Al_2O_3$ to $K_2O \cdot 9Al_2O_3$ in the temperature interval between 1200 °C and 1600 °C⁴⁴. Neither β - nor β'' -alumina phases are believed to exist below 1000 °C. Both phases were often found to coexist in the temperature interval between 1000 and 1200 °C. β'' -Alumina is assumed to be a single phase at temperatures between 1050 °C and 1100 °C, but it is metastable.

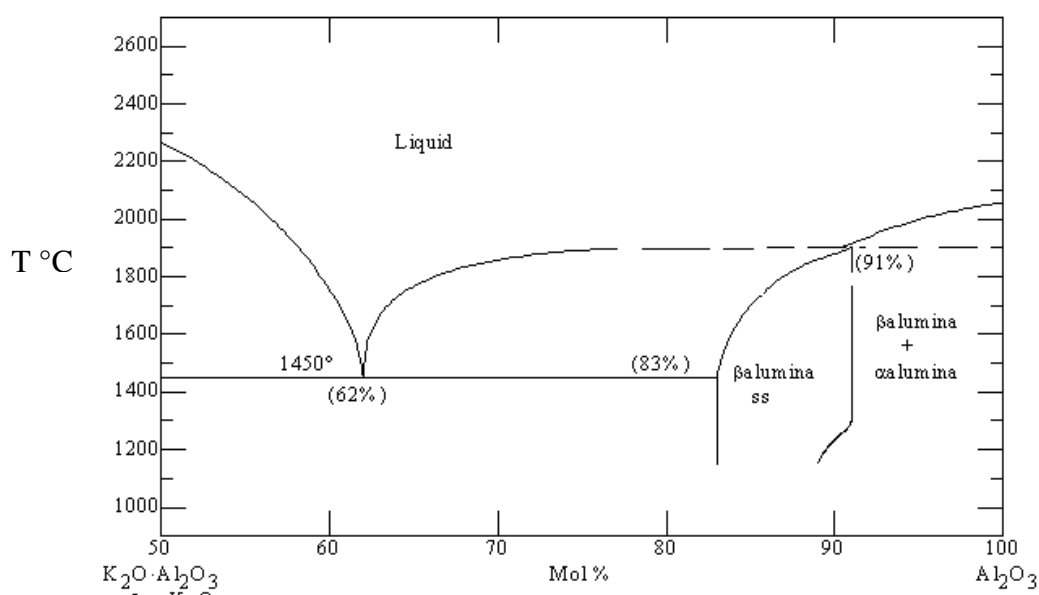


Fig. 11. Phase diagram of the system $KAIO_2-Al_2O_3$ reproduced from Moya⁴⁵

The diagram shown in **Fig. 11** was obtained by Moya et al.⁴⁵ by the use of DTA and X-ray diffraction measurements. The eutectic point was detected at 1450 °C. This is not confirmed by data obtained by Roth⁴³, who observed no sign of melting below 1910 °C. The homogeneity range of β -alumina is reported in Ref.⁴⁵ to be from about $\text{K}_2\text{O}\cdot 4.8\text{Al}_2\text{O}_3$ to $\text{K}_2\text{O}\cdot 10\text{Al}_2\text{O}_3$ near 1500 °C.

The discussion about the range of homogeneity of potassium β -alumina is like that regarding sodium β - and β'' -alumina. Na β - and β'' -alumina were considered by Jacob⁴² to have narrow ranges of stoichiometry close to the compositions $\text{NaAl}_9\text{O}_{14}$ and $\text{Na}_2\text{Al}_{12}\text{O}_{19}$, respectively. Potassium β - and β'' -alumina were therefore approximated as the stoichiometric compounds $\text{KAl}_9\text{O}_{14}$ and $\text{K}_2\text{Al}_{12}\text{O}_{19}$, respectively.

The temperatures of the ternary eutectics E_1 and E_2 were determined by quenching of previously crystallised preparations which were heated at the various appropriate temperatures and investigated by microscopy. These eutectic temperatures were found with an uncertainty of ± 10 °C, which was explained by the difficulty of recognising the first traces of glasses in the microscopic measurements.

The phase diagram of the quasi-binary K_2SiO_3 - Na_2SiO_3 system is shown in **Fig. 13(1)**. There is a simple eutectic between 43 mass percent K_2O , 15 Na_2O and 42 SiO_2 at 745 °C.

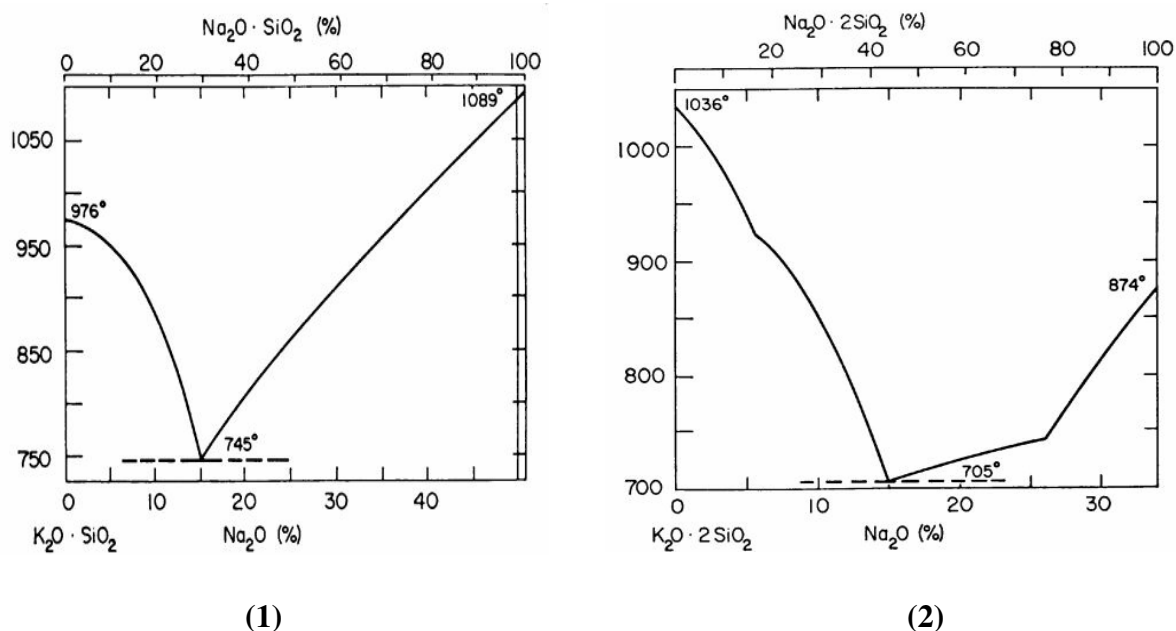


Fig. 13. Quasi-binary phase diagram reproduced from Kracek⁴⁶ for the alkali silicates: (1)- K_2SiO_3 - Na_2SiO_3 , (2) $K_2Si_2O_5$ - $Na_2Si_2O_5$

Fig. 13(2) shows the phase diagram of the alkali disilicates proposed by Kracek⁴⁶. The liquidus curves of both compounds exhibit breaks, at 920 °C for $K_2Si_2O_5$ and at 742 °C for $Na_2Si_2O_5$. Taking into account the phase relations in the binary systems Na_2O - SiO_2 ^{16,17,18} and K_2SiO_3 - SiO_2 ²³, corresponding breaks in the potassium system are encountered at 814 °C on the K_2O side and at 993 °C on the SiO_2 side of the $K_2Si_2O_5$ composition. In the sodium system, these heat effects were located at 706 °C on the Na_2O side, and at 768 °C on the SiO_2 side of the $Na_2Si_2O_5$ composition, below the liquidus temperature throughout.

Kracek⁴⁶ assumed that both $K_2Si_2O_5$ and $Na_2Si_2O_5$ enter into solid solutions with excess SiO_2 and excess K_2O and Na_2O , respectively. The different temperatures established are the unmixing temperatures of these solid solutions. The crystals are essentially the pure disilicates below the unmixing temperatures, as evidenced by the constancy of inversion temperatures, 596 °C for $K_2Si_2O_5$ I and $K_2Si_2O_5$ II, and 678 °C for $Na_2Si_2O_5$ I and $Na_2Si_2O_5$ II.

No possible compounds exist which might explain the presence of the breaks. The relations were summarised in Ref.⁴⁶ in the statement that both $\text{Na}_2\text{Si}_2\text{O}_5$ and $\text{K}_2\text{Si}_2\text{O}_5$ take up limited excess of SiO_2 , and Na_2O or K_2O , respectively, depending on the composition of the liquid from which they crystallise, in the compound-binary systems, and that $\text{K}_2\text{Si}_2\text{O}_5$ takes in a limited amount of Na_2O , while $\text{Na}_2\text{Si}_2\text{O}_5$ takes in a limited amount of K_2O in the ternary system.

3.2.2. $\text{Na}_2\text{O}-\text{Al}_2\text{O}_3-\text{SiO}_2$

The ternary system $\text{Na}_2\text{O}-\text{Al}_2\text{O}_3-\text{SiO}_2$ has been intensively investigated over many decades due to its fundamental importance for mineralogy, silicate ceramic, window glass, solid electrolytes and synthetic zeolites.

In the oxide system $\text{Na}_2\text{O}-\text{Al}_2\text{O}_3-\text{SiO}_2$ two ternary compounds exist at one atmosphere.

The compound with formula **NaAlSiO_4** can exist in two polymorphic forms, carnegieite and nepheline. The reversible inversion temperature is $1248\text{ }^\circ\text{C}$ ⁴⁷ for pure NaAlSiO_4 . This point was re-determined later as $1254\text{ }^\circ\text{C}$ in Ref.⁴⁸. This reconstructive high-temperature transformation of NaAlSiO_4 nepheline to carnegieite has been studied by light microscopy and X-ray precession photographs⁴⁹. The oriented transformation of nepheline to carnegieite is similar to that observed in the high-temperature transformation of tridymite to cristobalite. However, the transformation mechanisms were believed to be different. Thermally activated Na and weakening of the tetrahedral Al-O-bonds produce quickly migrating non-bridging O-atoms, which act as conversion nuclei, strongly accelerating the transformation process in comparison to SiO_2 .

NaAlSiO_4 melts congruently at $1526\text{ }^\circ\text{C}$ ^{47,48}. Pure carnegieite and its solid solution have not been found as natural minerals, but only as synthetic preparations. In contrast, nepheline has been found as a natural mineral.

Carnegieite can occur in high- and low-temperature forms as well. High carnegieite, stable at temperatures above $\approx 1250\text{ }^\circ\text{C}$, transforms to the low form by quenching below $667\pm 5\text{ }^\circ\text{C}$, for instance by immersing the crucible in a water bath⁵⁰. This form has cubic cristobalite structure with triclinic distortions.

The compound **$\text{NaAlSi}_3\text{O}_8$** is the well-known mineral soda feldspar or albite. This compound melts congruently at $1118\pm 3\text{ }^\circ\text{C}$ ⁴¹. The results of scanning calorimetric measurements⁵¹ on crystalline albite in the temperature range from 1027 to $1502\text{ }^\circ\text{C}$ confirmed that melting takes place during a $300\text{ }^\circ\text{C}$ temperature interval starting near the accepted equilibrium melting point of $1100\text{ }^\circ\text{C}$. The heat of fusion amounts to $70\text{ }230\text{ J/mol}$ after Stebbins et al.⁵².

In Ref.⁵³ congruent melting of albite was shown to be in the range from 1100 to $1120\text{ }^\circ\text{C}$. Melting rates are proportional to the amount of superheat and inversely proportional to the

viscosity of the melt phase. The melting point was determined to be approximately 1124 °C by extrapolating the normalised melting rate to zero melting.

A new speculation model for the melting of albite was proposed by Simakin⁵⁴. Albite was assumed to decompose into quartz and nepheline. These species were considered to represent a local medium range arrangement of the aluminosilicate network controlled by the interaction between sodium and aluminium ions. The stability of the albite feldspar-like complexes (4-membered rings) with a medium-sized sodium ion is lower than the corresponding potassium analogue (orthoclase).

The T (tetrahedral) sites in feldspar are arranged in linked four-membered rings and can be occupied by a perfect alternation of Al and Si atoms. The replacement of one-half of the Al by Si in albite leads to large entropy⁵⁵. The ordering phase transition temperature T_c for albite is $T_c \approx 2027\text{--}2227$ °C. The actual T_c for albite is complicated by the fact that the C2/m-C $\bar{1}$ transition is a combination of Al-Si ordering and lattice displacement. Analysis has shown that the displacive part of the transition first occurs on lowering the temperature from the disordered state, pulling the Al-Si ordering with it at lower temperatures, and that the latter would occur at 560 °C by itself.

A few natural pyroxenes consist largely of $\text{Na}_2\text{O} \cdot \text{Al}_2\text{O}_3 \cdot 4\text{SiO}_2$ or **NaAlSi₂O₆** (jadeite). Chemical study of many pyroxenes has indicated⁴¹ the presence of small amounts of jadeite $\text{Na}_2\text{O} \cdot \text{Al}_2\text{O}_3 \cdot 4\text{SiO}_2$ along with acmite ($\text{Na}_2\text{O} \cdot \text{Fe}_2\text{O}_3 \cdot 4\text{SiO}_2$), diopside ($\text{CaO} \cdot \text{MgO} \cdot 4\text{SiO}_2$) and other constituents in these complex solid solutions. Jadeite is not stable under atmospheric pressure.

Taylor and Brown⁵⁶ studied the distribution of short-range interatomic distances in NaAlSi₂O₆ and NaAlSiO₄ glass by X-ray radial distribution analysis. It was suggested that at one atmosphere the NaAlSi₂O₆ melt has a stuffed tridymite-like structure with Al in tetrahedral coordination rather than a pyroxene-like structure with Al in octahedral coordination. The radial distribution function of NaAlSiO₄ glass is also consistent with a stuffed tridymite-like structure similar to that of crystalline nepheline. Replacement of SiO₂ by NaAlO₂ across the SiO₂-NaAlSiO₄ join causes a progressive expansion of the stuffed tridymite structure. The stuffed tridymite model is consistent with the observed densities of glasses along the SiO₂-NaAlSiO₄ join and offers a molecular interpretation of the high viscosity of melts in the Na₂O-Al₂O₃-SiO₂ system at Na/Al ratios of 1.0.

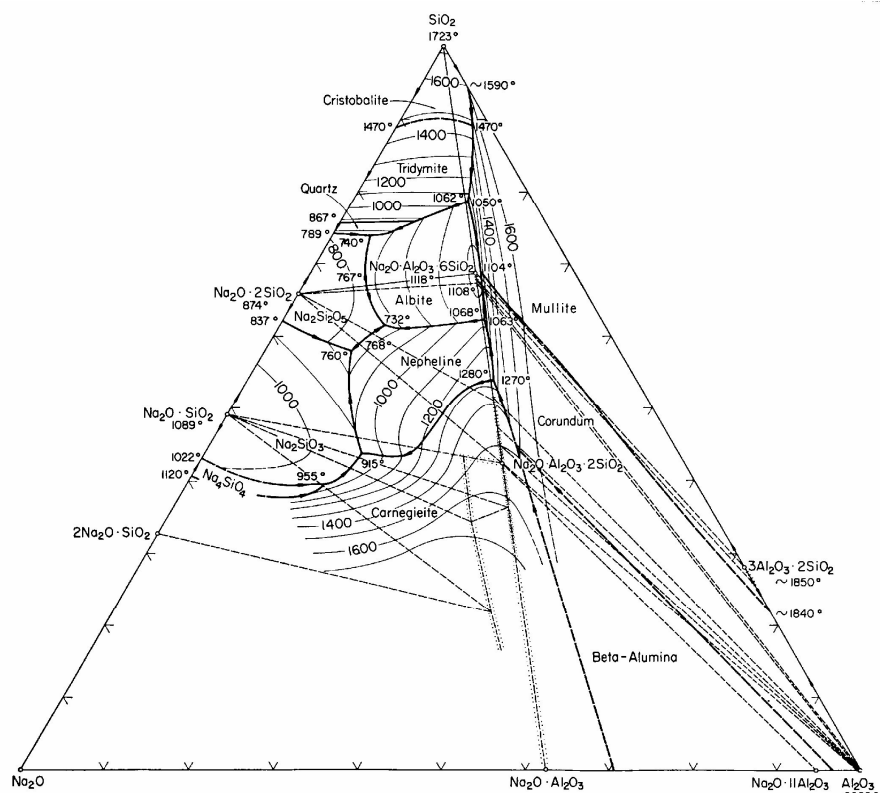


Fig. 14. Phase equilibrium diagram of the system $\text{Na}_2\text{O}-\text{Al}_2\text{O}_3-\text{SiO}_2$ with fields of the primary crystalline phases, isotherms and temperatures of binary and ternary invariant points after Schairer and Bowen⁴¹

Systematic study of the phase relations of the quasi-binary system in the $\text{Na}_2\text{O}-\text{Al}_2\text{O}_3-\text{SiO}_2$ system was performed by Schairer and Bowen⁴¹. Results of quenching experiments at temperatures between the liquid and that of complete crystallisation were reported for 340 synthetic compositions. These located the liquidus surfaces and the fields of the primary phases: cristobalite, tridymite, quartz, mullite $\text{Al}_6\text{Si}_2\text{O}_{13}$, corundum Al_2O_3 , albite $\text{NaAlSi}_3\text{O}_8$, nepheline $\text{NaAlSi}_3\text{O}_8$, carnegieite, sodium disilicate $\text{Na}_2\text{Si}_2\text{O}_5$, sodium metasilicate Na_2SiO_3 and sodium orthosilicate Na_4SiO_4 . Some of these solid phases are of variable composition because of solid solution. The equilibrium diagram for this ternary system is given in **Fig. 14**. The six quasi-binary subsystems were considered in Ref.⁴¹.

In the system **albite - silica** the eutectic point was detected at 1062 °C. All glasses in this system are extremely viscous. Periods of many months were required to obtain any crystallisation in these dry melts.

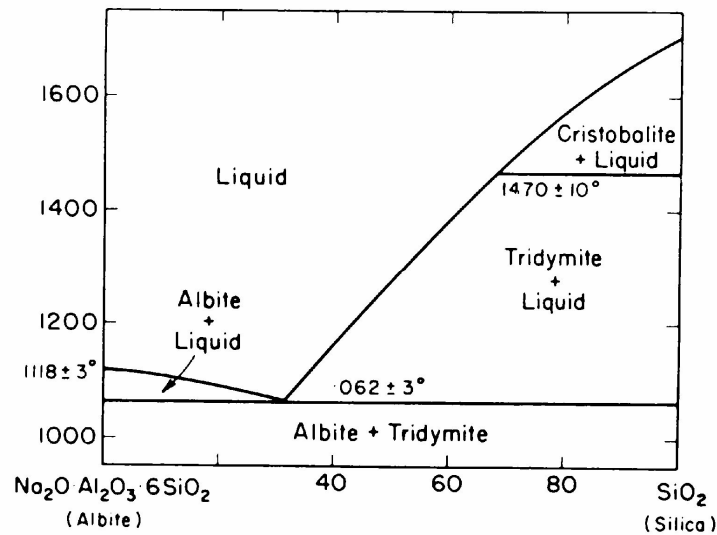


Fig. 15. Equilibrium diagram of the binary system albite-silica after Schairer, Bowen⁴¹

The phase diagram of the albite-silica system is given in **Fig. 15**. The temperatures of the eutectic and the inversion of cristobalite to tridymite are 1065°C and 1470°C , respectively.

The phase diagram of the system **carnegieite/nepheline - albite** is reproduced in **Fig. 16**. The system was studied in Ref.⁴⁸. Both nepheline and carnegieite take up limited amounts of albite in solid solution. The inversion temperature rises to about 1280°C .

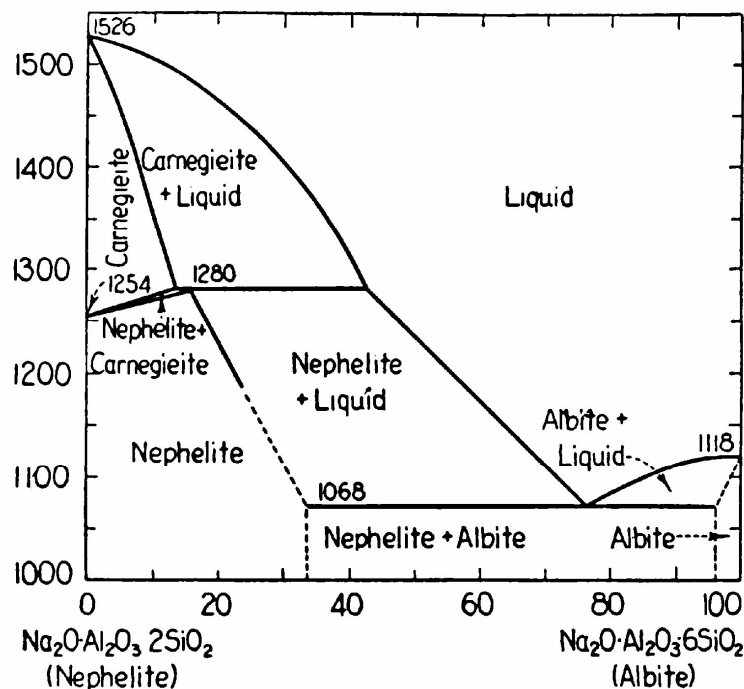


Fig. 16. Equilibrium diagram of the binary system NaAlSiO_4 - $\text{NaAlSi}_3\text{O}_8$ after Greig and Barth⁴⁸

The data for the **carnegieite - sodium aluminate** NaAlO_2 obtained by Schairer and Bowen⁴¹ were considered only as an approximation. A small loss of soda by volatilisation during the preparation of these compositions was observed.

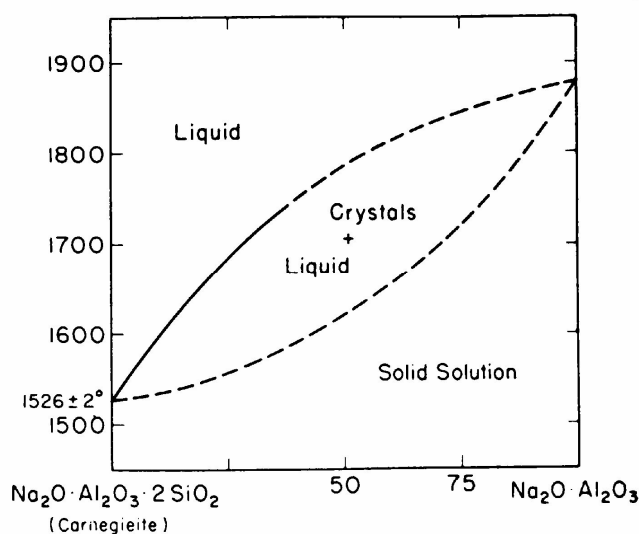


Fig. 17. Probable phase relations in the binary system NaAlSiO_4 (carnegieite)- NaAlO_2 after Schairer and Bowen⁴¹

The liquidus line could rise from 1526 °C at pure carnegieite to an estimated temperature of 1850±30 °C at $\text{Na}_2\text{O} \cdot \text{Al}_2\text{O}_3$. One observation obtained by Matignon⁴⁰ was not in agreement with that. He found the melting point of $\text{Na}_2\text{O} \cdot \text{Al}_2\text{O}_3$ at 1650 °C. This was not confirmed by Brownmiller and Bogue⁵⁷, who heated a homogeneous solid phase of the composition $\text{Na}_2\text{O} \cdot \text{Al}_2\text{O}_3$ to 1650 °C (the upper limit of the furnaces available to them) and found no melting or dissociation up to that temperature.

The phase diagram given in **Fig. 17** implies a continuous solid solution extending between sodium aluminate and carnegieite. Both of these phases have β -cristobalite-related structures. A new attempt to study the sodium aluminate-carnegieite system ($\text{Na}_{2-x}\text{Al}_{2-x}\text{Si}_x\text{O}_4$, $0 \leq x \leq 1$) in detail was made by Thompson et al.^{58,59}. They studied this system by XRD and the electron diffraction method in the temperature range from 800 to 1300 °C. The materials were prepared by gel synthesis followed by solid state reaction in air. The five new phases at intermediate compositions have β -cristobalite-related structures as well, so in one sense Schairer and Bowen⁴¹ were right.

All of the new phases can be described as modulated variants of an underlying β -cristobalite parent structure. At $x \approx 0.05$ the γ - NaAlO_2 -type structure is stabilised to room temperature; at $x \approx 0.2$ -0.45 an orthorhombic KGaO_2 -type structure is obtained, except at $x \approx 0.35$ where a new tetragonal phase is observed; at $x \approx 0.5$ -0.6 a new cubic phase is obtained; at $x \approx 0.7$ -0.9 a new orthorhombic phase is determined.

Thompson et al.⁵⁸ admitted that the proposed phase diagram is incomplete since equilibrium is only slowly reached, particularly toward the carnegieite composition. Furthermore, it only describes the phase relationships of specimens quenched to room temperature from 1300 °C. It is quite possible that reversible non-reconstructive phase transitions occur for the intermediate phases in the same way that they occur for the end members, i.e. $\gamma \rightarrow \beta$ -NaAlO₂, high \rightarrow low-carnegieite, and only low-temperature structures were observed. This work represents progress in solving and refining the structures of all five new phases from XRD data using the Rietveld method and starting from a modulation wave approach to the description of these phases⁵⁹.

The next quasi-binary phase diagram of **sodium disilicate - albite** system is depicted in **Fig. 18**. The eutectic temperature is 767 °C.

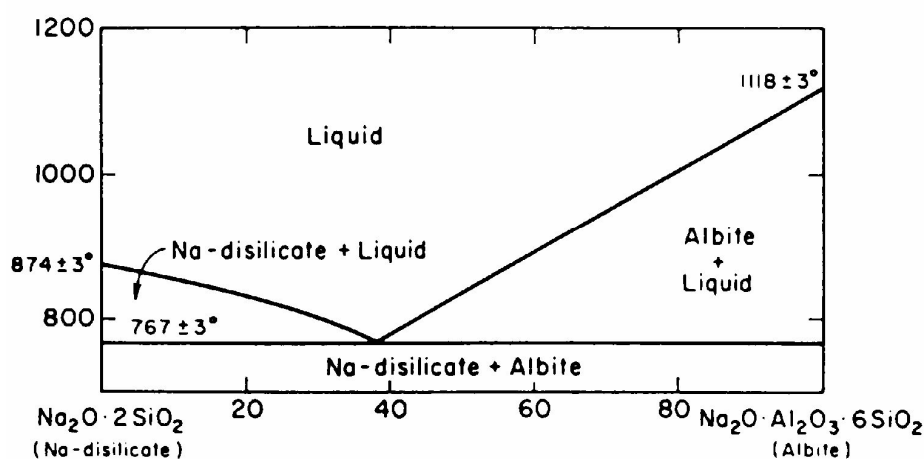


Fig. 18. Equilibrium diagram of the binary system sodium disilicate-albite after Schairer and Bowen⁴¹

All the compositions studied in the system **albite-corundum** (**Fig. 19**) were viscous and difficult to crystallise. The binary eutectic between albite and corundum was estimated at 1108±3 °C from quenching runs of several months duration.

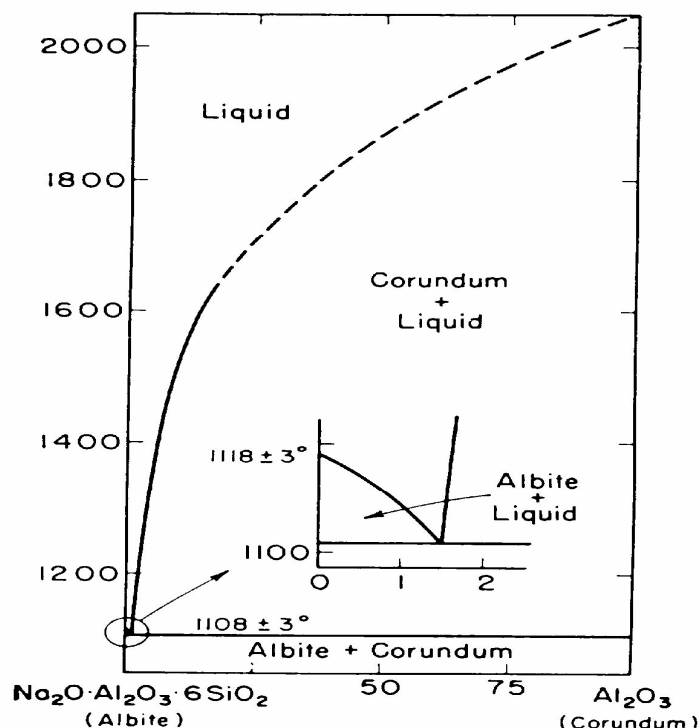


Fig. 19. Equilibrium diagram of the binary system albite-corundum after Schairer and Bowen⁴¹

The phase relations between **sodium disilicate** and **carnegieite/nepheline** are presented in Fig. 20.

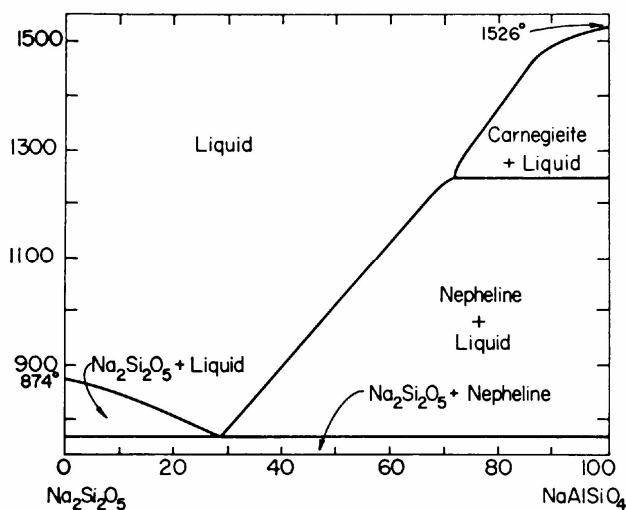


Fig. 20. Equilibrium diagram of the binary system $\text{Na}_2\text{Si}_2\text{O}_5$ (sodium disilicate)- NaAlSiO_4 (nepheline, carnegieite) after Tilley⁶⁰

The phase diagram for the system **carnegieite-corundum** is presented in Fig. 21 according to the data from Ref.⁴¹. Owing to the presence of some $\beta\text{-Al}_2\text{O}_3$ in all the crystallised glasses of compositions studied in this system, it was difficult to estimate the

temperature of the binary eutectic between carnegieite and corundum precisely. This eutectic is found at 1475 °C from the quenching data.

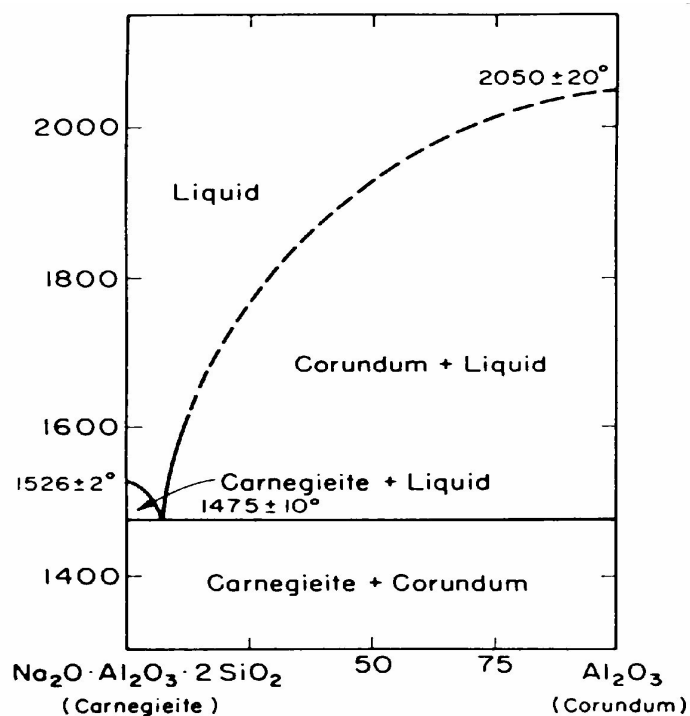


Fig. 21. Phase diagram of the system carnegieite-corundum taken from Ref. ⁴¹

The phase diagram for the system **sodium metasilicate- NaAlSiO_4** given in **Fig. 22** was studied in Ref.⁶⁰. Carnegieite NaAlSiO_4 is considered to contain up to 24 percent of sodium metasilicate Na_2SiO_3 in solid solution, while there is little or no solid solution of sodium metasilicate in nepheline. The inversion temperature is lowered from about 1248 °C in pure NaAlSiO_4 to 1163 °C. The eutectic between sodium metasilicate and nepheline is located at 906 °C. Spivak⁶¹ determined this eutectic point as at 900 ± 2 °C.

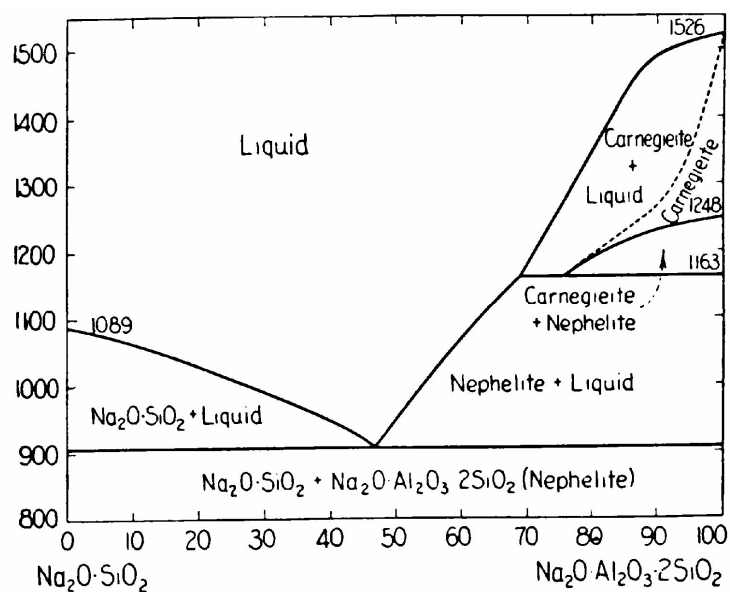


Fig. 22. Equilibrium diagram of the binary system Na₂SiO₃ (sodium metasilicate)-NaAlSiO₄ (nepheline, carnegieite) after Tilley⁶⁰

4. Optimisation routine

The object of the investigation is the complex oxide system containing silica and alumina as main slag constituents and alkali oxides (sodium and potassium). The liquid phase of such a type having strong interactions between components can be described by two suitable approaches: (1) the modified quasichemical model and (2) modified associate species model. In the present work, the modified associate species model was chosen since it allows an adequate representation of the thermodynamic properties, for instance, phase relations, in more extended concentration ranges for many oxide systems. Furthermore, this model is considered to be simpler for the presentation of the phase diagram and more easily modified.

The database based on the associate species model was created and developed by Besmann, Spear et al.^{7,8}. The basic thermodynamic functions involving the pure solid and liquid compounds are different from those given in the FACT database, which is considered as the primary database for the whole system. It would be necessary to incorporate the associate species model into the FACT database with a simultaneous adjustment of the solution data to describe the thermodynamic properties of the considered systems.

For this propose, the end binary and ternary systems have to be investigated in terms of thermodynamic description of the solution phase using the modified associate species model. The new model parameters for each subsystem can be found by the use of the optimisation procedure given in Chapter 2.3.4.

The optimisation procedure is performed using the **Optimisation Module** incorporated in the ChemSage computer program. The selected adjustable parameters are optimised according to the experimental data. The primary data are the phase diagram data for the systems considered and the available measured alkali activities as well. All available data have to be collected, and critically analysed to select the most reliable data.

A thermochemical data file consists of the thermodynamic functions for all phases which may exist in the system. These phases are the solid compounds and the liquid solution (slag). The data for pure solid compounds were taken from the FACT database and presented as shown in Chapter 2.3.1. They contain the standard formation enthalpy ΔH_f° , standard entropy S° and the heat capacity as a function of temperature.

The liquid slag is considered as a solution containing the pure liquid oxides, the congruent melting compounds and the appropriate species as well. The possible interactions between components are responsible for the non-ideality of the slag solution. According to this approach, the Gibbs energy of the solution is expressed as an equation in the form of the sum of its ideal part and its excess part

$$G_m = \sum x_i G_i^0 + RT \sum x_i \ln x_i + \sum_{i < j} \sum_v x_i x_j L_{ij}^{(v)} (x_i - x_j)^v, \quad (44)$$

where $L_{ij}^{(v)}$ is an interaction coefficient between corresponding i-th and j-th constituents, expressed as a Redlich-Kister polynomial (Eq.13).

Applied to the considered system, only the two first terms regarding temperature ($A_{ij}^{(v)}$ and $B_{ij}^{(v)}$) and composition (value of v may accept only the value 0 or 1) are taken into account. Thus, for each pair of species 1 and 2 interaction parameters are determined as

$$\begin{aligned} L_{12}^{(0)} &= A_{12}^{(0)} + B_{12}^{(0)}T \\ L_{12}^{(1)} &= A_{12}^{(1)} + B_{12}^{(1)}T \end{aligned} \quad (45)$$

The thermodynamic data for the pure solid and liquid compounds taken from FACT were kept as constants over the optimisation procedure. In order to represent the thermodynamic relations of the system as exactly as possible using the associate species approach, the following parameters were chosen to be adjustable:

- 1) standard formation enthalpies $\Delta H_{298,f}^0$ and entropies S_{298}^0 of the considered associate species,
- 2) the interaction parameters between solution constituents $L_{12}^{(v)}$, expressed by Redlich-Kister coefficients.

These parameters had to be optimised in order to obtain a satisfactory representation of the thermodynamic properties.

The parameter optimisation was carried out interactively by selecting the experimental data. Then initial estimates of the parameters and their standard deviations are entered. During the optimisation each experimental data point (composition and temperature) was given a certain weight by assigning an error to it. This weight is chosen by personal judgement and changed by trial and error in order to get the most acceptable result. For example, the temperature of the liquidus at a certain composition may be given within the error range of ± 10 K. If the melting point of a compound is known, it can be weighted heavily by giving it a small error. The adjustable parameters were allowed to be varied within their uncertainty limits during the optimisation, thus ensuring that reasonable values were considered.

As a first step of the optimisation, attempts are made to determine the standard formation enthalpies and entropies of species in order to obtain preliminary melting points of the compounds. During this step the interaction parameters remain untouched. Then, the adjustable solution interaction parameters are simultaneously fitted with respect to the experimental phase relation in the system under consideration.

The number of iterations with which the algorithm was carried out could also be specified for each optimisation process on request. After execution of the optimisation the new thermodynamic properties for the solution species and the set of interaction parameters are obtained as a result. This set of data was moved into the **Solution Model** of the FactSage

program, which allows a new user database to be created based on the associate species approach. Using this database the calculation of phase diagrams, for example, could be performed by **Equlib** and **Phase Diagram** modules of the ChemSage or FactSage programs, and the estimated phase diagrams were compared with experimental points until a proper convergence was obtained.

5. Results

5.1. Binary systems

5.1.1. $\text{Na}_2\text{O-SiO}_2$

The first system treated consists of sodium oxide and silica. One of the features of this system is the absence of reliable data involving the phase relation in the concentration range between pure Na_2O and sodium orthosilicate Na_4SiO_4 as mentioned in Chapter 3.1.1.

Analysis of the experimental data

The assessment is mainly based on the phase diagram data reported in Refs. ^{16,17,18}. The experimental points used for the optimisation procedure are presented in **Table A.1**.

The sodium orthosilicate Na_4SiO_4 is considered to melt congruently at a temperature of 1078 °C according to data from Loeffler²¹, otherwise it would not be adjusted with the accepted melting point of Na_2O as 1132 °C. The phase relations in the composition range between pure sodium oxide and Na_4SiO_4 were proposed by the authors⁶², who applied the modified associate species model taking into account the polymerisation⁶³ of silica

Regarding the phase relations in the Na_2O -rich region, it was suggested that a simple eutectic exists at 0.18 mole percent silica and 920 °C or at 0.267 mole percent silica and 930 °C as reported in Ref.⁶². The latter values were accepted for the optimisation.

The phase diagram data related to $\text{Na}_6\text{Si}_2\text{O}_7$, Na_2SiO_3 and $\text{Na}_2\text{Si}_2\text{O}_5$ were extracted from Refs. ^{16, 17, 18, 21}.

In order to determine the improved database by optimisation, the available Na_2O activity data were also considered. Activities of Na_2O in the liquid are reported by several researchers, who used different methods: Knudsen cell mass spectrometry⁶², EMF measurements in reversible concentration cells^{64, 65, 66, 67, 68, 69} and ionic-molecular equilibrium studies⁷⁰, mixed-phase equilibrium study⁷¹. Except from the data of Froberg⁶⁵, which show different temperature dependence, the data are generally in good agreement. Pure liquid sodium oxide is accepted as a reference state.

Modelling of the liquid phase in the $\text{Na}_2\text{O-SiO}_2$ system

To describe the phase relation in this system for the liquid phase the modified associate species model is applied. The slag in equilibrium with solids is considered as a real solution which consists of pure liquid oxides $\text{Na}_2\text{O}(\text{liq})$, $\text{SiO}_2(\text{liq})$, and so-called associate species. Their composition corresponds to that of some compounds present in the system $\text{Na}_2\text{O-SiO}_2$. These associate species are orthosilicate $\text{Na}_4\text{SiO}_4 \cdot 2/5(\text{liq})$ or $\text{Na}_{1.6}\text{Si}_{0.4}\text{O}_{1.6}(\text{liq})$, metasilicate $\text{Na}_2\text{SiO}_3 \cdot 2/3(\text{liq})$ or $\text{Na}_{1.333}\text{Si}_{0.667}\text{O}_2(\text{liq})$, and disilicate $\text{Na}_2\text{Si}_2\text{O}_5 \cdot 1/2(\text{liq})$ or

NaSiO_{2.5}(liq). All corresponding solid compounds melt congruently. Solution species stoichiometries are explained by empirical requirements according to the associate species approach to represent the phase relations and other thermodynamic properties in the considered system. Each species must have two non-oxygen atoms per mole of the species.

The thermodynamic data for the chosen species, taken from Ref.⁹, differ from those included in the FACT database accepted in this work as the main database. Therefore, the standard formation enthalpies and entropies were to be optimised to represent the phase relations in this system. Moreover, these data must be adjusted with the general FACT database for solid, pure liquid and gaseous phases. Thermodynamic data for pure liquid compounds (FACT database) were used as initial values of the thermodynamic functions for the oxide species in the Na₂O-SiO₂ system, taking into account the stoichiometry required by the modified associate species approach. These data had to be optimised using the **Optimisation** module of the ChemSage program from the beginning in order to obtain accurate values for the melting points of binary compounds. The new thermodynamic functions obtained for the chosen species are given in **Table 1** in comparison with the initial data from the FACT database.

Table 1. Liquid species data for the Na₂O-SiO₂ system

Species	Database	ΔH_f^{298} , J/mol	S^{298} , J/(mol•K)
Na ₄ SiO ₄ ·2/5	FACT	-803 075.52	105.9
	New database	-804 302.46	104.9
Na ₂ SiO ₃ ·2/3	FACT	-1 000 834.0	103.95
	New database	-1 009 578.2	93.25
Na ₂ Si ₂ O ₅ ·1/2	FACT	-1 218 003.6	97.06
	New database	-1 218 812.7	93.19

According to the associate species model the deviation of the associate solution from ideal behaviour can be taken into account by a consideration of the interactions between the associate species. The interaction parameter between Na₂Si₂O₅·1/2(liq) and Si₂O₄(liq) introduced by Spear in Ref.⁹ allows thermodynamic properties of the liquid to be represented in the composition range in which a metastable immiscibility gap has been reported for glass phases in the Na₂O (or K₂O)-SiO₂ system. In contrast to this, in this work an attempt was made to add other interactions between the available associate species. The choice of suitable parameters, which could be important for representing the phase diagram, and their adjustment were carried out by trial and error.

The Gibbs energy of the solution according to this approach is given by Eq. (44), expressed as the sum of the ideal part in the total Gibbs energy and the excess Gibbs energy, including the Redlich-Kister polynomial as Eq.(45).

Usually the interaction parameter is responsible for the phase relations between the corresponding compounds. **Fig. 23** gives an example of the associate species distribution depending on the mixture composition at a given temperature. One can see what kind of species prevails in each region of the phase diagram. For instance, if the phase equilibria near the supposed eutectic between $\text{Na}_6\text{Si}_2\text{O}_7$ and Na_2SiO_3 (this composition is shown by the straight line) are considered, then one can assume that the interaction parameter between the nearest associate species, $\text{Na}_4\text{SiO}_4 \cdot 2/5(\text{liq})$ and $\text{Na}_2\text{SiO}_3 \cdot 2/3(\text{liq})$, will determine this eutectic equilibrium.

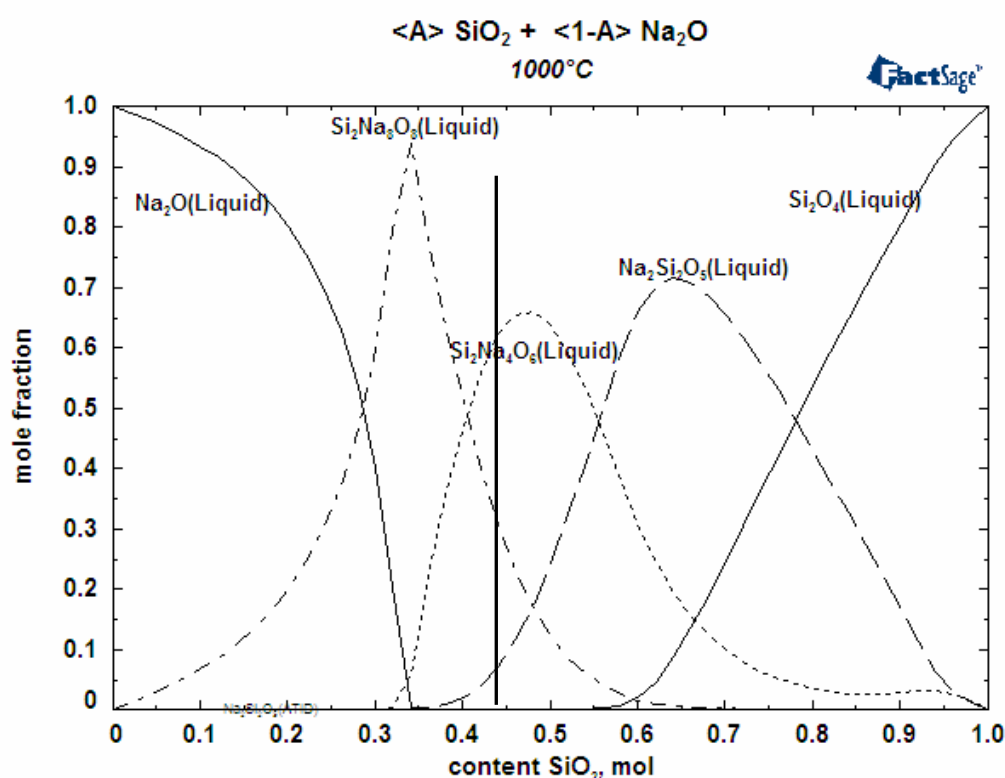


Fig. 23. Composition distribution of associate species depending on the silica content in the melt $\text{Na}_2\text{O}-\text{SiO}_2$ at 1000°C . The calculation is performed using the associate species model and the new database for the slag

The interaction parameters between different species are presented in **Table 2**. They are found to achieve the correct representation of the phase relations in the oxide system considered.

Table 2. Improved interaction parameters for the system Na₂O-SiO₂

Species 1	Species 2	A_{12}^0	B_{12}^0	A_{12}^1	B_{12}^1
Na ₂ O	Na ₄ SiO ₄ ·2/5	6 643	0	0	0
Na ₄ SiO ₄ ·2/5	Na ₂ SiO ₃ ·2/3	48.6	0	-66.4	0
Na ₂ SiO ₃ ·2/3	Na ₂ Si ₂ O ₅ ·1/2	164.6	0	-110.9	0
Si ₂ O ₄	Na ₂ Si ₂ O ₅ ·1/2	49 334	-34	-19 954	-6.5

All obtained parameters for the species and the interactions between them are entered by the **Solution** module of FactSage as a new improved database for the liquid.

Comparison with previous solution descriptions

The phase diagrams calculated using different solution models and databases are compared in **Fig. 24**. The solid line depicts the optimised phase diagram according to the modified quasichemical approach (FACT database), where the excess Gibbs energy of the liquid phase was estimated through a model parameter, depending on composition and temperature given in Ref.⁷².

$$\begin{aligned}\omega &= -114345 - 381598Y_{\text{SiO}_2} + 123010Y_{\text{SiO}_2}^7, \text{J/mol} \\ \eta &= -43.932 - 20.920Y_{\text{SiO}_2}^7, \text{J/(mol} \cdot \text{K)}\end{aligned}\quad (46)$$

In the composition range from Na₄SiO₄ to silica the phase diagram is reproduced very well.

Near the melting point of SiO₂, the calculated liquidus does not agree well with the experimental points of Kracek¹⁷. Wu et al.⁷² supposed that Na₂O dissociates in a solution into two independent Na⁺ ions. It can be argued that in solutions which are very rich in SiO₂, sodium ions actually form Na₂²⁺ groupings around “broken oxygen bridges” (Si-O⁻-O-Si). This would give a limiting liquidus slope at pure SiO₂ of one-half of the calculated value, thereby giving a liquidus closer to Kracek’s points. On the other hand, measurements at very high temperatures in very viscous liquids are difficult. Vaporisation of Na₂O during the experiments shifts the liquidus to higher temperatures. It was supposed by Wu et al.⁷² that there is some solubility of Na₂O in solid SiO₂.

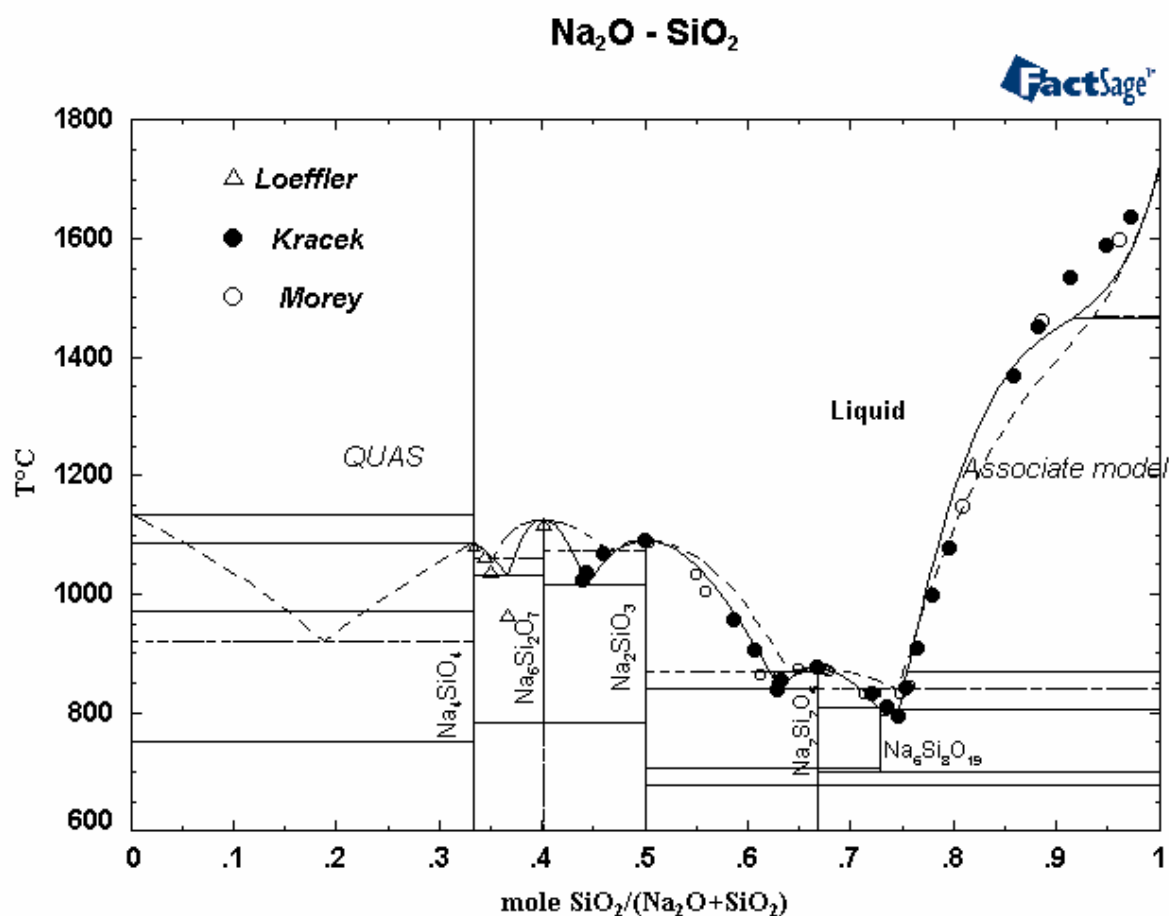


Fig. 24. Comparison of experimental phase equilibrium data with calculations performed using different thermodynamic data and different solution models

The phase diagram reproduced by the dotted line in **Fig. 24** corresponds to calculations using the modified associate species model. In the Na_2O - SiO_2 binary system, described in Ref.⁹, the liquid is composed of the liquid species $\text{Na}_2\text{O}(\text{liq})$, $\text{Na}_4\text{SiO}_4 \cdot 2/5(\text{liq})$, $\text{Na}_2\text{SiO}_3 \cdot 2/3(\text{liq})$, $\text{Na}_2\text{Si}_2\text{O}_5 \cdot 1/2(\text{liq})$, and $\text{Si}_2\text{O}_4(\text{liq})$. Only one pair of parameters between $\text{Na}_2\text{Si}_2\text{O}_5 \cdot 1/2(\text{liq})$, and $\text{Si}_2\text{O}_4(\text{liq})$ was taken into account. These lines demonstrate the noticeable divergences at high silica content, but the main equilibria are reproduced quite well in principle.

The calculated phase diagram using the associate species model with new interaction parameters compatible with the FACT database is presented in comparison with the experimental points in **Fig. 25**. One point from Loeffler²¹ lying below the eutectic between sodium orthosilicate and $\text{Na}_6\text{Si}_2\text{O}_7$ is not taken into account because it disagrees with other data. A good agreement with the experimental points is observed with the exception of the phase relations at high silica content. In contrast to the quasichemical model, the calculation using the modified associate species approach is able to describe the phase relations in the Na_2O -rich region by keeping an acceptable agreement with the experimental points.

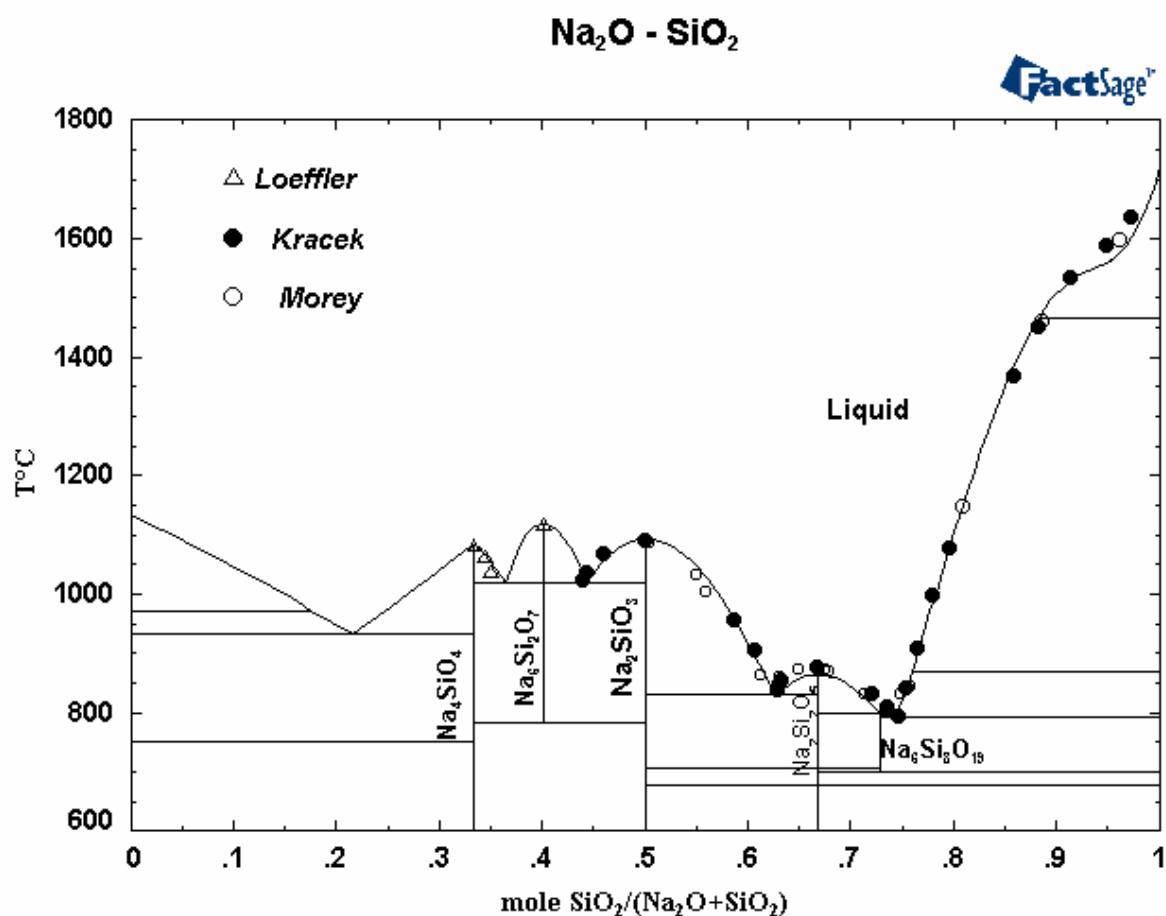


Fig. 25. Phase diagram of the Na₂O-SiO₂ system calculated using the new optimised database

The new improved data set can be also used for the calculation of the activity of sodium oxide. The available experimental data were used to optimise the solution parameters in this system. After that they could be compared with the calculated data estimated according to the model. **Fig. 26** shows a comparison of the experimental activity data obtained by different authors with calculated values. The calculations were carried out using the different solution approaches and database as well. A quite good agreement of the calculation performed using the optimised data set with experimental data is observed.

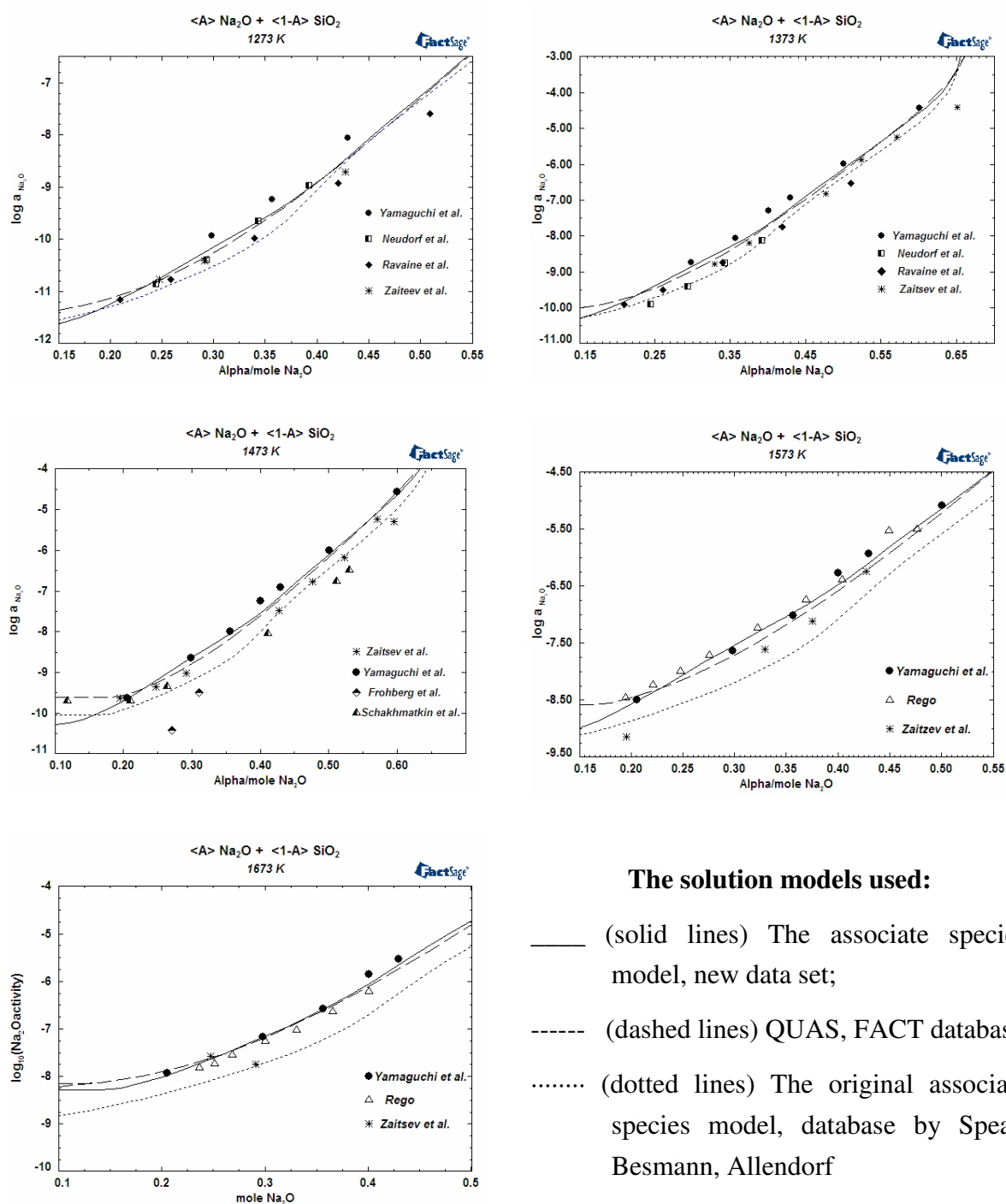


Fig. 26. Na₂O activity in the Na₂O-SiO₂ melt at different temperatures: comparison of experimental data with the calculated values. Reference state – pure liquid Na₂O. The calculations are performed using the different solution approach and databases

5.1.2. K_2O-SiO_2

The next system considered containing potassium oxide and silica reveals similar behaviour to the Na_2O-SiO_2 system. The equilibrium diagram in the composition range from potassium metasilicate K_2SiO_3 to silica was measured by Kracek²³ by quenching techniques. Melting points of potassium metasilicate K_2SiO_3 , disilicate $K_2Si_2O_5$ and tetrasilicate $K_2Si_4O_9$ were reported as 976 °C, 1045 °C and 770 °C, respectively. Further, three eutectic equilibria are considered, which are located as follows: the eutectics between K_2SiO_3 and $K_2Si_2O_5$ at 0.566 mole percent of silica and 781 °C, between $K_2Si_2O_5$ and $K_2Si_4O_9$ at 0.773 mole percent of silica and 743 °C, and the last eutectic between $K_2Si_4O_9$ and quartz at 0.81 mole silica and 770 °C. All these measured points are used to estimate the data in this system as well as some experimental K_2O activities in the K_2O-SiO_2 melts.

Modelling of the liquid phase in the K_2O-SiO_2 system

The liquid solution in this system according to the modified associate species model⁹ is represented as a solution which consists of pure liquid potassium oxide and silica and associate species, whose compositions correspond to those of congruently melting compounds. They can be written as $K_2SiO_3 \cdot 2/3(liq)$, $K_2Si_2O_5 \cdot 1/2(liq)$ and $K_2Si_4O_9 \cdot 1/3(liq)$ taking into account the required stoichiometry to provide the presence of two non-oxygen atoms in their formulas.

In order to obtain the improved data for the liquid phase in this system the standard formation enthalpies and entropies taken from the FACT database were used as starting data in the optimisation procedure. These values are mostly adjusted to provide the melting points of the binary compounds. The initial and estimated thermodynamic values of the species used are presented in **Table 3**.

Table 3. Liquid species data for the K_2O-SiO_2 system

Species	Database	ΔH_f^{298} , J/mol	S^{298} , J/(mol•K)
$K_2SiO_3 \cdot 2/3$	FACT	-1 030 315.9	105.37
	New database	-1 012 800	119.31
$K_2Si_2O_5 \cdot 1/2$	FACT	-1 235 700.7	111.49
	New database	-1 248 200.0	95.09
$K_2Si_4O_9 \cdot 1/3$	FACT	-1 433 642.2	100.79
	New database	-1 431 900.0	89.72

To represent the phase equilibria over the whole composition range the interactions among the associate species were considered. Their adjustment for standard formation enthalpies and standard entropies was realised using the **Optimisation** module of ChemSage. All available experimental data were collected and used to get a new data set which can provide satisfactory agreement with experimental data that permit the prediction of the thermodynamic behaviour of this system. The new interaction parameters are presented in **Table 4**.

Table 4. Improved interaction parameters for the liquid phase in the system K₂O-SiO₂

Species 1	Species 2	A_{12}^0	B_{12}^0	A_{12}^1	B_{12}^1
K ₂ O	K ₂ SiO ₃ ·2/3	3 484	0	0	0
K ₂ SiO ₃ ·2/3	K ₂ Si ₂ O ₅ ·1/2	-9 376.6	8	200	0
K ₂ Si ₂ O ₅ ·1/2	K ₂ Si ₄ O ₉ ·1/3	-1 041.9	-16.9	-2 595	-4.3
K ₂ Si ₄ O ₉ ·1/3	Si ₂ O ₄	560.1	0	10 046	7.6

Comparison of different approaches applicable to the K₂O-SiO₂ liquid

For the liquid solution in this system, the following quasi-chemical parameters were obtained⁷²:

$$\begin{aligned}\omega &= -409986 - 1647688Y_{\text{SiO}_2}^6 + 1593677Y_{\text{SiO}_2}^7, \text{J/mol} \\ \eta &= -58.576 + 33.472Y_{\text{SiO}_2}^7, \text{J/(mol} \cdot \text{K)}\end{aligned}\quad (47)$$

The terms $Y_{\text{SiO}_2}^6$ and $Y_{\text{SiO}_2}^7$, which become important only at high SiO₂ content, are required only to reproduce the “sigmoid shaped” liquidus above 80% mole SiO₂, which results from the tendency to liquid immiscibility. The calculated phase diagram (FACT database) is shown in **Fig. 27** by the solid line. This approach is not able to represent the phase relations in the composition range below 50 mol percent silica.

According to the associate species model, the molten slag of the K₂O-SiO₂ system is represented as a solution containing the associate species K₂SiO₃·2/3(liq), K₂Si₂O₅·1/2(liq) and K₂Si₄O₉·1/3(liq), which reproduce the negative free-energy terms caused by non-ideal mixing of the end-member components in the system. In order to describe the region of phase separation, positive interaction parameters between the associate species K₂Si₄O₉·1/3(liq) and Si₂O₄(liq) were added. The phase diagram of the K₂O-SiO₂ system calculated according to the associate model (dotted lines) is given in **Fig. 27** for comparison with the equilibrium lines estimated using the quasichemical model for liquid slag (solid line).

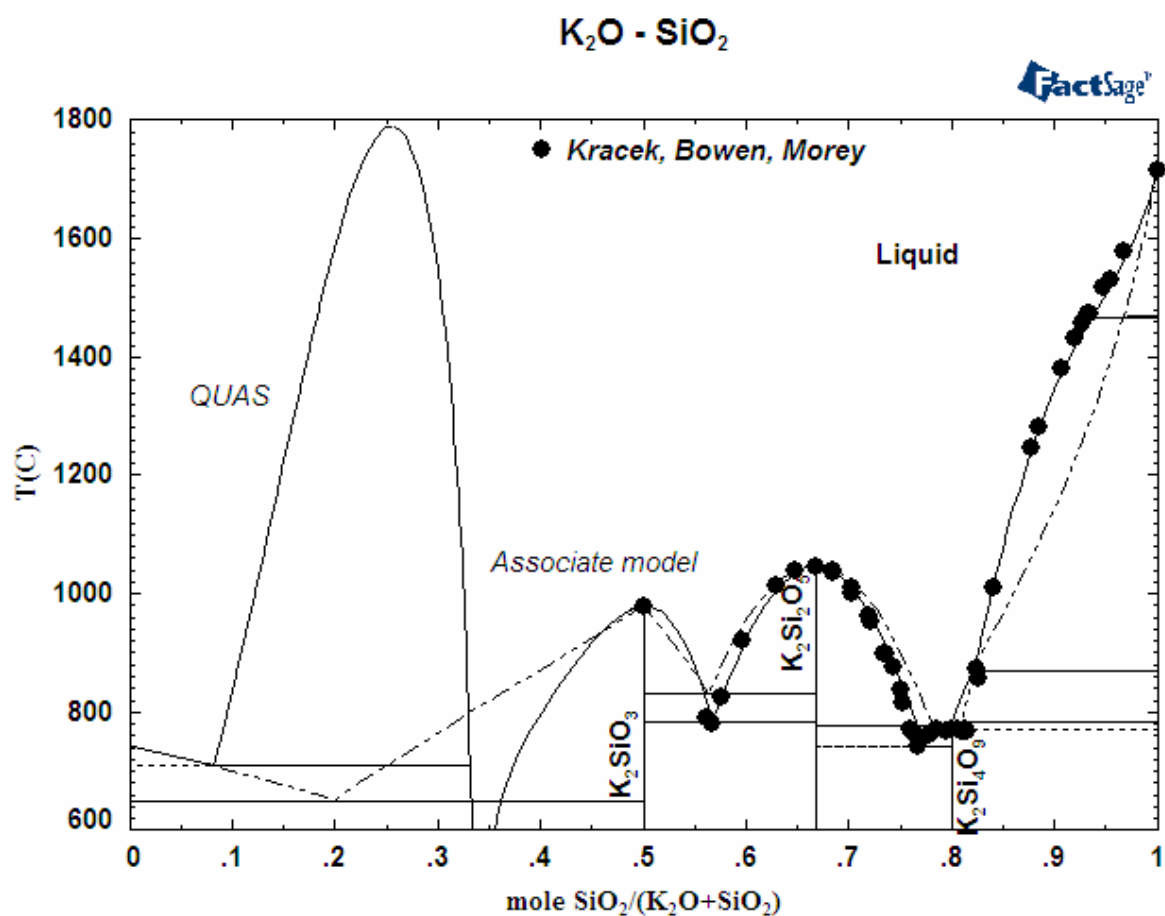


Fig. 27. Calculated phase diagram of the K_2O-SiO_2 system. Experimental points are taken from Kracek et al²³. The liquid slag is described using the quasichemical model⁷² (solid line) and the modified associate approach⁹ (dotted line)

The phase diagram calculated using the associate species approach and new data concerning the species data and interaction parameters is shown in Fig. 28 for the whole concentration range. The phase diagram in the K_2O -rich region was calculated in terms of the data by Allendorf and Spear. These data were used in the present work to optimise along all other experimental points. Unlike the data published in Ref.⁹, the new adjusted data set correctly allows the equilibria between liquid slag and silica (quartz, tridymite, cristobalite) to be represented.

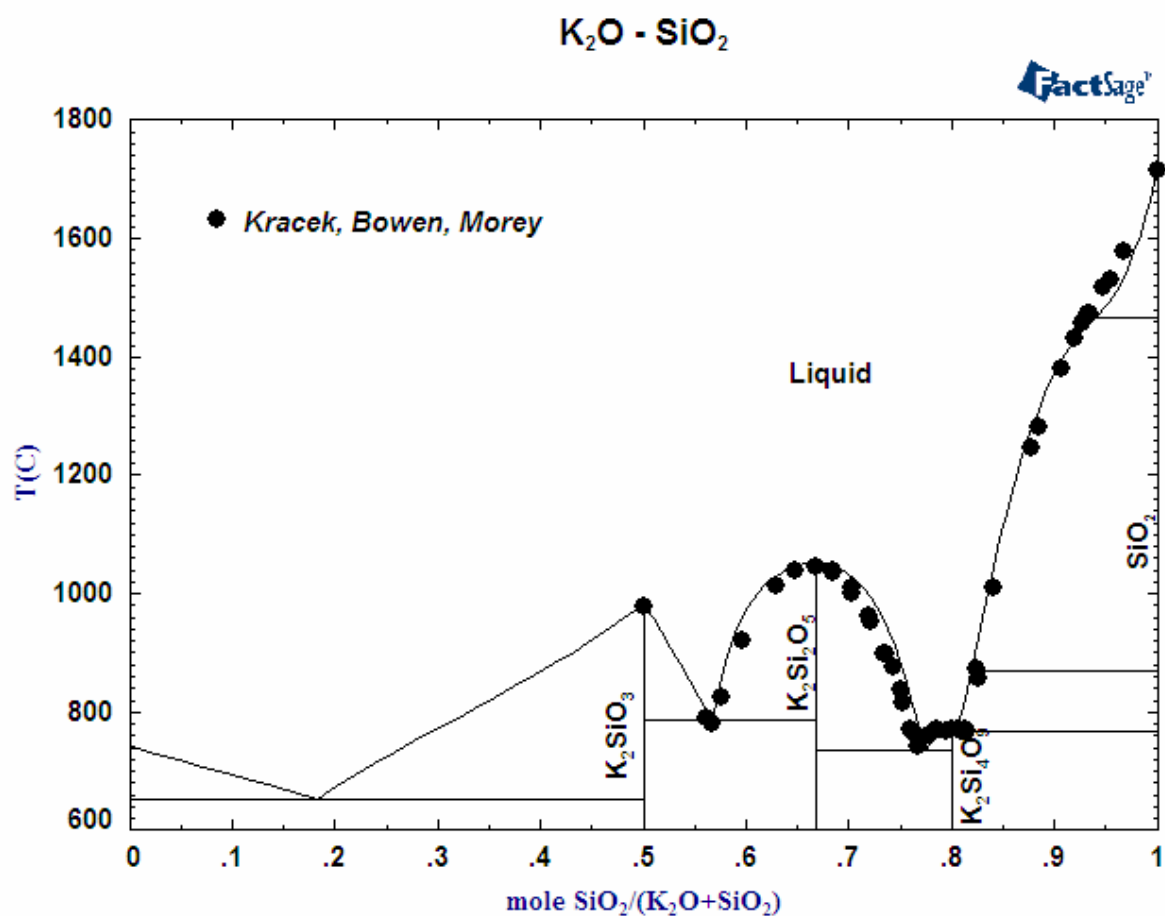


Fig. 28. Phase diagram of the K_2O-SiO_2 system calculated using the new optimised database

The potassium oxide activities in the K_2O-SiO_2 melt are plotted in Fig. 29. The activities were measured in Refs.^{65,68} by galvanic cell techniques in the temperature range 850 °C to 1100 °C. Zaitsev et al.⁷³ investigated the thermodynamic properties of K_2O-SiO_2 melts in the temperature and composition ranges 1057-1730 K and 10.8-50.0 mole% K_2O , respectively, by Knudsen effusion mass spectrometry (KEMS). Their selected data were reported in Ref.⁷⁴. The experimental values are given in comparison with the activities calculated using the quasichemical (dotted line) model (FACT database) and the modified associate species model using the database by Spear et al.⁹ (dashed line) and the new database (solid line).

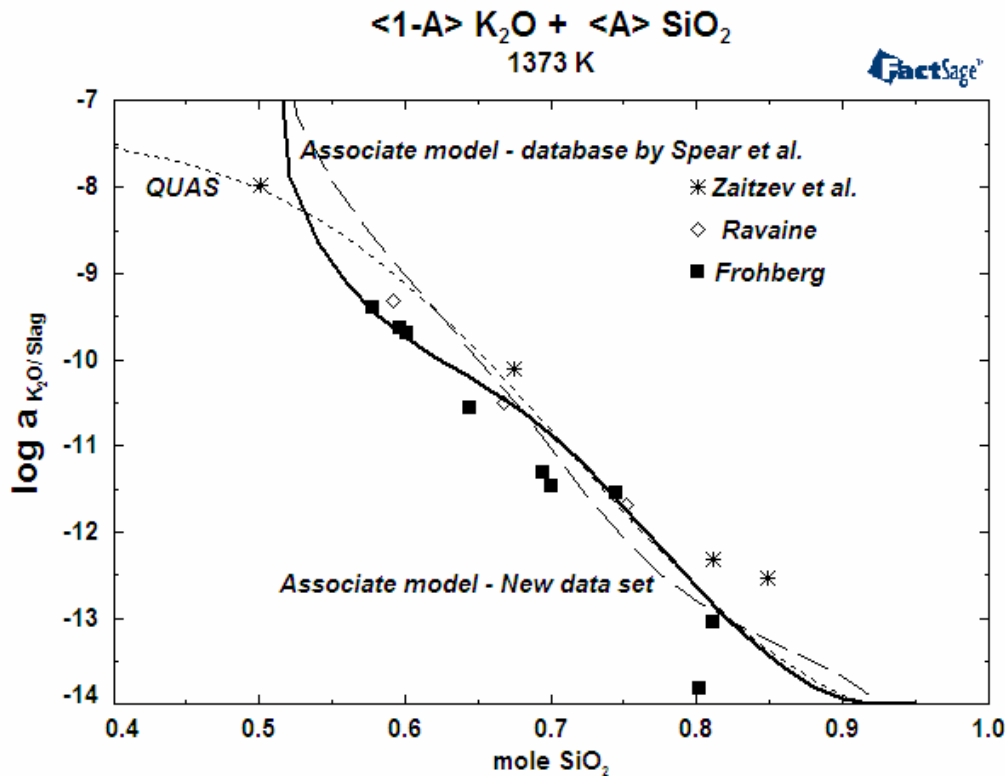


Fig. 29. Comparison of potassium oxide activities in the K_2O - SiO_2 melt at 1373 K (standard state is pure liquid) with calculations performed using the quasichemical and the modified associate species approaches

5.1.3. Al_2O_3 - SiO_2

The Al_2O_3 - SiO_2 system is characterised by some differing phase diagram data. In order to get a new set of thermodynamic data for liquid aluminosilicate in the Al_2O_3 - SiO_2 system the most reliable phase diagram data for optimisation had to be chosen. To that end, the data revised by Klug et al. were used for the optimisation. They studied the region of the phase diagram close to the melting point as well as the non-stoichiometry of mullite above 1600 °C. Along these data the experimental points of Aramaki and Roy were chosen for the optimisation at low temperatures, because they are in quite good agreement with each other. The eutectic is considered to be at 1587 °C and 4 mole percent Al_2O_3 . The mullite is considered as a non-stoichiometric phase, melting at 1890 °C, as is reported in Ref.²⁸. All points used for optimisation are collected in **Table A.2**.

Application of the associate species model to aluminosilicate liquid

The binary Al_2O_3 - SiO_2 system was considered in Ref.^{7,75} as part of the quaternary Na_2O - Al_2O_3 - B_2O_3 - SiO_2 system. The complete set of thermochemical information for the

considered system was refined and tested to give reasonable thermodynamic and phase diagram information over wide ranges of temperature and composition. Although many phases can have significant homogeneity ranges, Besmann and Spear⁷ considered only mullite and nepheline NaAlSiO_4 as solid solutions. For these crystalline solid solutions the associate species model was successfully developed. Mullite was assumed to be composed of $\text{Al}_6\text{Si}_2\text{O}_{13}$ - $\text{Al}_6\text{B}_{1.33}\text{O}_{11}$, because these compositions represent the compositional bounds of the phase.

The aluminosilicate slag is considered to consist of $\text{Al}_2\text{O}_3(\text{liq})$, $\text{SiO}_2 \cdot 2(\text{liq})$ and the associate species $\text{Al}_6\text{Si}_2\text{O}_{13} \cdot 1/4(\text{liq})$. In Ref.⁷⁵ the optimisation of the phase diagram and the thermodynamic data show that the intermediate species never dominate the liquid phase in this system. In this approach, two pair interactions between alumina and silica, and mullite and silica were considered. The phase diagram calculated according to the associate approach is given in **Fig. 30**.

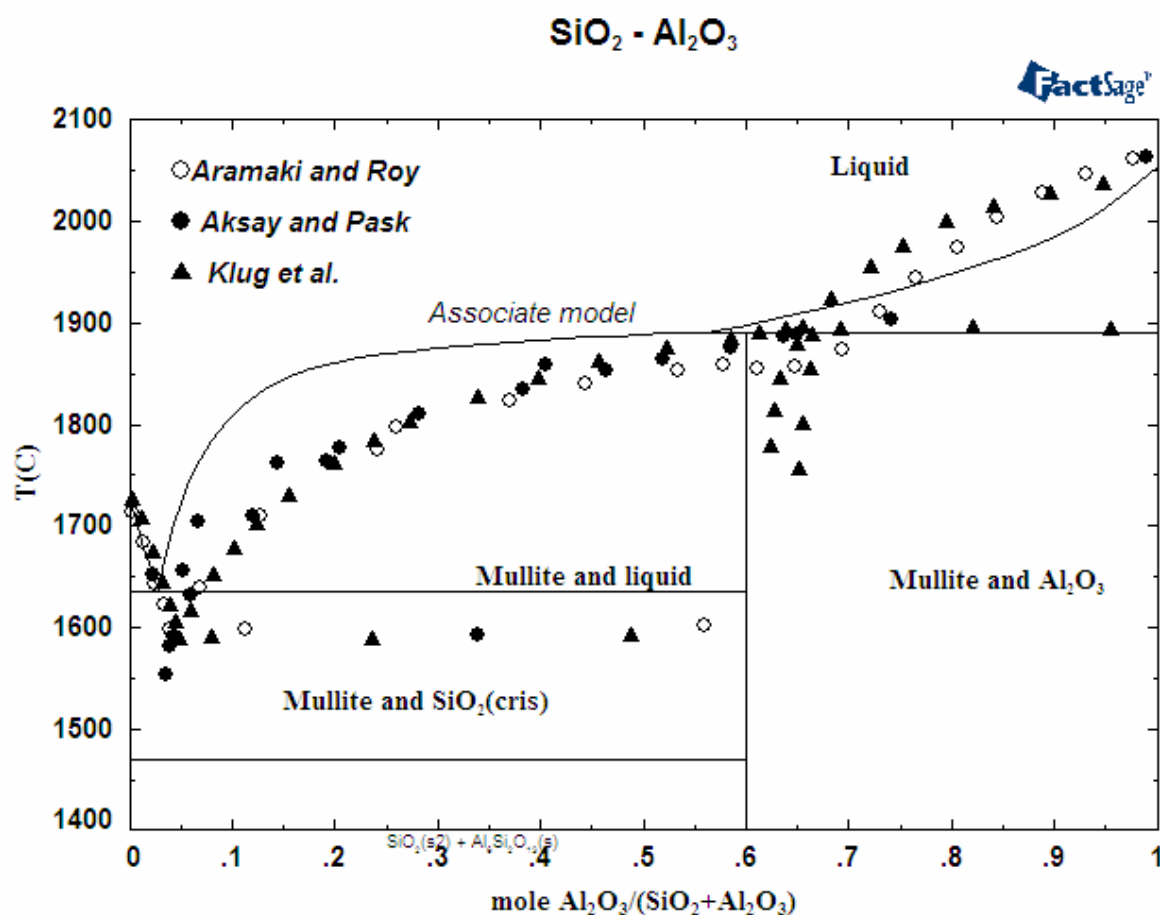


Fig. 30. Calculated phase relations in the Al_2O_3 - SiO_2 system using the associate species model after data reported in Refs.^{7,75}

In order to obtain a more accurate description of this system using the associate species model the model parameters had to be adjusted. In according with the associate species model the liquid of the aluminosilicate system can be represented as complex solution, containing the oxides $\text{Al}_2\text{O}_3(\text{liq})$, $\text{SiO}_2\cdot 2(\text{liq})$ or $\text{Si}_2\text{O}_4(\text{liq})$ and the associate species $\text{Al}_6\text{Si}_2\text{O}_{13}\cdot 1/4(\text{liq})$. In spite of the fact that mullite is accepted as an incongruently melting compound, it is incorporated as a solution constituent to represent the phase equilibria in the region near to mullite. The compositions of the solution constituents are chosen so that each solution associate species contains two non-oxygen atoms. The thermodynamic data of the considered species are invariable during optimisation: standard formation enthalpy and entropy data on liquid silica and alumina were taken from the FACT database, for the associate species $\text{Al}_6\text{Si}_2\text{O}_{13}\cdot 1/4(\text{liq})$ the data reported in Ref.⁷ were used (standard formation enthalpy and entropy of mullite species $\text{Al}_6\text{Si}_2\text{O}_{13}\cdot 1/4(\text{liq})$ are -1600 kJ/mol and $99.43 \text{ J/mol}\cdot\text{K}$, respectively).

The interaction parameters found, which may be responsible for interactions between solution species in the liquid, are given in **Table 5** in the same form as used in the **Solution module** of FactSage, which is applied to create the new database using the available mathematic polynomial for solution Gibbs energy. The interaction parameters, which were obtained according to the associate species model and published in Ref.⁷, are enclosed in brackets. The interaction parameters expressing the temperature dependence were used to give a more correct representation of the experimental properties in this system.

Table 5. Improved interaction parameters for the liquid phase in the Al_2O_3 - SiO_2 system

Species 1	Species 2	A_{12}^0	B_{12}^0	A_{12}^1	B_{12}^1
Al_2O_3	Si_2O_4	240 000 (30 000)	-121	57 144	-28
$\text{Al}_6\text{Si}_2\text{O}_{13}\cdot 1/4$	Al_2O_3	-30 000	5	-10 000	0
$\text{Al}_6\text{Si}_2\text{O}_{13}\cdot 1/4$	Si_2O_4	0 (30 000)	0	0	0

Thermodynamic data for the mullite phase were taken from the FACT database, where the non-stoichiometry of mullite is described by a general defect model similar to the Wagner-Shottky model, which is outlined in Ref.⁷⁶ (**Appendix**).

The energy parameters for the formation of both majority defects for mullite were set to $121903+38.17\cdot T$, J/mol, with the constants $\beta_1=\beta_2=1$ as given in Ref.⁷⁷.

The data for the mullite phase remained invariable during optimisation.

In the framework of the quasichemical approach, the liquid in the Al_2O_3 - SiO_2 system is described using the following optimised quasichemical parameters⁷⁷:

$$\omega = 4800 + 100784Y_{\text{SiO}_2}^3 - 142068Y_{\text{SiO}_2}^5 + 78571Y_{\text{SiO}_2}^7, \text{ J/mol} \quad (48)$$

with $\eta=0$. This gives small positive deviations in the liquid, with a maximum integral excess Gibbs energy of about 5 kJ/mol.

In the present study, the data related to the liquid slag are optimised in order to represent the phase equilibria in the Al_2O_3 - SiO_2 system using the modified associate species model, which are compatible with the FACT database. The phase diagram calculated using the new improved data set in the framework of the associate model is given in **Fig. 31** for comparison with the calculation performed by the quasichemical approach (dotted line).

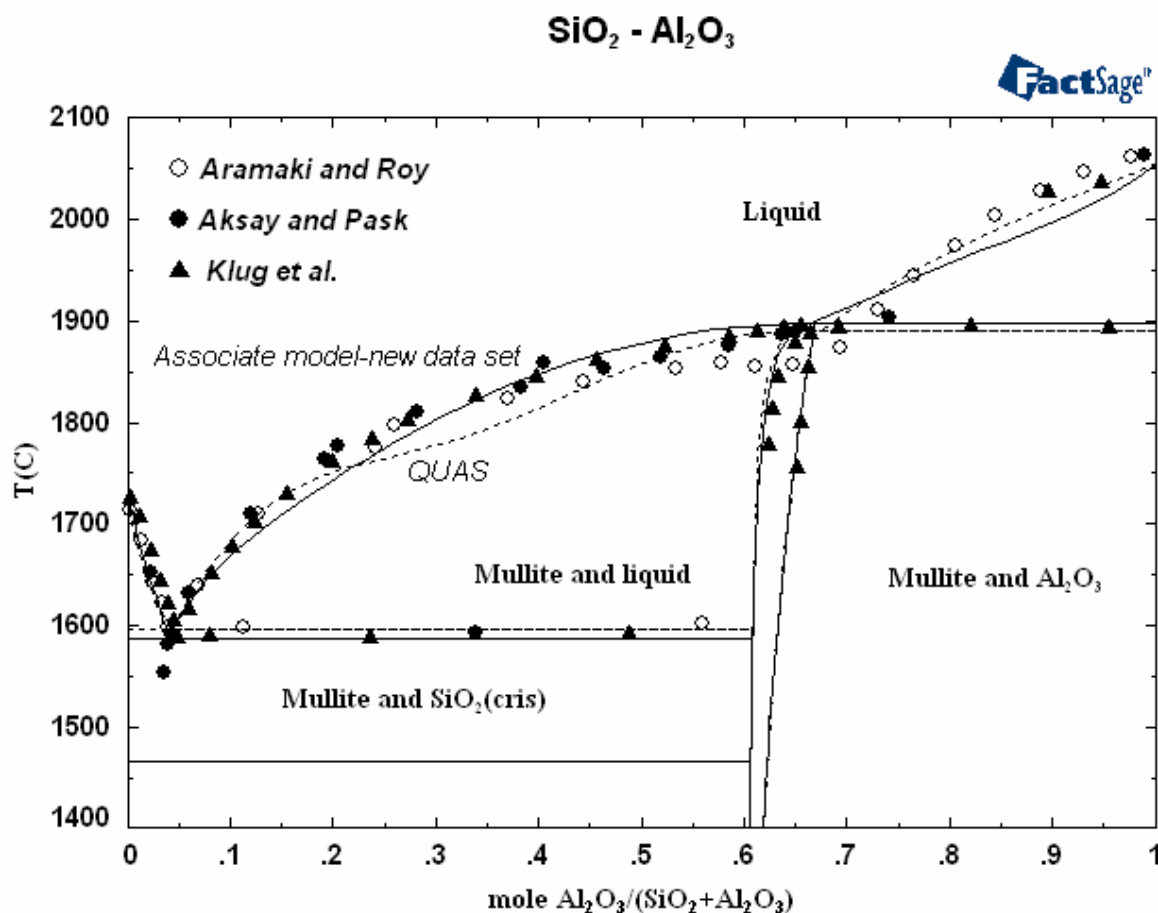


Fig. 31. Comparison of the two model approaches conformable to the Al_2O_3 - SiO_2 system: quasichemical model (database FACT, dotted line) and associate species model (new improved database, solid line). For mullite both calculated lines overlap with each other

5.1.4. Na_2O - Al_2O_3

In the literature, the system containing sodium and aluminium oxides is investigated in terms of phase relations only for alumina concentrations above 50 mole percent.

Description of the liquid in the Na₂O-Al₂O₃ system: comparison of quasichemical and associate approaches

The Na₂O-Al₂O₃ binary system was described by Eriksson et al.⁷⁸ using the modified quasichemical model. The following optimised quasichemical parameters for the liquid solution (for the components NaO_{0.5}-AlO_{1.5}) were obtained to reproduce the liquidus data, including the melting point of NaAlO₂ of 1867 °C and the eutectic reported by Weber and Venero³⁷:

$$\begin{aligned}\omega &= -483888Y_{\text{AlO}_{1.5}} - 447772Y_{\text{AlO}_{1.5}}^7, \text{J/mol} \\ \eta &= -167.360Y_{\text{AlO}_{1.5}} - 221.752Y_{\text{AlO}_{1.5}}^7, \text{J/(mol} \cdot \text{K)}\end{aligned}\quad (49)$$

The liquidus data (FACT database) were fitted reasonably well. The NaAlO₂-liquidus of Weber and Venero, which starts off nearly horizontally and then drops rapidly near the eutectic, is extremely difficult to reproduce thermodynamically. The unusually large excess entropy terms in the equation suggest that the liquidus data may be inaccurate. The probably maximum inaccuracy in the assessed diagram is estimated as ± 50 K. The optimised phase diagram is plotted in **Fig. 32** by solid lines.

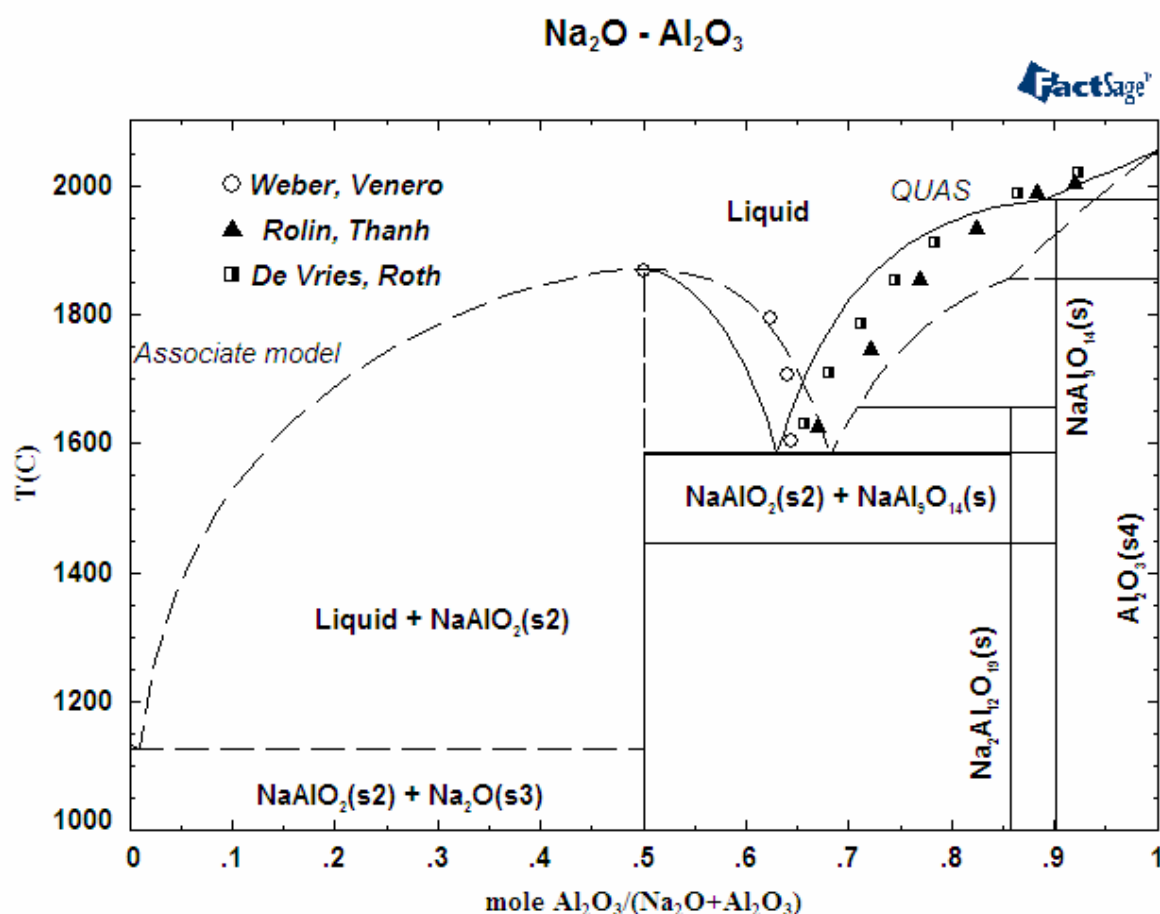


Fig. 32. Modified quasichemical and modified associate species models applied for the slag in the Na₂O-Al₂O₃ system

The associate species approach can be applied to represent the thermodynamic properties of the liquid phase in the $\text{Na}_2\text{O}-\text{Al}_2\text{O}_3$ binary system in the whole concentration region. Since there are no other compounds between sodium oxide and sodium aluminate, the simple eutectic located close to Na_2O is assumed to be quite reasonable.

The $\text{Na}_2\text{O}-\text{Al}_2\text{O}_3$ melt was considered in Refs.^{8,75} to be an ideal solution of the end-member liquid components $\text{Na}_2\text{O}(\text{liq})$ and $\text{Al}_2\text{O}_3(\text{liq})$, and the intermediates (associate species) $\text{NaAlO}_2(\text{liq})$ and $\text{Na}_2\text{Al}_4\text{O}_7 \cdot 1/3(\text{liq})$. The utility of including the $\text{NaAlO}_2(\text{liq})$ associate species was apparent from its existence in the system as a crystalline phase. The additional use of $\text{Na}_2\text{Al}_4\text{O}_7 \cdot 1/3(\text{liq})$, which has no crystalline duplicate, was necessary to accurately reproduce the phase relations in the compositional region near $\text{Na}_2\text{O}:\text{Al}_2\text{O}_3=1:2$. The initial thermodynamic values for $\text{NaAlO}_2(\text{liq})$ were derived from the crystalline phase during optimisation, whereas the $\text{Na}_2\text{Al}_4\text{O}_7 \cdot 1/3(\text{liq})$ species initial values were estimated using techniques reported in Ref.⁷⁵. The calculated phase diagram of the $\text{Na}_2\text{O}-\text{Al}_2\text{O}_3$ binary system according to the associate species approach is depicted in **Fig. 32** by the dotted line. In contrast to the quasichemical approach, the consideration of liquid slag as an associate species solution is able to assume the phase relations in the whole concentration range as a first approximation.

Solution data optimisation for the liquid phase in the $\text{Na}_2\text{O}-\text{Al}_2\text{O}_3$ system

In the present work, the parameter optimisation in the $\text{Na}_2\text{O}-\text{Al}_2\text{O}_3$ system is based mainly on the experimental points obtained by Weber and Venero³⁷ and revised in Ref.³⁶. All of these points are related to the phase equilibria at concentrations above 50 mole percent alumina. The sodium aluminate is considered to melt congruently at 1867 °C as reported in Ref.³⁷ and confirmed by data from Ref.⁴¹. The data from Ref.³⁵ concerning the equilibrium NaAlO_2 -liquid is not taken into account owing to their disagreement with the other data. The eutectic point is considered to be at 64 mole percent Al_2O_3 and 1586 °C.

The thermodynamic data for the solid compounds which exist in this system were taken from the FACT database and kept constant during the optimisation.

The associate species, needed to represent the phase relations in this system, were the same as noted in Refs.^{8,75}. The solution parameters which had to be optimised were (1) the standard data of formation for the associate species and (2) the interaction parameter between the solution components. The data for the pure end-members of the solution, liquid sodium and aluminium oxide were taken from the FACT database and remained invariable during the optimisation. The thermodynamic data for liquid $\text{NaAlO}_2(\text{liq})$ are available in the FACT database and was employed for the optimisation. The standard enthalpy and entropy of formation for the intermediate species $\text{Na}_2\text{Al}_4\text{O}_7 \cdot 1/3(\text{liq})$ estimated in Ref.⁸ were used as initial data. The initial and optimised parameters are given in **Table 6**.

Table 6. Data for the binary intermediate associate species in the Na₂O-Al₂O₃ system

Species	Database	ΔH_f^{298} , J/mol	S^{298} , J/(mol•K)
NaAlO ₂	FACT	-1 093 254.8	77.619
	New database	-966 297.4	134.76
Na ₂ Al ₄ O ₇ ·1/3	Spear ⁸	-1 234 000	95
	New database	-973 971.7	52.0

Interaction parameters between the oxide species which are not taken into account by the original associate approach were added in order to fit the associate species model to the system considered. The parameters given in **Table 7** are expressed according to Eqs.(44, 45) and applied to describe the phase diagram in conformity with available experimental data.

Table 7. New interaction parameter for associate liquid in the Na₂O-Al₂O₃ system

Species 1	Species 2	A_{12}^0	B_{12}^0	A_{12}^1	B_{12}^1
Na ₂ O	Al ₂ O ₃	-80 271.9	0	0	0
Na ₂ O	NaAlO ₂	58 096.6	-30.4	57 158.4	-22
Al ₂ O ₃	NaAlO ₂	-252 287	110.8	-482 604.6	217.3

The results of the calculations performed using the associate species model are depicted in **Fig. 33** in comparison with experimental points. The data of Rolin and Thanh³⁵ located below the eutectic temperature are excluded from the consideration.

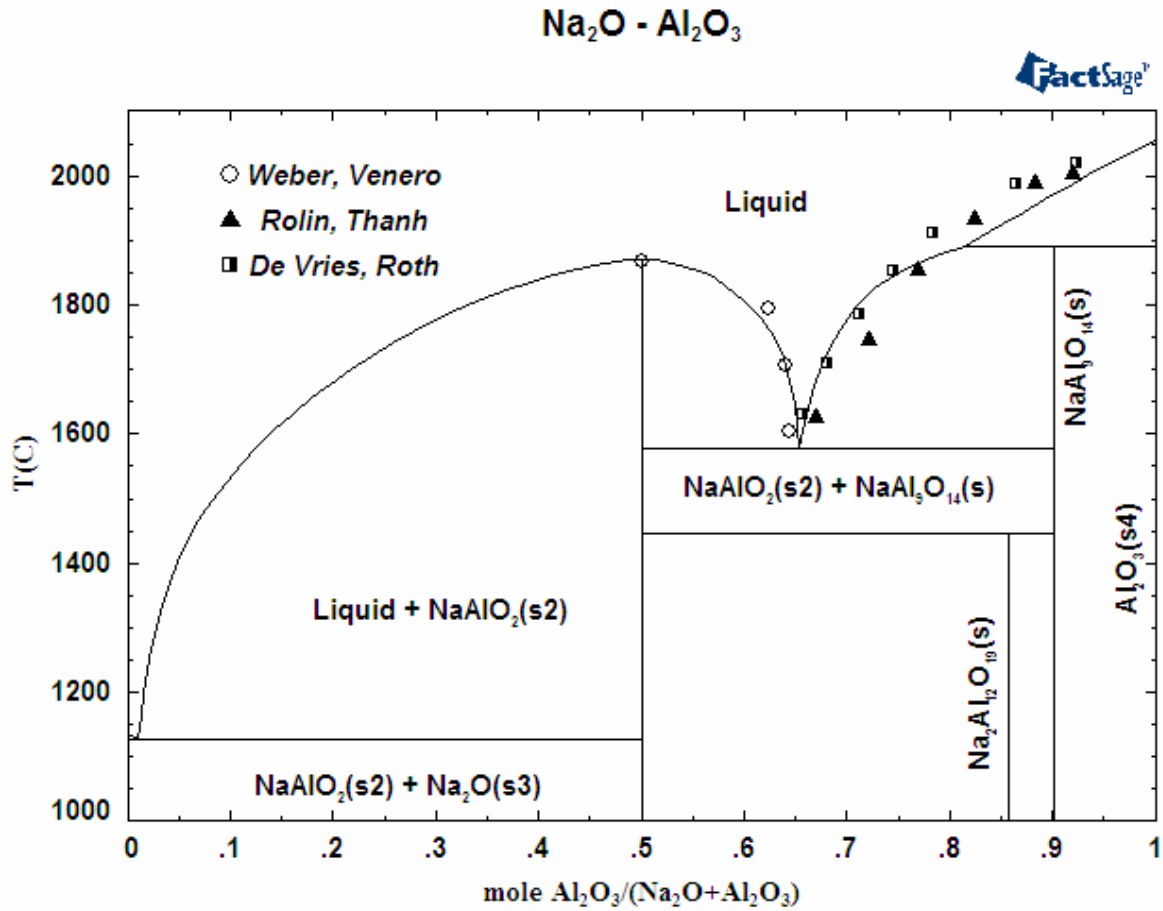


Fig. 33. Comparison of experimental points in the binary system Na₂O-Al₂O₃ with the phase diagram calculated according to the modified associate species model using the new improved data

5.1.5. K₂O-Al₂O₃

The experimental phase diagram data for the binary system K₂O-Al₂O₃ are known for Al₂O₃ concentrations above 50 mole percent as well as for the sodium oxide-alumina system. The assessment using the quasichemical approach was based on the phase diagram published in Ref.⁴³. The melting point of KAlO₂ and the eutectic point were reproduced by the following optimised quasichemical parameters for the liquid reported in Ref.⁷⁸:

$$\begin{aligned}\omega &= -531460Y_{\text{AlO}_{1.5}} + 160971Y_{\text{AlO}_{1.5}}^7, \text{ J/mol} \\ \eta &= -62.760Y_{\text{AlO}_{1.5}}, \text{ J/(mol} \cdot \text{K)}\end{aligned}\quad (50)$$

A peritectic melting of β -alumina at 1920 °C was calculated in good agreement with the earlier value of 1900 °C predicted in Ref.⁷⁹. The probable maximum inaccuracy in the assessed diagram is estimated as ± 100 K. β -Alumina was calculated to decompose to KAlO₂ and β -alumina above 1146 °C.

The liquid phase in the $K_2O-Al_2O_3$ system according to the modified associated species model was described using as solution constituents the same species which were used for the system containing sodium and aluminium oxides. These are the end-member oxides $K_2O(liq)$ and $Al_2O_3(liq)$, and the intermediates (associate species) $KAlO_2(liq)$ and $K_2Al_4O_7 \cdot 1/3(liq)$. The calculated phase diagram published in Ref.⁸ is in good agreement with the phase diagram optimised by Eriksson⁷⁸. Only the data of the melting temperature of KAl_9O_{14} differ. Eriksson et al. assumed that the β -alumina melts by a peritectical reaction at 1920 °C to give α -alumina and liquid at 0.75 mole percent of Al_2O_3 . In contrast to that, the calculation using the associate species model proposed a congruent melting β -phase at 1989 °C and an α -alumina- β -alumina eutectic at 1984 °C.

The predicted phase diagram calculated using both these approaches is shown in **Fig. 34**.

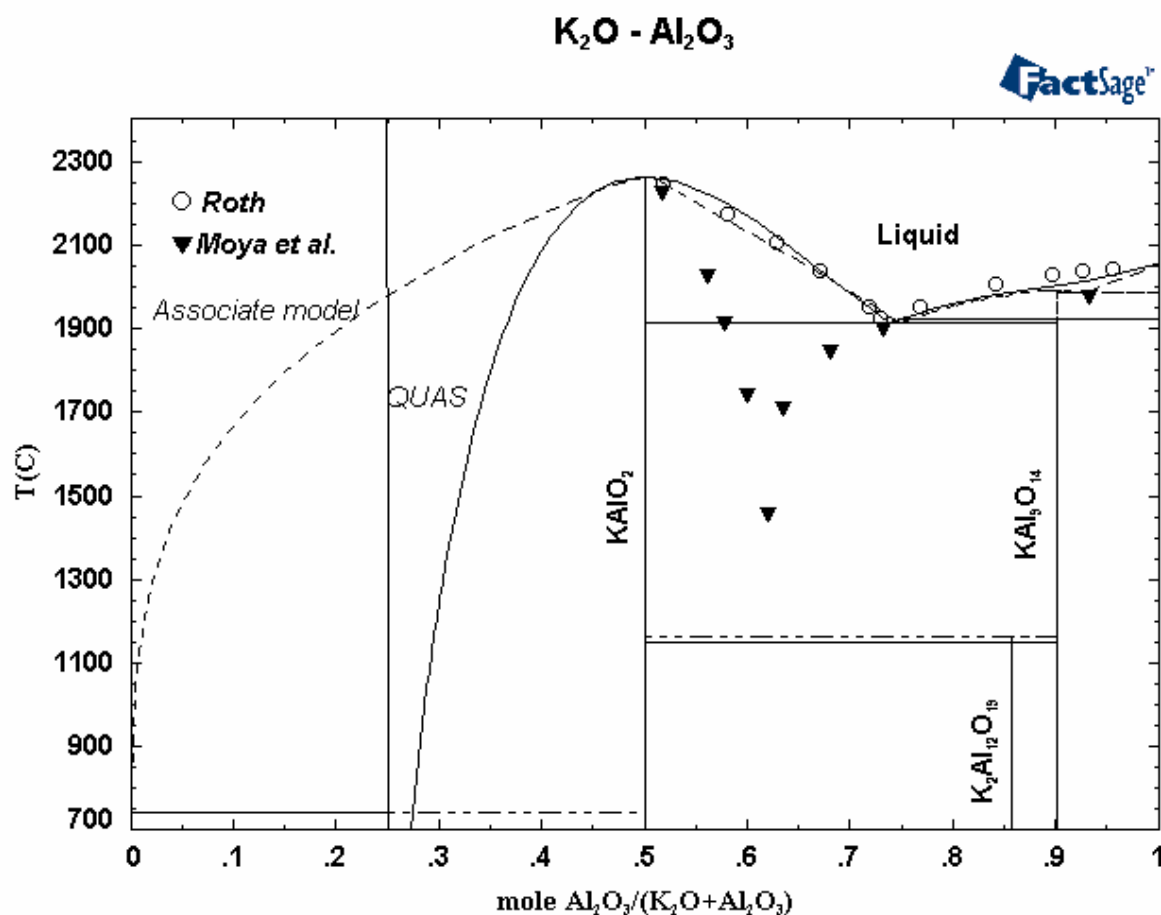


Fig. 34. Comparison of the calculated phase relations in the $K_2O-Al_2O_3$ system using the quasichemical model (solid lines) and the associate species model (dotted line)

In the present work the attempt was made to change the thermodynamic data for solution constituents proposed by the associate species model and also to incorporate

interaction parameters among the species. The solution constituent's compositions correspond to those determined by Spear⁸. The initial data for pure liquid K₂O, Al₂O₃ and KAlO₂ were taken from the FACT database. The complex oxide species K₂Al₄O₇·1/3(liq) does not exist as a chemical entity that can be isolated and characterised. It is used to represent the negative interaction energies that occur between K₂O and Al₂O₃ in an oxide solution. The composition was dictated by the compositional region of the phase diagram where a better fit is needed. The initial thermodynamic data for K₂Al₄O₇·1/3(liq) are taken from Ref.⁸. The initial data for the complex liquid species are estimated to correctly describe the phase diagram. The results of the optimisation of standard formation enthalpies and entropies in comparison with initial values are shown in **Table 8**.

Table 8. Liquid species data for the K₂O-Al₂O₃ system

Species	Database	ΔH_f^{298} , J/mol	S^{298} , J/(mol•K)
KAlO ₂	FACT	-1 058 402.6	120.606
	New database	-1 036 478.1	128.64
K ₂ Al ₄ O ₇ ·1/3	Spear ⁸	-1 210 000	102
	New database	-396 667.6	433.23

Unlike the associated species approach proposed in Ref.⁸ the interaction parameters are added and optimised by the trial and error method to correctly represent the phase relations in the considered system. The adjustable parameters are thus the thermodynamic data for the associate species and the values of interaction parameters, which are entered as noted by Eqs.(44, 45) to represent the excess Gibbs energy for the liquid phase. These pair interaction parameters are noted in **Table 9**.

Table 9. Optimised interaction parameters obtained for the liquid phase of the K₂O-Al₂O₃ system

Species 1	Species 2	A_{12}^0	B_{12}^0	A_{12}^1	B_{12}^1
Al ₂ O ₃	KAlO ₂	19 591.7	-7.3	-8 884.6	-5.9

These parameters obtained by the optimisation module of the ChemSage program allow the phase equilibria to be depicted as shown in **Fig. 35**. It is necessary to note that the thermodynamic data for all available condensed phases were taken from the FACT database without any changes during the optimisation procedure.

The experimental equilibrium points required for optimisation were mainly taken from Ref.⁴³. They relate to the concentration region above 50 mole percent alumina. The points obtained by Moya et al.⁴⁵ were excluded from the consideration because of their inconsistency with the other data.

There are no reliable phase diagram data for the composition range between pure potassium oxide and potassium aluminate. The quasichemical model is not able to represent this region as indicated in **Fig. 34**. Since there are no compounds in this region, the liquidus line can be suggested to start from the melting point of potassium aluminate KAlO_2 to a eutectic located near the melting point of potassium oxide. The liquidus of the composition range with less than 50 mole percent alumina is therefore assumed by Spear et al.⁷ as an approximation. The eutectic is calculated to be at 740 °C and 0.001 mole alumina.

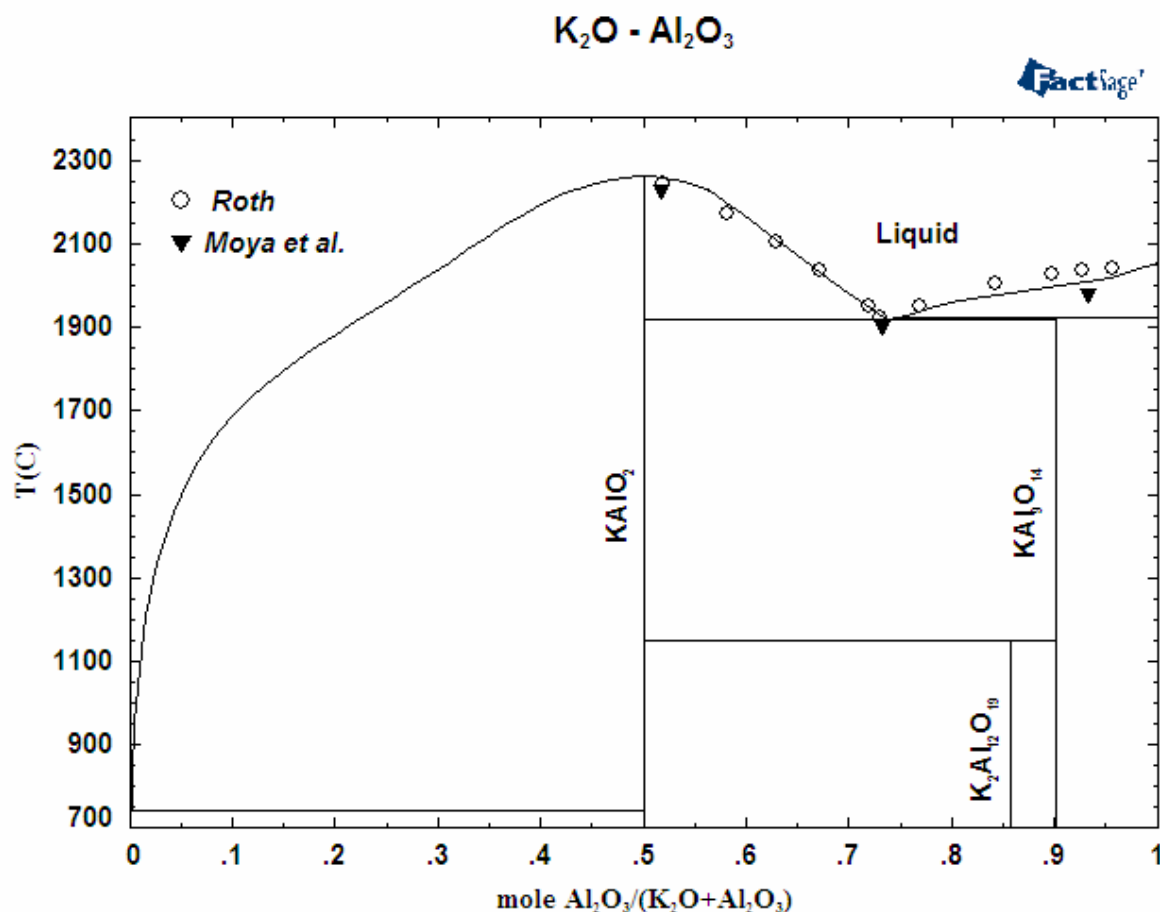


Fig. 35. Application of the modified associate species model for the $\text{K}_2\text{O}-\text{Al}_2\text{O}_3$ system using the new optimised data set

5.2. Ternary systems

5.2.1. $\text{Na}_2\text{O}-\text{K}_2\text{O}-\text{SiO}_2$

As a first approximation, the description of the liquid in the ternary system containing both alkalis with silica is based mainly on the experimental points obtained by Kracek⁴⁶. The phase diagram in the composition range above 50 mole percent of potassium and sodium oxide was studied by the quenching method. The phase relations of the binary boundaries are already considered in Chapter 3.2.1. The alkali activities measured by Knudsen effusion mass spectrometry depending on composition and temperature were also employed as experimental data.

The modified associate species model can be applied to represent the phase equilibria in this ternary system. Since there are no ternary compounds in the system, one can assume that the ternary liquid can be represented as a solution containing only known binary constituents. These are pure liquid potassium, sodium and silicon oxide and also the binary associate species, which were used to describe the binary slags. The interaction parameters between binary species estimated for the binary system have to be taken into consideration without any changes.

In order to represent the ternary liquid it may be reasonable to consider the interaction between associate species containing the different alkalis.

The search for suitable parameters was carried out using the optimisation module of the ChemSage program. The thermodynamic data of the binary systems, standard formation enthalpies and entropies of the binary constituents and interaction parameters among them, were kept invariable during optimisation of the “ternary” parameters. The values which had to be optimised include the interaction parameters between species containing heterogeneous alkalis to represent specific interactions concerning different alkali silicates. Generally, all possible pair interactions among available species can be considered, but only certain pairs could be applied to represent the phase relations in the ternary system.

The selection of suitable pairs can be performed on the assumption that those pair interactions are of great importance whose concentrations are dominant in the certain region. For example, the preliminary calculation of the equilibrium in the solution at fixed temperature carried out using the Equilib module of FactSage shows that the dominant species along the quasi-binary section $\text{Na}_2\text{Si}_2\text{O}_5$ - $\text{K}_2\text{Si}_2\text{O}_5$ are potassium and sodium disilicates $\text{K}_2\text{Si}_2\text{O}_5 \cdot 1/2$ and $\text{Na}_2\text{Si}_2\text{O}_5 \cdot 1/2$, respectively. **Fig. 36** demonstrates the associate species distribution calculated according to the associate species approach.

It can be supposed that these constituents are responsible for interactions in this concentration region and these pairs should be optimised. A similar consideration can be made for the quasi-binary section Na_2SiO_3 - K_2SiO_3 .

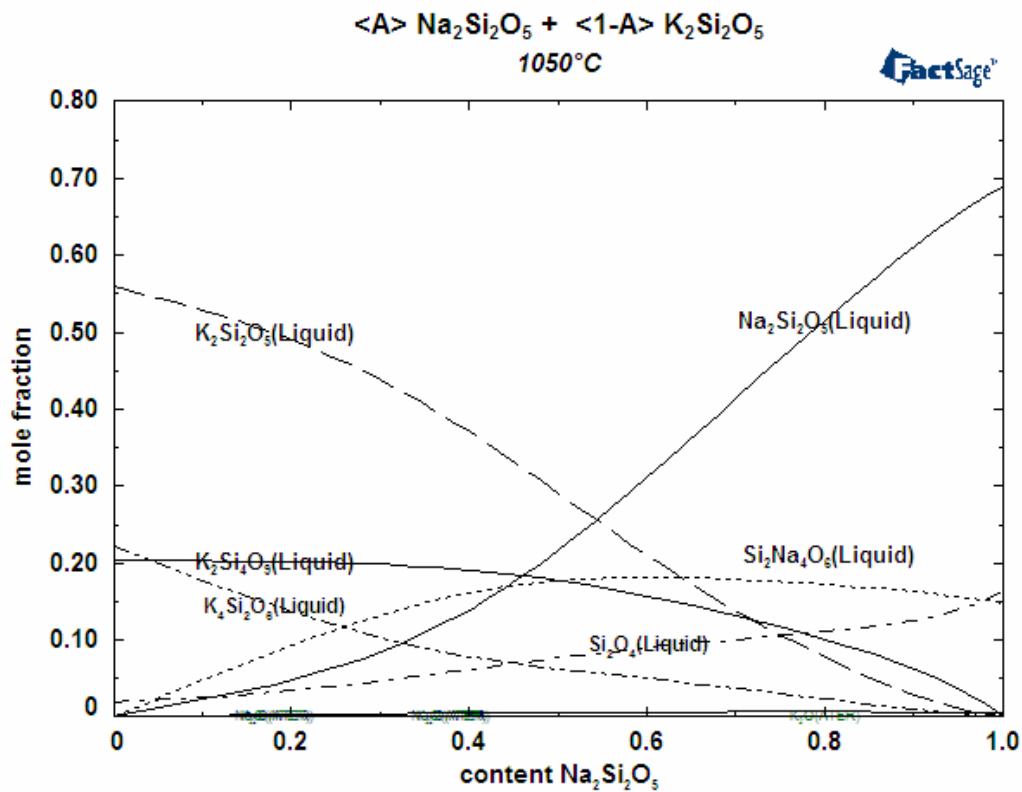


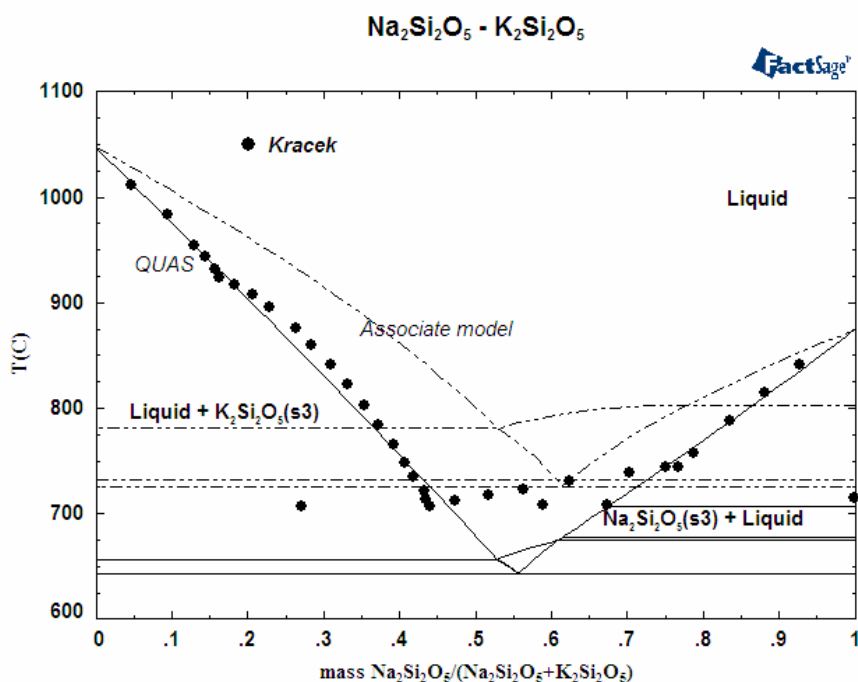
Fig. 36. Composition of the Na_2O - K_2O - SiO_2 liquid at 1050 °C calculated using the data set before the optimisation

The Gibbs energy of the solution is expressed by the sum of the ideal part and the excess part of Gibbs energy according to Eq.(44). In order to describe the behaviour of the ternary system the interactions between heterogeneous constituents were added to the existing binary parameter.

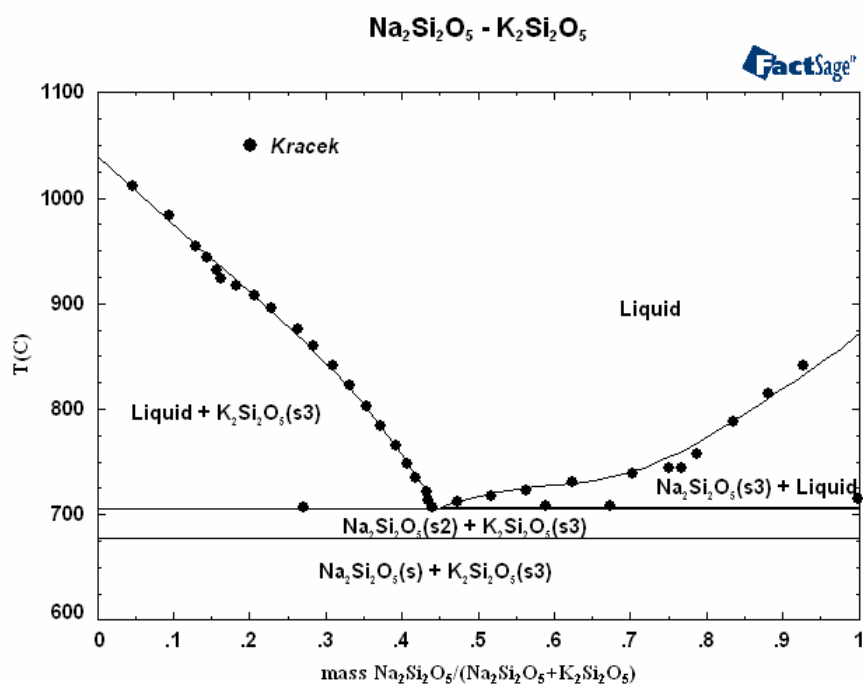
The accuracy of the parameters found is given in **Table 10** and can be tested by representing of the phase relations in the quasi-binary sections with respect to alkali disilicates $\text{Me}_2\text{Si}_2\text{O}_5$ and metasilicates Me_2SiO_3 . The comparison of experimental points and the phase diagrams calculated using the new data set are presented in **Fig. 37** and **Fig. 38**.

Table 10. Optimised interaction parameters in the K_2O - Na_2O - SiO_2 ternary system

Species 1	Species 2	A_{12}^0	B_{12}^0	A_{12}^1	B_{12}^1
$\text{K}_2\text{SiO}_3 \cdot 2/3$	$\text{Na}_2\text{SiO}_3 \cdot 2/3$	-21 415.4	24.7	100 000	-90.9
$\text{K}_2\text{SiO}_3 \cdot 2/3$	$\text{Na}_2\text{Si}_2\text{O}_5 \cdot 1/2$	45 188.46	-64.1	0	0
$\text{K}_2\text{Si}_2\text{O}_5 \cdot 1/2$	$\text{Na}_2\text{SiO}_3 \cdot 2/3$	-38 440.7	29	0	0
$\text{K}_2\text{Si}_2\text{O}_5 \cdot 1/2$	$\text{Na}_2\text{Si}_2\text{O}_5 \cdot 1/2$	87 780.6	-62.2	-13 614.8	15.5



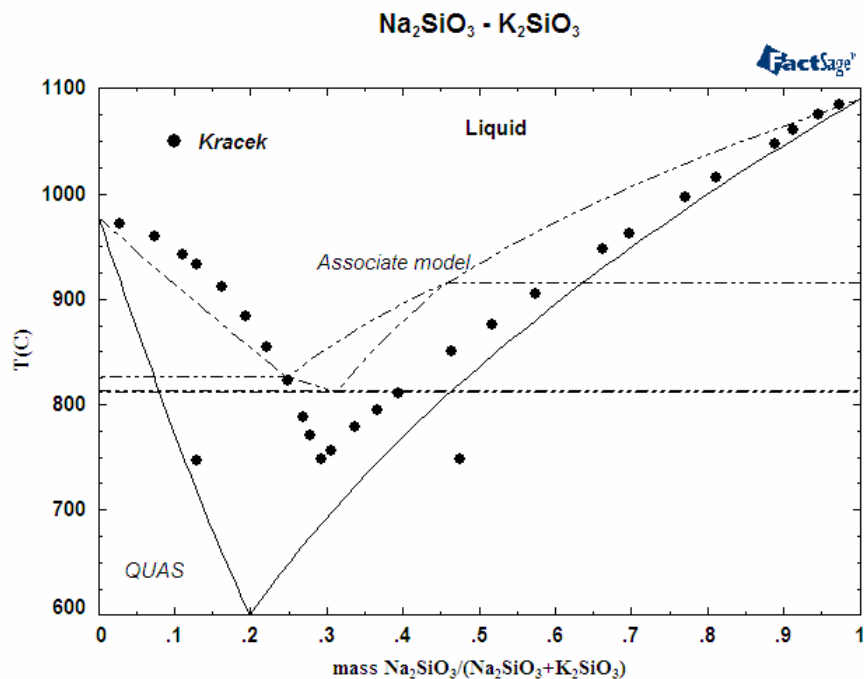
(1)



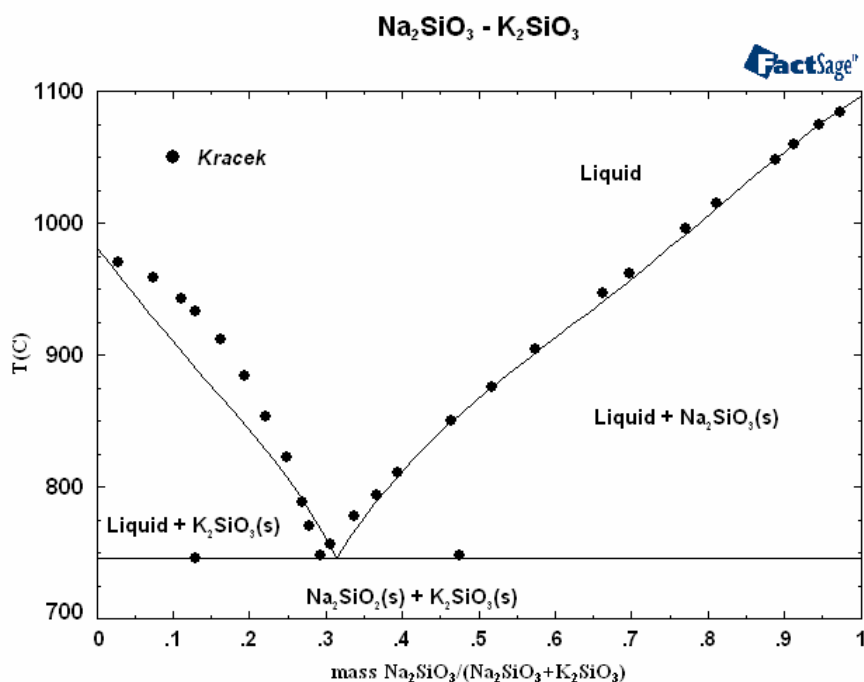
(2)

Fig. 37. Comparison of experimental points with phase diagram in the quasi-binary $\text{Na}_2\text{Si}_2\text{O}_5$ - $\text{K}_2\text{Si}_2\text{O}_5$ system calculated using different solution models

- (1) quasichemical model (solid line) and associate species (dotted line) approaches (before optimisation)
- (2) associate model using the new improved database



(1)



(2)

Fig. 38. Quasi-binary section K_2SiO_3 - Na_2SiO_3 : comparison of quasichemical and associate species approach with experimental data

- (1) quasichemical model (solid) and associate species (dotted line) approaches (before optimisation)
- (2) associate model using the new improved database

The preliminary calculations concerning the phase relations in the ternary system are shown in **Fig. 39**. The experimental quenched data are depicted by points at different temperatures in the range between 800 and 1600 °C.

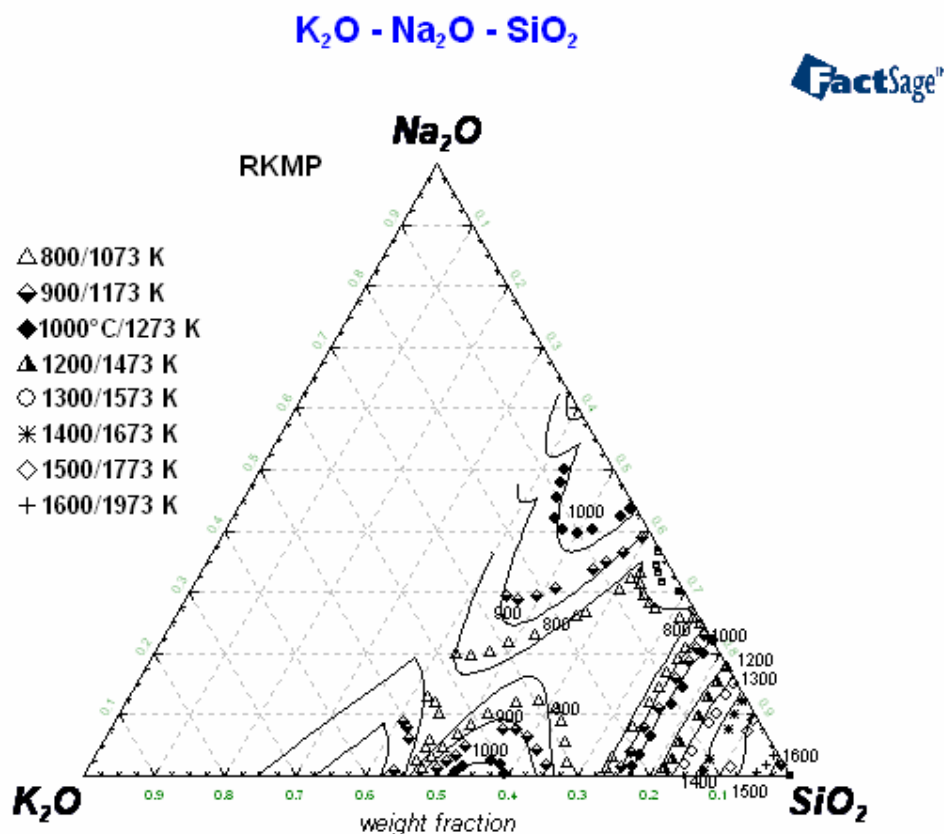


Fig. 39. Ternary system K₂O-Na₂O-SiO₂: isotherms of the liquidus surfaces of the various compounds. The liquidus calculations are performed according to the modified associate species model using the new optimised data set

5.2.2. Na₂O-Al₂O₃-SiO₂

The thermodynamic description of the complex oxide system can be performed by considering the available phase relations in quasi-binary sections. The present chapter is devoted to preliminary calculations in the Na₂O-Al₂O₃-SiO₂ system.

As mentioned in the literature review, there are two ternary compounds, namely NaAlSi₃O₈ albite and NaAlSiO₄, which exists in the two polymorphs, carnegieite and nepheline, in the ternary Na₂O-Al₂O₃-SiO₂ system. The reversible inversion temperature is considered to be of pure NaAlSiO₄ at 1254 °C in Ref.⁴⁸.

Besmann and Spear⁷ made an attempt to model the solid solutions on the basis of NaAlSiO₄ (nepheline) using the associate species approach. Nepheline was treated as an ideal

solution of NaAlSiO_4 , $\text{NaAlSi}_2\text{O}_6$ and NaAlO_2 . All these entire compounds are located on the same line joining silica and sodium aluminate NaAlO_2 , where the relation $\text{Na}_2\text{O}/\text{Al}_2\text{O}_3$ remains constant.

The ternary liquid can be simultaneously considered in the framework of the modified associate species model. In contrast to the ternary system containing silica and both alkali oxides sodium and potassium oxide, this liquid seems to be more complicated because there are two solid ternary compounds (at 1 atm) which melt congruently, and, in general, can be considered as associate species in the liquid slag. According to previous approximations performed in Ref.⁷, ternary liquid in the $\text{Na}_2\text{O}-\text{Al}_2\text{O}_3-\text{SiO}_2$ system consists of $\text{NaAlSiO}_4(\text{liq})$ and $\text{NaAlSi}_2\text{O}_6(\text{liq})$ as ternary constituents and the other already known binary associate species.

This approach is able to represent the liquidus temperature, but involves only one of the available solid solutions. Some inconsistency between experimental and calculated data is observed.

The present problems regarding the thermodynamic description of the $\text{Na}_2\text{O}-\text{Al}_2\text{O}_3-\text{SiO}_2$ system are the description of both solid solutions on the basis of NaAlSiO_4 , and liquid ternary phase using the modified associate species model. The phase relations of the quasi-binary cross-sections of this ternary system have to be described simultaneously.

Since the presence of a continuous solid solution extending between sodium aluminate and carnegieite, both having β -cristobalite-related structures, is not considered to be proved, only two compounds can be chosen as solid solution constituents: NaAlSiO_4 (nepheline or carnegieite, depending on the temperature range) and $\text{NaAlSi}_2\text{O}_6$. In order to obtain information about the solid solutions, the thermodynamic data of the considered associate species are to be found. The interaction parameters among them can be added to represent the phase relations concerning these solid phases, if necessary.

Since $\text{NaAlSi}_3\text{O}_8$ (albite) and NaAlSiO_4 have congruent melting points, it is quite reasonable to choose them as ternary associate species. Regarding the ternary liquid phase the binary associate species are considered to be invariable during searching of the ternary data. The possible interactions in the ternary liquid can be presumably represented by the introduction of interaction parameters, which are responsible for the excess part of the solution Gibbs energy expressed by Eqs(44, 45).

To this end, the adjustable solution parameters (standard formation enthalpies and entropies for the chosen ternary associate species and also interaction parameters) can be estimated using the **Optimisation** module of the ChemSage program. Initial data for the associate species $\text{NaAlSiO}_4 \cdot 1/3(\text{liq})$ are taken from Ref.⁷. The solid solutions on the basis of nepheline and carnegieite are considered to contain as components the $\text{NaAlSiO}_4(\text{s3})$ and $\text{NaAlSi}_2\text{O}_6(\text{s})$, and $\text{NaAlSiO}_4(\text{s4})$ and $\text{NaAlSi}_2\text{O}_6(\text{s})$, respectively. Possible interactions are also added to represent the phase relation.

The standard formation enthalpy and entropy for the considered species of liquid and solid solutions, and interaction parameters are found by trial and error to achieve the most adequate accordance with experimental phase relation data. The obtained values are given in **Tables 11-14**. The unusual stoichiometry of species is assigned by empirical requirements of the modified associate species model to have two non-oxygen atoms per mole.

Table 11. Liquid species data for the Na₂O-Al₂O₃-SiO₂ system

Species	Database	ΔH_f^{298} , J/mol	S^{298} , J/(mol•K)
NaAlSiO ₄ ·1/3(liq)	Initial from Ref. ⁷	1 373 150	110.0
	New database	-1 355 655.5	105.6
NaAlSi ₃ O ₈ ·2/5(liq)	Initial from Ref. ⁷	-1 500 000	105.0
	New database	-1 468 562	154.85

Table 12. New interaction parameters for the associate liquid in the Na₂O-Al₂O₃-SiO₂ system

Species 1	Species 2	A_{12}^0	B_{12}^0	A_{12}^1	B_{12}^1
NaAlSiO ₄ ·1/3	NaAlSi ₃ O ₈ ·2/5	-164 253.8	102.7	-122 092	90.7
Si ₂ O ₄ (liq)	NaAlSi ₃ O ₈ ·2/5	-58 899	44	-20 092	6.3
Si ₂ O ₄ (liq)	NaAlSi ₃ O ₈ ·2/5	-105 207.9	96.2	0	0

Table 13. Solid solution species data for the nepheline phase

Species	Database	ΔH_f^{298} , J/mol	S^{298} , J/(mol•K)
NaAlSiO ₄ (s3)	FACT	-2 078 114.68	143.705
NaAlSi ₂ O ₆ (s)	Initial FACT	-3 025 118.23	133.574
	New database	-3 027 483.5	153.34

Interaction parameters					
Species 1	Species 2	A_{12}^0	B_{12}^0	A_{12}^1	B_{12}^1
NaAlSiO ₄ (s3)	NaAlSi ₂ O ₆	-13 042.5	-0.1	-485	-2

Table 14. Solid solution species data for the carnegieite phase

Species	Database	ΔH_f^{298} , J/mol	S^{298} , J/(mol•K)
NaAlSiO ₄ (s4)	FACT	-2 078 101.467	143.713
NaAlSi ₂ O ₆ (s)	Initial FACT	-3 025 118.23	133.574
	New database	-2 944 973.6	205.85

Interaction parameters					
Species 1	Species 2	A_{12}^0	B_{12}^0	A_{12}^1	B_{12}^1
NaAlSiO ₄ (s4)	NaAlSi ₂ O ₆ (s)	-14 139	0.7	-597.9	-0.6

Table 15. Optimised data for the albite

Albite	Database	ΔH_f^{298} , J/mol	S^{298} , J/(mol•K)
NaAlSi ₃ O ₈ (s1)	FACT	-3 933 008.2	207.4
	New database	-3 887 019.71	243.7
NaAlSi ₃ O ₈ (s2)	FACT	-3 919 526.2	224.4
	New database	-3 873 537.7	260.7

The calculated phase diagram for the quasi-binary cross-section is given in **Fig. 40**. The quasichemical model cannot represent these phase relations, because the solid solutions are not taken into account. The modified associate consideration reported in Ref.⁷ relates to one of the available solid solutions, namely nepheline (dashed line in **Fig. 40**).

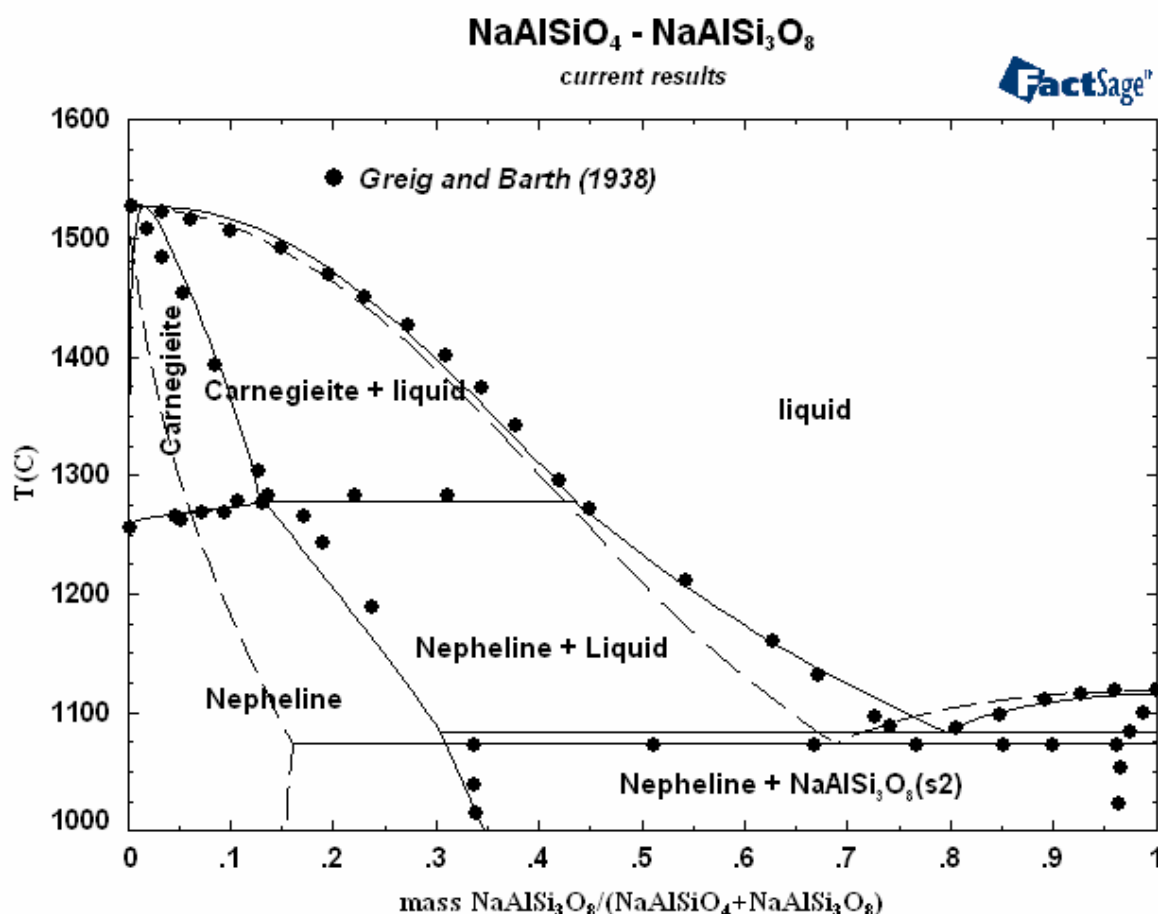


Fig. 40. Comparison of the preliminary calculated phase diagram with experimental data obtained by Greig and Barth⁴⁸

The calculation of the phase equilibria regarding this part of the ternary system Na₂O-Al₂O₃-SiO₂ demonstrates that the performed optimisation of the phase allows the phase relations to be represented quite well. The estimated liquidus lines show a good agreement with experimental data in general.

5.2.3. Application of the associate species model to calculate K_2O activities

The obtained solution data in the framework of the associate species solution model can be applied to represent the activities of the slag components. Measurements of partial pressure were carried out using Knudsen effusion mass-spectrometry for the multicomponent system containing SiO_2 , Al_2O_3 , M_2O ($M=Na, K$) and additionally CaO , FeO and others ². The vaporisation reaction for the alkali Me (Na or K) can be written as:



The equilibrium constant is expressed as:

$$K_p = \frac{P_{Me}^2 \cdot P_{O_2}^{1/2}}{a_{Me_2O_{liq}}} , \quad (52)$$

where K_p is calculated according to the FACT database and the alkali partial pressure is a measured value. The oxygen pressure can be estimated directly by the mass-spectrometric method or by consideration of the oxygen-dependent equilibrium (for instance, between Fe and $FeO_{1-\delta}$). Assuming stoichiometric vaporisation of the M_2O_{liq} from slag the oxygen partial pressure can be determined as the expression:

$$P_{O_2} = \frac{1}{4} P_{Me} . \quad (53)$$

The activities of the alkali oxides in the slag can then be calculated from the following equation:

$$a_{Me_2O_{liq}} = \frac{P_{Me}^{5/2}}{2 \cdot K_p} . \quad (54)$$

The measurements were carried out in the temperature range from 1550 to 1900 K. **Fig. 41** shows the K_2O activity in the slag and partial pressure of potassium over the liquid slag. The calculations of the partial pressures and activities were executed using the Equilib module of the FactSage program. In this case the equilibrium between an ideal gas phase and liquid slag, which is described as an associate species solution, is considered. The thermodynamic data for the gas phase are taken from the FACT database. In comparison to the calculated values obtained using the FACT database (quasichemical model for slag) and original data after Spear, Besmann, Allendorf (modified associate species model), the new optimised data set can represent these experimental points more accurately.

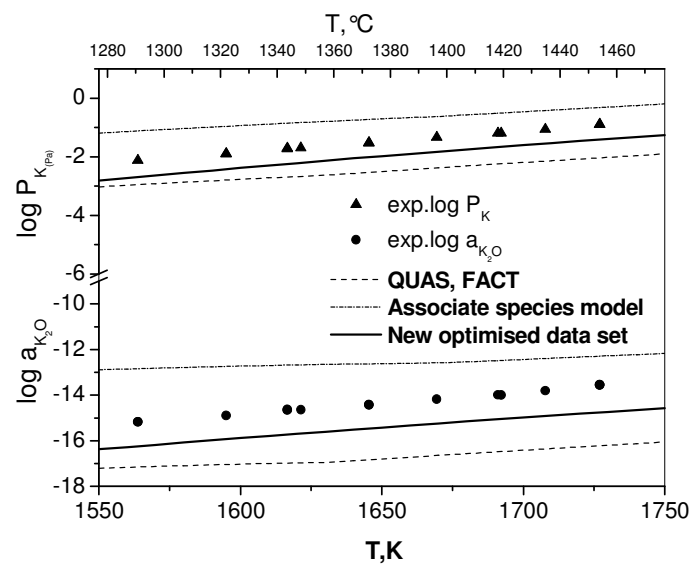


Fig. 41. Potassium partial pressure over the liquid and potassium oxide activities in the $\text{K}_2\text{O-Na}_2\text{O-Al}_2\text{O}_3\text{-SiO}_2$ melt containing 78.31 mass percent SiO_2 , 17.15 Al_2O_3 , 4.14 K_2O and 0.4 Na_2O . Comparison of experimental points with the activities calculated using different models and data sets

6. Discussion

The binary and ternary subsystems of the $\text{Na}_2\text{O-K}_2\text{O-Al}_2\text{O}_3\text{-SiO}_2$ system were studied regarding the thermodynamic description of the liquid slag. The modified associate species model was chosen to represent the solution containing the chemical components (i.e. the basic oxides) and so-called associate species. The deviation from the ideal behaviour of the slag was taken into account by the formation of the species and interactions between these species and the component oxides. The improvement of the database was carried out using an optimisation procedure involving the solution parameters used in the excess Gibbs energy function (Redlich-Kister polynomial). These parameters had to be added and optimised to obtain a good agreement in comparison with the experimental data as far as possible. The thermodynamic data of the solid phases (pure compounds as well as solid solutions, e.g. mullite) and pure component liquid were taken from the FACT database without changes during the optimisation procedure.

In the literature, the binary systems $\text{Me}_2\text{O-SiO}_2$ ($\text{Me}=\text{Na, K}$) were not investigated regarding their experimental phase diagrams in the composition range between pure alkali oxide and Na_4SiO_4 and K_2SiO_3 , respectively. **Fig. 24** and **Fig. 27** demonstrate the comparison of the calculated phase diagrams of the alkali silicate systems with the experimental data. The quasichemical approach cannot represent the phase relations in the alkali-rich composition range. In contrast to that, the modified associate species model allows the liquidus line to be assumed close to pure sodium oxide. However, the liquidus lines in the silica rich region for both systems calculated using the original associate species model data (Spear, Besmann, Allendorf) show some discrepancies with experimental points.

The improved database permitted the phase relations to be described for the alkali silicate systems as given in **Fig. 25** and **Fig. 28** for $\text{Na}_2\text{O-SiO}_2$ and $\text{K}_2\text{O-SiO}_2$ systems, respectively. In contrast to the quasichemical model, the calculation using the modified associate species approach is able to describe the phase relations in the Na_2O -rich region by keeping an acceptable agreement with the experimental points. The calculated phase diagrams for the considered system using the optimised database show much better agreement with the experimental data compared with the original associate species model and the quasichemical model.

The series of figures given in **Fig. 26** show the activity of Na_2O as a mole fraction of Na_2O at various temperatures and display a good agreement of the calculated activity values with experimental points obtained by different methods. The optimisation of the associate solution data allows the sodium oxide activity in the $\text{Na}_2\text{O-SiO}_2$ melt depending on the composition to be represented more correctly in comparison with the calculations performed using the original associate species model, which show some disagreement with the measured values, especially at temperatures above 1473 K. This can be explained by the more accurate

description of the liquid phase in the high temperature region, which is also reflected by better agreement of the calculated and experimental phase diagram.

Similar to the $\text{Na}_2\text{O-SiO}_2$ system, the new database is applicable to describe the potassium oxide activity in the $\text{K}_2\text{O-SiO}_2$ melt more accurately as demonstrated in **Fig. 29**. The scattering of experimental points can be partly explained by the difference in the measurement methods used to obtain these data and by some difficulties concerning the volatility of alkalis. The performed calculations show a good agreement with experimental data. This indicates the correctness of the application of the modified associate species model to the potassium silicate liquid.

In the $\text{Al}_2\text{O}_3\text{-SiO}_2$ system, differences between experimental points obtained by different authors and calculated equilibria using the original associate species model (Spear, Besmann⁷) were observed as shown in **Fig. 30**. Moreover, mullite was calculated without taking into account its non-stoichiometry. The FACT database includes the thermodynamic description of the mullite having the non-stoichiometry region mentioned in the literature. The phase equilibria calculated using the modified associate model with the optimised slag solution data, which is compatible with the FACT data for the solid phases, show a good agreement with the experimental points (**Fig. 31**).

The comparison of the experimental points available for the binary systems $\text{Me}_2\text{O-Al}_2\text{O}_3$ ($\text{Me}=\text{Na}, \text{K}$) with the calculated phase diagrams are depicted in **Fig. 32** and **Fig. 34**. There are no reliable phase diagram data for the composition range between pure alkali oxide Me_2O and potassium or sodium aluminate MeAlO_2 . The quasichemical model is not able to represent this region. Since there are no compounds in this region, in the framework of the modified associate species model the liquidus line was suggested by Besmann, Spear, Allendorf^{7,8} to start from the melting point of MeAlO_2 to a eutectic located near the melting point of the respective pure alkali oxide. The liquidus of the composition range with less than 50 mole percent alumina is therefore an approximation.

The modified associate species of the $\text{Me}_2\text{O-Al}_2\text{O}_3$ melt mentioned in the literature⁸ were used, and new interaction parameters between associate species were added and optimised to represent the properties of $\text{Me}_2\text{O-Al}_2\text{O}_3$. The phase relations calculated using the new improved data set of solution parameters are shown by solid lines in **Fig. 33** and **Fig. 35**. Reasonably good agreement with measured equilibrium data was obtained and also a reasonable liquidus line in the alkali-rich range was predicted.

The modified associate species model was applied for the optimisation of the solution data in the ternary system $\text{Na}_2\text{O-K}_2\text{O-SiO}_2$ as well. In this case, the associate liquid is represented as a solution containing as constituents the binary associate species which resulted from the assessment of the binary systems, also taking into account the interactions between binary components. The binary solution data remained constant during the optimisation procedure. The available ternary experimental data regarding the phase relations

in the system $\text{Na}_2\text{O}-\text{K}_2\text{O}-\text{SiO}_2$ were analysed and used to obtain the new solution data including the added ternary interaction parameters. As can be seen from **Fig. 37** and **Fig. 38**, the chosen interacting pairs with the added parameters represent the liquidus lines well and also the eutectics which occur in the quasi-binary sections considered relating to the alkali metasilicate and alkali disilicate systems, respectively.

The phase equilibria of the ternary system $\text{K}_2\text{O}-\text{Na}_2\text{O}-\text{SiO}_2$ are demonstrated as liquidus lines in the temperature interval 800-1600 °C in **Fig. 39**. A good agreement between calculated and measured isothermal lines is observed. This indicates that the associate approach can be extended to the ternary system taking into account “ternary” interactions.

The current calculations indicate that the modified associate species model can also be applied in general to describe the liquid in the ternary $\text{Na}_2\text{O}-\text{Al}_2\text{O}_3-\text{SiO}_2$ system. Furthermore, the solid solutions nepheline and carnegieite were also treated. In contrast to the original database by Spear, Besmann, Allendorf, which treats only one solid solution, a successful attempt to develop data for both solid solutions was made. The consideration of NaAlSiO_4 (nepheline and carnegieite) and $\text{NaAlSi}_2\text{O}_6$ as solution constituents allows the phase relation in the quasi-binary section NaAlSiO_4 (nepheline, carnegieite) - $\text{NaAlSi}_3\text{O}_8$ (albite) to be represented (**Fig. 40**). Quite good agreement is observed between the experimental points and the estimated phase diagram from the literature. This indicates that the associate species approach can be used for different phases (solids and liquids) taking into account the proper solution components and the interactions among them.

The alkali activity as an important property of the slag can be obtained using the thermodynamic calculation. The comparison of the measured partial pressures of K over the liquid and the potassium oxide activities in the $\text{Na}_2\text{O}-\text{K}_2\text{O}-\text{Al}_2\text{O}_3-\text{SiO}_2$ melt with calculated values is given in **Fig. 41**. There are still some differences between the measured values and those calculated using the new data. However, the new calculated curves are already those which are closer to the experimental than both old curves, although in the present work quaternary experimental information has not yet been used. The optimisation of the associate solution data was performed mainly on the basis of the experimental phase equilibria points in the ternary system $\text{K}_2\text{O}-\text{Na}_2\text{O}-\text{SiO}_2$ without taking into account the activity data of the quaternary system. However, the improved data set for the complex solution is already able to represent the activities of the considered quaternary composition as a function of temperature much better than the databases using the modified quasichemical and original associate solution model. This indicates that the associate approach using the optimised solution data is acceptable to describe and predict the thermodynamic properties of such kinds of systems.

The considered binary and ternary systems can be treated as a basis for the future addition of further slag relevant oxides such as Fe_2O_3 and the alkali earth oxides CaO and MgO . The calculations of the phase diagrams and the alkali activities performed using the new database for the slag solution show that the modified associate approach can be

successfully extended for multicomponent systems taking into account the interactions in the complicated solution. The modified associate species model may be considered as an appropriate approach for ternary liquids and, in future, for other ternary and multicomponent systems.

7. Summary and conclusions

Complex oxide slag systems containing silica and alumina are important in many fields of science and industry. The alkali-oxide-containing systems are of great interest in the field of power production because of the alkali release during coal combustion. The allowed alkali concentration in the hot flue gas is limited by the gas turbine manufacturers because of the high corrosiveness of the alkalis.

Measurements on complex and reactive systems such as slags at high temperatures are difficult and not practical for the whole range of composition and temperature of technological interest. A thermodynamic description allows the properties of many complex systems to be represented and predicted within a shorter time and at less expense. Thermodynamic calculations can be applied to get information about phase equilibria, thermochemical and other properties based on extrapolation and interpolation of temperature and/or composition ranges which cannot be investigated in the laboratory. The accuracy of the calculation depends on the reliability of the database and adaptability of the model. Therefore, a database had to be developed which is optimised for the relevant oxide system.

In the present work, the quaternary oxide system containing SiO_2 , Al_2O_3 , Na_2O , and K_2O was investigated regarding the thermodynamic description of the liquid solution (slag). The available thermodynamic data were collected, analysed and modified for the purpose of improvement of the solution database. The modified associate species model was adapted to the accepted data for the appropriate solid phases from the FACT database. This allows calculations to be performed applying the FACT database for solid and gaseous phases and simultaneously the new optimised database for the liquid and a few solid solution phases.

The thermodynamic properties of the binary and ternary systems in the framework of the quaternary system SiO_2 - Al_2O_3 - Na_2O - K_2O were investigated. The modified associate species model was used to describe the liquid phase in the binary systems Me_2O - SiO_2 , Me_2O - Al_2O_3 ($\text{Me}=\text{Na}$, K), and SiO_2 - Al_2O_3 and the ternary systems Na_2O - K_2O - SiO_2 and Na_2O - SiO_2 - Al_2O_3 . The associate species approach was applied owing to its adaptability for the representation of the phase relations in the whole composition range of the complex oxide system in contrast to the quasichemical approach, which is used in the FACT database to describe the liquid solution and which shows limits in its compositional applicability.

The data for the modified associate species approach introduced by Besmann et al.^{7,8,9} were optimised in order to determine more correctly the thermodynamic properties of the considered systems (phase diagram and activity data). The thermodynamic data of the solution components (standard formation enthalpy and entropy) and interaction parameters introduced to express the excess solution Gibbs energy were added and assessed using the optimisation procedure of the ChemSage software package.

In the literature, the binary systems $\text{Me}_2\text{O-SiO}_2$ and $\text{Me}_2\text{O-Al}_2\text{O}_3$ ($\text{Me}=\text{Na, K}$) were not investigated regarding their phase diagrams in the composition range between pure alkali oxide and alkali silicate and aluminate, respectively. Also, it is not possible to use the commercially available FACT database to describe the phase relations in the alkali-rich regions of the binary systems. The new database allows the description of the whole composition range of the binary systems. The assessments performed are in very good agreement with the available experimental data indicating that the modified associate species model can in general be applied to liquid solutions containing alkali silicates and alkali aluminates. In addition, the new solution parameters of the modified associate species model allow the correct representation of the partial pressure of alkali metals over the liquid solution and the alkali oxide activity in the liquid solution.

The binary system $\text{Al}_2\text{O}_3\text{-SiO}_2$ is very well represented by the new database. Since there are some differences in the experimental data points available in the literature, the most reliable experimental data points were chosen for the optimisation considering mullite as a non-stoichiometric, incongruently melting solution phase as available in the FACT database.

The modified associate species approach was extended to the ternary systems $\text{Na}_2\text{O-K}_2\text{O-SiO}_2$ and $\text{Na}_2\text{O-SiO}_2\text{-Al}_2\text{O}_3$. In these cases, the liquid solution is represented as a solution containing the binary associate species which were applied for the binary systems possibly taking into account interactions between them and the ternary associates. The binary solution data remained constant during optimisation.

For the ternary system $\text{Na}_2\text{O-K}_2\text{O-SiO}_2$ there are experimental data points available for phase equilibria within the two quasi-binary systems $\text{Na}_2\text{Si}_2\text{O}_5\text{-K}_2\text{Si}_2\text{O}_5$ and $\text{Na}_2\text{SiO}_3\text{-K}_2\text{SiO}_3$. In contrast to the old databases, the phase relations in these quasi-binary systems are very well represented by the new optimised database. In addition, a very good agreement between calculated and measured isothermal liquidus lines in the SiO_2 -rich region of the ternary system is observed. These results allow the conclusion that the solution parameters for the modified associate species model are suitable and that the new database can be successfully employed for the thermodynamic description of the liquid solution phase in the whole composition range of the ternary system.

In the ternary system $\text{Na}_2\text{O-Al}_2\text{O}_3\text{-SiO}_2$ the congruent melting compounds NaAlSiO_4 (nepheline) and $\text{NaAlSi}_3\text{O}_8$ (albite) were introduced as new ternary associate species in the liquid. Their thermodynamic formation data as well as interaction parameters among the available binary and the new ternary constituents were determined and optimised to represent the phase relations in the quasi-binary section $\text{NaAlSiO}_4\text{-NaAlSi}_3\text{O}_8$. The calculations are in very good agreement with the experimental data points. In contrast to the old database, which treats one solid solution, the new database contains two solid solutions, nepheline and carnegieite. This result demonstrates that the associate species approach cannot only be used

for the representation of liquid solutions but also for the representation of solid solutions without giving full account of the structure of the solid solution.

The comparison of measured partial pressures of potassium over the liquid phase and potassium oxide activities in the quaternary $\text{Na}_2\text{O-K}_2\text{O-SiO}_2\text{-Al}_2\text{O}_3$ melt with calculated values already show a relatively good agreement although these data were not yet taken into account for the optimisation. There are still some differences between calculated and measured data. However, the differences decreased to less than one order of magnitude with the new database whereas the results obtained with the old databases differ from the measured values by up to more than two orders of magnitude.

The results indicate that the modified associate species approach using the optimised solution data is suitable to describe and predict the thermodynamic properties of the considered quaternary oxide system. The considered system can be treated as a basis for the future addition of further slag relevant oxides such as Fe_2O_3 and the alkaline earth oxides CaO and MgO . The calculations performed show that the modified associate species approach can be successfully extended to multicomponent systems taking into account the interactions in the complex liquid and even solid solutions.

Outlook

In the framework of the quaternary system $\text{SiO}_2\text{-Al}_2\text{O}_3\text{-Na}_2\text{O-K}_2\text{O}$, the remaining ternary systems should be investigated regarding their features of phase relations and thermodynamic properties.

In order to use the thermodynamic calculations for solutions of technical problems it will be necessary to take into account other important slag species, namely MgO , CaO , and Fe_2O_3 . The modified associate species model can be applied to consider the multicomponent oxide systems in the future. The newly established data set for the liquid solution will be employed to estimate not only phase diagrams but different thermodynamic and thermochemical properties, e.g., components activities. It will also serve as the basis of an assessment of the higher order systems.

8. Acknowledgements

The present work was performed at the Institute for Materials and Processes in Energy Systems (IWV-2) of Forschungszentrum Juelich. I want to thank Prof. Dr. L. Singheiser for the opportunity to perform my work in his institute.

The author would like to thank Prof. Dr. J. M. Schneider and Prof. Dr. K. Hilpert for their supervision and stimulating support for my work.

I thank Dr. M. Mueller for practical advice and for the continuous interest he showed in the progress of my work.

The author is grateful to Dr. K. Hack (GTT-Technologies, Herzogenrath) for the theoretical discussions concerning the thermodynamic modelling and the great influence on my thinking.

Sincere thanks go to Dr. A. Zuev for his valuable support and useful explanation concerning theoretical aspects of my work.

I thank my respected teachers from Ural's State University who aroused my interest in scientific research. I appreciate the support and attention of all my friends who assisted me while writing.

Finally, I would like to express my gratitude to my parents and my sisters. I dedicate my thesis to my family.

9. References

- ¹ Hannes K., Neumann F., Thielen W., Pracht M.: “Kohlenstaub-Druckverbrennung”, VGB Kraftwerkstechnik, **77**, p.393-400 (1997)
- ² Willenborg W.: “Untersuchungen zur Alkalireinigung von Heißgasen für die Druckkohlenstaubfeuerung”, PhD thesis, 2003
- ³ Redlich O., Kister A.T.: “Algebraic Representation of Thermodynamic Properties and the Classification of Solution”, Industrial and Engineering Chemistry, **48**, N.2, pp.345-348 (1948)
- ⁴ Pelton Arthur D., Blander M.: “Thermodynamic analysis of ordered Liquid Solutions by a Modified Quasichemical Approach – Application to Silicate Slags”, Metall.Trans. **17B** [4], p.805-815 (1986)
- ⁵ Hastie J.W., Bonnell D.W.: “A Predictive Phase Equilibrium Model for Multicomponent Oxide Mixtures”, High Temperature Science, **19**, p.275-306 (1985)
- ⁶ Hastie J.W., Bonnell D.W.: “A Predictive Thermodynamic Model for Complex High Temperature Solution Phases XI”, High Temperature Science, **26**, p.313-334 (1990)
- ⁷ Besmann T.M., Spear K.E.: “Thermodynamic Modelling of Oxide Glasses”, J.Am.Ceram.Soc., **85** [12], p.2887-94 (2002)
- ⁸ Spear K.E., Allendorf M.D.: “Thermodynamic Analysis of Alumina Refractory Corrosion by Sodium or Potassium Hydroxide in Glass Melting Furnaces”, J.Electrochem.Soc., **149** [12], B551-B559 (2002)
- ⁹ Allendorf M.D., Spear K.E.: “Thermodynamic Analysis of Silica Refractory Corrosion in Glass-Melting Furnaces”, J.Electrochem.Soc., **148** (2), B59-B67 (2001)
- ¹⁰ Pelton Arthur D., Thompson W.T., Bale C.W., Eriksson G.: “F*A*C*T Thermochemical Database for Calculations in Materials Chemistry at High Temperature”, High Temperature Science, **26**, p.231-249 (1990)
- ¹¹ Bale C.W., Chartrand P., Degterov S.A., Eriksson G., Hack K., R.Ben Mahfoud, Melançon J., Pelton Arthur D., Petersen S.: “FactSage Thermochemical Software and Databases”, Calphad, **26**, N.2, p.189-228 (2002)
- ¹² www.factsage.com
- ¹³ Eriksson G., Hack K.: “ChemSage-A Computer Program for the Calculation of Complex Chemical Equilibria”, Metall.Trans. **21B**, p.1013-1023 (1990)
- ¹⁴ Gupta H., Morral J.E., Nowotny H. Scripta Metall., **20**, p.889 (1986)

- ¹⁵ Koenigsberger E., Eriksson G.: "A New Optimisation Routine for Chemsage", *Calphad*, **19**, N.2, p.207-214 (1995)
- ¹⁶ Morey G.W., Bowen N.L.: "The binary system sodium metasilicate-silica", *J.Phys.Chem.*, **28**, p.1167-1179 (1924)
- ¹⁷ Kracek F.C.: "The System Sodium Oxide-Silica", *J.Phys.Chem.*, **34**, p.1583-1598 (1930)
- ¹⁸ Kracek F.C.: "Phase Equilibrium Relations in the System $\text{Na}_2\text{SiO}_3\text{-Li}_2\text{SiO}_3\text{-SiO}_2$ ", *J.Amer.Chem.Soc.*, **61**, p.2863-2877 (1939)
- ¹⁹ JANAF Thermochemical Tables, 3rd ed., *J.Phys.Vhem.Ref.Data*, 14 (1985)
- ²⁰ D`Ans J., Loeffler J.: „Untersuchungen im system $\text{Na}_2\text{O-SiO}_2\text{-ZrO}_2$ ", *Z.Anorg.Allg.Chem.*, **191**, p.1-34 (1930)
- ²¹ Loeffler J.: "Über den alkalischen Teil des Systems $\text{Na}_2\text{O-SiO}_2$ ", *Glastechn.Ber.*, **42** [3], p.92-96 (1969)
- ²² Williamson J., Glasser F.P.: "Phase Relations in the System $\text{Na}_2\text{Si}_2\text{O}_5\text{-SiO}_2$ ", *Science*, **148** [6], p.1589-1591 (1965)
- ²³ Kracek F.C., Bowen N.L., Morey G.W.: "Equilibrium Relations and Factors Influencing Their Determination in the System $\text{K}_2\text{SiO}_3\text{-SiO}_2$ ", *J.Phys.Chem.*, **41**, p.1183-1193 (1937)
- ²⁴ Aramaki S., Roy R.: "Revised Equilibrium Diagram for the System $\text{Al}_2\text{O}_3\text{-SiO}_2$ ", *J.Am.Ceram.Soc.*, **45** [5], p.229-42 (1962)
- ²⁵ Aksay I.A., Pask J.A.: "The Silica-Alumina System: Stable and Metastable Equilibria at 1.0 Atmosphere", *Science*, **183**, p.69-71 (1973); Aksay I.A., Pask J.A.: "Stable and Metastable Equilibria in the System $\text{SiO}_2\text{-Al}_2\text{O}_3$ ", *J.Am.Cer.Soc.*, **58**, N.11-12, p.507-512 (1975)
- ²⁶ Risbud S.H., Pask J.A.: " $\text{SiO}_2\text{-Al}_2\text{O}_3$ Metastable Phase Equilibrium Diagram without Mullite", *J.Mater.Sci.*, **13** [11], p.1449-54 (1978)
- ²⁷ Staronka A., Pham H., Rolin M.: "Study of system $\text{SiO}_2\text{-Al}_2\text{O}_3$ by cooling curve method", *Revue Internationale des Hautes Temperatures et des Réfractaires*, **5** (2), p.111-115 (1968)
- ²⁸ Klug F.J., Prochazka S., Doremus R.H.: "Alumina-Silica Phase Diagram in the Mullite Region", *J.Am.Ceram.Soc.*, **70**, p.750-759 (1987)
- ²⁹ Welch J.H.: "New Interpretation of the Mullite Problem", *Nature (London)*, **186** [4724], p.545-46 (1960)

- ³⁰ Shornikov S.I. : “Thermodynamic Study of the Mullite Solid Solution Region in the Al_2O_3 - SiO_2 System by Mass Spectrometric Techniques”, *Geochem.Int.*, **40**, Suppl.1, p.S46-S60 (2002)
- ³¹ Kummer J.T.: “ β -Alumina Electrolytes”, *Progr.Solid State Chem.*, **7**, p.141-175 (1972)
- ³² Rankin G.A., Merwin H.E. *J.Am.Chem.Soc.*, **38**, p.568 (1916)
- ³³ Scholder R., Mansmann M., *Z.Anorg.Allg.Chem.*, **321**, p.246 (1963)
- ³⁴ Yamaguchi G., *J.Japan Electrochemical Soc.*, **11**, p.260 (1943)
- ³⁵ Rolin M., Thanh P.H.: “Phase diagrams of mixtures not reacting with molybdenum [$\text{Ca}(\text{AlO}_2)_2$ -, NaAlO_2 -and La_2O_3 - Al_2O_3]”, *Rev.Hautes Temp.Refract.*, **2**, p.175-185 (1965)
- ³⁶ De Vries R.C., Roth W.L.: “Critical Evaluation of the Literature Data on Beta Alumina and Related Phases: I, Phase Equilibria and Characterization of Beta Alumina Phases”, *J.Amer.Ceram.Soc.*, **52**, N.7, p.364-369 (1969)
- ³⁷ Weber N., Venero A.F.: “Revision of the Phase Diagram NaAlO_2 - Al_2O_3 ”, *Am.Ceram.Soc.Bull.*, **49** (4), p.491-492 (1970)
- ³⁸ Ray A.K., Subbarao E.C.: “Synthesis of Sodium β and β'' -Alumina”, *Mat.Res.Bull.*, **10**, p.583-590 (1975)
- ³⁹ Dzieciuch M.A., Weber N.; *Fr.Pat.* 1,491,673, July 3 (1967); assigned to Ford Motor Co.
- ⁴⁰ Matignon C.: “Action of High Temperatures on Some Refractory Substances”, *Compt.Rend.*, **177**, p.1290-1293 (1923)
- ⁴¹ Schairer J.F., Bowen N.L.: “The System Na_2O - Al_2O_3 - SiO_2 ”, *American Journal of Science*, **254** (3), p.129-195 (1956)
- ⁴² Jacob K.T., Swaminathan K., Sreedharan O.M.: “Potentiometric Determination of Activities in the Two-phase fields of the System Na_2O -(α) Al_2O_3 ”, *Electrochim.Acta*, **36**, p.791-798 (1991)
- ⁴³ Roth R.S.: “Phase equilibrium research in portions of the potassium oxide-magnesium oxide-iron(III) oxide-aluminium oxide-silicon dioxide system”, *Adv.Chem.Ser.(Am.Chem.Soc)*, N.186, p.391-408 (1980)
- ⁴⁴ Choudhury N.S., *J.Electrochem.Soc.*, **133**, p.425-431 (1986)
- ⁴⁵ Moya J.S., Criado E., De Aza S.: “The $\text{K}_2\text{O}\cdot\text{Al}_2\text{O}_3$ - Al_2O_3 system”, *J.Mater.Sci.*, **17**, p.2213-2217 (1982)
- ⁴⁶ Kracek F.C.: “The ternary system K_2SiO_3 - Na_2SiO_3 - SiO_2 ”, *J.Phys.Chem.*, **36** [10], p.2529-2542 (1932)

- ⁴⁷ Bowen N.L.: “The binary system $\text{Na}_2\text{Al}_2\text{Si}_2\text{O}_8$ (nepheline, carnegieite) $\text{CaAl}_2\text{Si}_2\text{O}_8$ (anorthite)”, *Am.Jour.Sci.*, 4th ser., **33**, p.551-573 (1912)
- ⁴⁸ Greig J.W., Barth T.F.W.: “The system $\text{Na}_2\text{O} \cdot \text{Al}_2\text{O}_3 \cdot \text{SiO}_2$ (nepheline, carnegieite)- $\text{Na}_2\text{O} \cdot \text{Al}_2\text{O}_3 \cdot 6\text{SiO}_2$ (albite)”, *Am.Jour.Sci.*, 5th ser., **35A**, p.93-112 (1938)
- ⁴⁹ Schneider H., Flörke O.W., Stoeck R.: “The NaAlSiO_4 nepheline-carnegieite solid-state transformation”, *Z.für Kristallografie*, **209**, p.113-117 (1994)
- ⁵⁰ Klingenberg R., Felsche J.: “Crystal data for the low-temperature form of carnegieite NaAlSiO_4 ”, *J.Appl.Cryst.*, **14**, p.66-68 (1981)
- ⁵¹ DeYoreo J.J., Lange R.A., Navrotsky A.: “Scanning calorimetric determinations of the heat contents of diopside-rich systems during melting and crystallisation”, *Geochimica et Cosmochimica Acta*, **59**, N.13, p.2701-2707 (1995)
- ⁵² Stebbins J.F., Carmichael I.S.E., Weill D.A.: “The high temperature liquid and glass heat contents and the heats of fusion of diopside, albite, sanidine and nepheline”, *Amer.Mineral.*, **68**, p.717-730 (1983)
- ⁵³ Greenwood J.P., Hess P.C.: “Congruent melting kinetics of albite: Theory and experiment”, *Journal of Geophysical Research*, **103**, N.B12, p.29,815-29,828 (1998)
- ⁵⁴ Simakin A.G.: “Structural thermodynamic model of the melt in the system albite ($\text{NaAlSi}_3\text{O}_8$)-quartz(SiO_2) [Ab-Q]”, *Phys.Chem.Glasses*, **43** (4), p.184-188, (2002)
- ⁵⁵ Dove M.T., Thayaparam S., Heine V., Hammonds K.D.: “The phenomenon of low Al-Si ordering temperatures in aluminosilicate framework structures”, *American Mineralogist*, **81**, p.349-362 (1996)
- ⁵⁶ Taylor M., Brown G.E., Jr.: “Structure of mineral glasses-II. The SiO_2 - NaAlSiO_4 join”, *Geochimica et Cosmochimica Acta*, **43**, p.1467-1473 (1979)
- ⁵⁷ Brownmiller L.T., Bogue R.H.: “The system CaO - Na_2O - Al_2O_3 ”, *Am.Jour.Sci.*, 5th ser., **23**, p.505-524 (1932); *Nat.Bur.Standards Jour.Research*, **8**, p.289-307
- ⁵⁸ Thompson J.G., Melnitchenko A., Palethorpe S.R., Withers R.L.: “An XRD and Electron Diffraction Study of Cristobalite-Related Phases in the NaAlO_2 - NaAlSiO_4 System”, *J.Solid State Chem.*, **131**, p.24-37 (1997)
- ⁵⁹ Thompson J.G., Withers R.L., Melnitchenko A., Palethorpe S.R.: “Cristobalite-Related Phases in the NaAlO_2 - NaAlSiO_4 System. I. Two Tetragonal and Two Orthorhombic Structures”, *Acta Cryst.*, **B54**, p.531-546 (1998)
- ⁶⁰ Tilley C.E.: “The ternary system Na_2SiO_3 - $\text{Na}_2\text{Si}_2\text{O}_5$ - NaAlSiO_4 ”, *Min.pet.Mitt.*, **43**, p.406-421 (1933)
- ⁶¹ Spivak J.: “The system NaAlSiO_4 - CaSiO_3 - Na_2SiO_3 ”, *Jour.Geology*, **52**, p.24-52 (1944)

- ⁶² Zaitsev A.I., Shelkova N.E., Mogutnov B.M.: “Thermodynamics of Na₂O-SiO₂ Melts”, *Inorganic Materials*, **36**, N.6, p.529-543 (2000); translated from *Neorganicheskie Materialy*, **36**, N.6, p.647-662 (2000)
- ⁶³ Zaitsev A.I., Mogutnov B.M.: “Thermodynamic of CaO-SiO₂ and MnO-SiO₂ Melts: II. Thermodynamic Modelling and Phase-Equilibrium Calculations”, *Inorganic Materials*, **33**, N.8, p.823-831 (1997). Translated from *Neorganicheskie Materialy*, **33**, N.8, p.975-984 (1997)
- ⁶⁴ Yamaguchi S., Imai A., Goto K.S.: “Activity Measurement of Na₂O in Na₂O-SiO₂ Melts Using the Beta-Alumina as the Solid Electrolyte”, *Scand.J.Metall.*, **11**, p.263-264 (1982)
- ⁶⁵ Froberg M.G., Caung E., Kapoor M.L.: “Measurement of the Activity of the Oxygen Ions in the Liquid Systems Na₂O-SiO₂ and K₂O-SiO₂”, *Arch.Eisenhuttenwes.*, **44**, N.5, p.585-588 (1973)
- ⁶⁶ Kohsaka S., Sato S., Yokokawa T.E.: “Measurement of Molten Oxide Mixtures: III. Sodium Oxide+Silicon Dioxide”, *J.Chem.Thermodyn.*, **11**, p.547-551 (1979)
- ⁶⁷ Neudorf D.A., Elliot J.F.: “Thermodynamic Properties of Na₂O-SiO₂-CaO” Melts at 1000 to 1100 °C”, *Metall.Trans.*, **11B**, p.607-614, December (1980)
- ⁶⁸ Ravaine D., Azandegbe E., Souquet J.L.: « Mesures potentiométriques de chaînes électrochimiques comprenant des silicates fondus: Interprétation des résultats par un modèle statistique », *Silic.Ind.*, **12**, p.333-340 (1975)
- ⁶⁹ Schakhmatkin B.A., Schul'ts M.M.: “Thermodynamic Properties of Na₂O-SiO₂ Glass-Forming Melts in the Range 800-1200 °C”, *Fiz.Khim.Stekla*, **6**, N.2, p.129-135 (1980)
- ⁷⁰ Rudnyi E.B., Korobov M.V., Vovk O.M., Kaibicheva E.A., Sidorov L.N.: “A New Technique for Measurement of Low O₂ and Alkali Partial Pressures”, *High Temperature Science*, **26**, p.165-174 (1990)
- ⁷¹ Rego D.N., Sigworth G.K., Philbrook W.O.: “Thermodynamic Study of Na₂O-SiO₂ Melts at 1300 and 1400 °C”, *Metall.Trans.B*, **16**, p.313-323 (1985)
- ⁷² Wu P., Eriksson G., Pelton Arthur D.: “Optimisation of the Thermodynamic Properties and Phase Diagrams of the Na₂O-SiO₂ and K₂O-SiO₂ Systems”, *J.Am.Ceram.Soc.*, **76** [8], p.2059-2064 (1993)
- ⁷³ Zaitsev A.I., Shelkova N.E., Lyakishev N.P., Mogutnov B.M.: “The thermodynamic Properties of K₂O-SiO₂ Melts”, *Russian Journal of Physical Chemistry*, **74**, N.6, p.907-913 (2002). Translated from *Zhurnal Fizicheskoi Khimii*, **74**, N.6, p.1021-1028 (2000)
- ⁷⁴ Zaitsev A.I., Shelkova N.E., Lyakishev N.P., Mogutnov B.M.: “Modeling of the Thermodynamic Properties of Silicate Melts and Calculation of Phase Equilibria in the

- K₂O-SiO₂ System”, Russian Journal of Physical Chemistry, **74**, N.7, p.1033-1038 (2002).
Translated from Zhurnal Fizicheskoi Khimii, **74**, N.7, p.1159-1164 (2000)
- ⁷⁵ Spear K.E., Besmann T.M., Beahm E.C.: “Thermochemical Modelling of Glass: Application to High-Level Nuclear Waste Glass”, MRS Bull., **24**, p.37-44 (1999)
- ⁷⁶ Eriksson G., Wu P., Blander M., Pelton Arthur D.: “Critical Evaluation and Optimisation of the Thermodynamic Properties and Phase Diagrams of the Mn-O and CaO-SiO₂ Systems”, Canadian Met. Quarterly, **33**, N.1, p.13-21 (1994)
- ⁷⁷ Eriksson G., Pelton Arthur D.: “Critical Evaluation and Optimisation of the Thermodynamic Properties and Phase Diagrams of the CaO-Al₂O₃, Al₂O₃-SiO₂ and CaO-Al₂O₃-SiO₂ Systems”, Met.Trans., **24B**, p.807-816 (1993)
- ⁷⁸ Eriksson G., Wu P., Pelton Arthur D.: “Critical Evaluation and Optimisation of the Thermodynamic Properties and Phase Diagrams of the MgO-Al₂O₃, MnO-Al₂O₃, FeO-Al₂O₃, Na₂O-Al₂O₃ and K₂O-Al₂O₃ Systems”, CALPHAD, **17**, N.2, p.189-205 (1993)
- ⁷⁹ Eliezer I., Howald R.A.: “High-Temperature Thermodynamics and Phase Equilibria in the Potassium Oxide-Aluminium Oxide System”, High Temp.Sci, **10**, p.1-16 (1978)

10. Appendix

Table A.1. Basic phase diagram points in the system Na₂O-SiO₂ taken into account for optimisation.

Nº	Equilibrium	Comp. wt.%SiO ₂	Comp. mol SiO ₂	T°C, exp.	T, K	reference
(1)	Equilibrium Na ₂ O-liq	7.5 13.6 22.45	0.077 0.140 0.230	1123 1098 1019	1396 1371 1292	Calculation by Zaitzev et al ⁶²
(2)	Eutectic Na ₂ O- Na ₄ SiO ₄ -liq	26.10	0.267	930	1203	by Zaitzev et al ⁶²
(3)	Melting of Na ₄ SiO ₄	32.64	0.333	1078	1351	Loeffler ²¹
(4)	Equilibrium Na ₄ SiO ₄ -liquid	34.20 33.60	0.349 0.343	1033 1060	1306 1333	Loeffler ²¹
(5)	Eutectic Na ₄ SiO ₄ -Na ₆ Si ₂ O ₇ -liq	35.78	0.365	962	1235	Loeffler ²¹
(6)	Equilibrium Na ₆ Si ₂ O ₇ -liquid	37.07	0.378	1037	1310	Loeffler ²¹
(7)	Melting of Na ₆ Si ₂ O ₇	39.26	0.4	1115	1388	Loeffler ²¹
(8)	Eutectic Na ₆ Si ₂ O ₇ -Na ₂ SiO ₃ -liq	53.73 43.1	0.4386	1022	1295	Kracek ¹⁷
(9)	Equilibrium Na ₂ SiO ₃ -liquid	43.57 45.11 57.91 59.98	0.4435 0.4589 0.5868 0.6074	1035 1065 955 904	1308 1338 1228 1177	Kracek ¹⁷
(10)	Melting of Na ₂ SiO ₃	49.18	0.5	1089	1362	Kracek ¹⁷
(11)	Eutectic Na ₂ SiO ₃ -Na ₂ Si ₂ O ₅ -liq	62.1	0.6283	837	1110	Kracek ¹⁷
(12)	Equilibrium Na ₂ Si ₂ O ₅ -liquid	62.49 71.49 73.00	0.6323 0.7213 0.7362	851 829 806	1124 1102 1079	Kracek ¹⁷
(13)	Melting of Na ₂ Si ₂ O ₅	65.94	0.6665	874	1147	Kracek ¹⁷
(14)	“Peritectic” Na ₂ Si ₂ O ₅ - Na ₆ Si ₈ O ₁₉ -liq	72.49	0.731	807	1080	Zaitzev et al ⁶²
(15)	Eutectic Na ₆ Si ₈ O ₁₉ -quartz-liq	74.00 74.02 74.31	0.7461 0.745 0.749	793 803	1066 1073	Kracek ¹⁷ Zaitzev et al ⁶²
(16)	Equilibrium quartz-liquid	74.81 74.49	0.754 0.75	838 820	1111 1093	Kracek ¹⁷
(17)	Equilibrium tridymite-liquid	75.98 77.48 78.97 85.44 87.97 80.46 88.33	76.56 78.03 79.59 85.83 88.30 0.8094 0.8865	905 995 1075 1365 1450 1145 1457	1178 1268 1348 1638 1723 1418 1730	Kracek ¹⁷ Morey et al. ¹⁶
(18)	Equilibrium cristobalite-liquid	91.05 94.66 97.09 95.93	0.913 0.948 0.972 0.9605	1532 1586 1633 1596	1805 1859 1905 1869	Kracek ¹⁷ Morey et al. ¹⁶

Table A.2. Basic phase diagram points in the system Al_2O_3 - SiO_2 taken into account for optimisation.

Nº	Equilibrium	Comp. wt.% Al_2O_3	Comp. mol Al_2O_3	T°C, exp.	T, K	reference
1.	Equilibrium SiO_2 -liquid		0.012 0.033	1683.3 1621		Aramaki ²⁴
			0.0224 0.039	1674.2 1622.3		Klug ²⁸
2.	Eutectic		0.0473(calc)	1587		Klug ²⁸
3.	Equilibrium mullite-liquid		0.0678 0.1269 0.2416 0.259 0.368 0.534	1638.5 1709.3 1773.4 1796 1822 1853		Aramaki ²⁴
			0.0815 0.1017 0.155 0.3352 0.612	1650 1677 1730.4 1826.7 1890		Klug ²⁸
4.	Mullite		0.664	1890		Klug ²⁸
5.	Equilibrium Al_2O_3 -liquid		0.6909 0.7523 0.895 0.948	1893.3 1974.8 2028 2037		Klug ²⁸
			0.7305 0.765 0.8051	1910.1 1943 1974.2		Aramaki ²⁴

Defect model for mullite according to Eriksson, Wu ⁷⁶

For a compound of nominal stoichiometry $A_{1-y}B_y$, let X_1 and X_2 be the mole fractions of the majority point defects on the A-rich and B-rich sides of stoichiometry, respectively. The molar Gibbs energy of the solid relative to the hypothetical defect-free compound is then written as Eq.A.1:

$$G = \frac{RT}{\beta_1} (X_1 \ln X_1 + (1 - X_1) \ln(1 - X_1)) + \frac{RT}{\beta_2} (X_2 \ln X_2 + (1 - X_2) \ln(1 - X_2)) + \frac{1}{\beta_1} g_1 X_1 + \frac{1}{\beta_2} g_2 X_2 \quad (\text{A.1})$$

where $1/\beta_1$ and $1/\beta_2$ are the numbers of moles of lattice sites available to each type of point defect, and where g_1 and g_2 are the molar energies of formation of the majority defects on the A-rich and B-rich sides, respectively. It is assumed, for simplicity, that the defect concentrations are sufficiently small that the numbers of lattice sites do not change appreciably from those in the defect-free compound. For a given deviation from the stoichiometric composition represented by $A_{1-y-\delta}B_{y+\delta}$, it can be shown that:

$$\delta = \frac{X_2}{\beta_2} - \frac{X_1}{\beta_1} \quad (\text{A.2})$$

$$\left(\frac{X_1}{1 - X_1} \right)^{1/\beta_1} \left(\frac{X_2}{1 - X_2} \right)^{1/\beta_2} = \exp \left(\frac{-(g_1/\beta_1 + g_2/\beta_2)}{RT} \right) \quad (\text{A.3})$$

If the values of the energy parameters, g_1 and g_2 , are given, Eqs. (A.2) and (A.3) can be solved for any δ to give X_1 and X_2 , which can then be substituted back into equation (A.1) to give G . An expression for G° of stoichiometric $A_{1-y}B_y$ can also be written as a function of g_1 and g_2 .

The energy parameters for the formation of both majority defects for mullite were set to $121903 + 38.17 \cdot T$, J/mol, with the constants $\beta_1 = \beta_2 = 1$ as given in Ref.⁷⁷.

11. List of figures

- Fig. 1. Enthalpy and entropy of mixing of a binary system for different degrees of ordering at about $x_a=x_b=0.5$. Curves are calculated⁴ from the modified quasichemical theory at $T=1000\text{ }^{\circ}\text{C}$ with $z=2$ for a constant values of ω (kcal) and $\eta=0$
- Fig. 2. Temperature composition diagram of the binary system $\text{Na}_2\text{SiO}_3\text{-SiO}_2$ according to Morey, Bowen¹⁶
- Fig. 3. Equilibrium phase diagram of the binary system $\text{Na}_2\text{O-SiO}_2$ (after Kracek^{17,18})
- Fig. 4. Part of the equilibrium phase diagram of the system $\text{Na}_2\text{Si}_2\text{O}_5\text{-SiO}_2$, showing a stability field of $\text{Na}_6\text{Si}_8\text{O}_{19}$
- Fig. 5. Experimental phase diagram for $\text{K}_2\text{O-SiO}_2$ system reproduced from Ref.²³
- Fig. 6. Comparison of the experimental phase diagrams for the $\text{Al}_2\text{O}_3\text{-SiO}_2$ system. Reproduced from: (1) Aramaki and Roy and (2) Aksay and Pask, modified by Risbud and Pask
- Fig. 7. Composite alumina - silica phase diagram. Reproduced from Klug et al²⁸
- Fig. 8. Phase diagram for the $\text{NaAlO}_2\text{-Al}_2\text{O}_3$ system reproduced from Rolin and Thanh³⁵
- Fig. 9. $\text{NaAlO}_2\text{-Al}_2\text{O}_3$ phase diagrams proposed by DeVries and Roth³⁶
- Fig. 10. Phase diagram of the system $\text{K}_2\text{O-Al}_2\text{O}_3$ according to Roth⁴³
- Fig. 11. Phase diagram of the system $\text{KAlO}_2\text{-Al}_2\text{O}_3$ reproduced from Moya⁴⁵
- Fig. 12. Ternary system $\text{K}_2\text{SiO}_3\text{-Na}_2\text{SiO}_3\text{-SiO}_2$ after Kracek⁴⁶
- Fig. 13. Quasi-binary phase diagram reproduced from Kracek⁴⁶ for the alkali silicates: (1)- $\text{K}_2\text{SiO}_3\text{-Na}_2\text{SiO}_3$, (2) $\text{K}_2\text{Si}_2\text{O}_5\text{-Na}_2\text{Si}_2\text{O}_5$
- Fig. 14. Phase equilibrium diagram of the system $\text{Na}_2\text{O-Al}_2\text{O}_3\text{-SiO}_2$ with fields of the primary crystalline phases, isotherms and temperatures of binary and ternary invariant points after Schairer and Bowen⁴¹

- Fig. 15. Equilibrium diagram of the binary system albite-silica after Schairer, Bowen⁴¹
- Fig. 16. Equilibrium diagram of the binary system NaAlSiO_4 - $\text{NaAlSi}_3\text{O}_8$ after Greig and Barth⁴⁸
- Fig. 17. Probable phase relations in the binary system NaAlSiO_4 (carnegieite)- NaAlO_2 after Schairer and Bowen⁴¹
- Fig. 18. Equilibrium diagram of the binary system sodium disilicate-albite after Schairer and Bowen⁴¹
- Fig. 19. Equilibrium diagram of the binary system albite-corundum after Schairer and Bowen⁴¹
- Fig. 20. Equilibrium diagram of the binary system $\text{Na}_2\text{Si}_2\text{O}_5$ (sodium disilicate)- NaAlSiO_4 (nepheline, carnegieite) after Tilley
- Fig. 21. Phase diagram of the system carnegieite-corundum taken from Ref. ⁴¹
- Fig. 22. Equilibrium diagram of the binary system Na_2SiO_3 (sodium metasilicate)- NaAlSiO_4 (nepheline, carnegieite) after Tilley ⁶⁰
- Fig. 23. Composition distribution of associate species depending on the silica content in the melt Na_2O - SiO_2 at 1000 °C. The calculation is performed using the associate species model and the new database for the slag
- Fig. 24. Comparison of experimental phase equilibrium data with calculations performed using different thermodynamic data and different solution models
- Fig. 25. Phase diagram of the Na_2O - SiO_2 system calculated using the new optimised database
- Fig. 26. Na_2O -activity in the Na_2O - SiO_2 melt at different temperatures: comparison of experimental data with the calculated values. Reference state – pure liquid Na_2O . The calculations are performed using the different solution approach and databases
- Fig. 27. Calculated phase diagram of the K_2O - SiO_2 system. Experimental points are taken from Kracek et al²³. The liquid slag is described using the quasichemical model⁷² (solid line) and the modified associate approach ⁹(dotted line)

- Fig. 28. Phase diagram of the K_2O-SiO_2 system calculated using the new optimised database
- Fig. 29. Comparison of potassium oxide activities in the K_2O-SiO_2 melt at 1373 K (standard state is pure liquid) with calculations performed using the quasichemical and the modified associate species approaches
- Fig. 30. Calculated phase relations in the $Al_2O_3-SiO_2$ system using the associate species model after data reported in Refs.^{7,75}
- Fig. 31. Comparison of the two model approaches conformable to the $Al_2O_3-SiO_2$ system: quasichemical model (database FACT, dotted line) and associate species model (new improved database, solid line). For mullite both calculated lines overlap with each other
- Fig. 32. Modified quasichemical and modified associate species models applied for the slag in the $Na_2O-Al_2O_3$ system
- Fig. 33. Comparison of experimental points in the binary system $Na_2O-Al_2O_3$ with the phase diagram calculated according to the modified associate species model using the new improved data
- Fig. 34. Comparison of the calculated phase relations in the $K_2O-Al_2O_3$ system using the quasichemical model (solid lines) and the associate species model (dotted line)
- Fig. 35. Application of the modified associate species model for the $K_2O-Al_2O_3$ system using the new optimised data set
- Fig. 36. Composition of the $Na_2O-K_2O-SiO_2$ liquid at 1050 °C calculated using the data set before optimisation
- Fig. 37. Comparison of experimental points with phase diagram in the quasi-binary $Na_2Si_2O_5-K_2Si_2O_5$ system calculated using different solution models
- (1) quasichemical model (solid line) and associate species (dotted line) approaches (before optimisation)
 - (2) associate model using the new improved database

Fig. 38. Quasi-binary section $\text{K}_2\text{SiO}_3\text{-Na}_2\text{SiO}_3$: comparison of quasichemical and associate species approach with experimental data

- (1) quasichemical model (solid) and associate species (dotted line) approaches (before optimisation)
- (2) associate model using the new improved database

Fig. 39. Ternary system $\text{K}_2\text{O-Na}_2\text{O-SiO}_2$: isotherms of the liquidus surfaces of the various compounds. The liquidus calculations are performed according to the associate species model using the new optimised data set

Fig. 40. Comparison of the preliminary calculated phase diagram with experimental data obtained by Greig and Barth⁴⁸

Fig. 41. Potassium partial pressure over the liquid and potassium oxide activities in the $\text{K}_2\text{O-Na}_2\text{O-Al}_2\text{O}_3\text{-SiO}_2$ melt containing 78.31 mass percent SiO_2 , 17.15 Al_2O_3 , 4.14 K_2O and 0.4 Na_2O . Comparison of experimental points with the activities calculated using different models and data sets

12. List of tables

- Table 1. Liquid species data for the $\text{Na}_2\text{O-SiO}_2$ system
- Table 2. Improved interaction parameters for the system $\text{Na}_2\text{O-SiO}_2$
- Table 3. Liquid species data for the $\text{K}_2\text{O-SiO}_2$ system
- Table 4. Improved interaction parameters for the liquid phase in the system $\text{K}_2\text{O-SiO}_2$
- Table 5. Improved interaction parameters for the liquid phase in the $\text{Al}_2\text{O}_3\text{-SiO}_2$ system
- Table 6. Data for the binary intermediate associate species in the $\text{Na}_2\text{O-Al}_2\text{O}_3$ system
- Table 7. New interaction parameter for associate liquid in the $\text{Na}_2\text{O-Al}_2\text{O}_3$ system
- Table 8. Liquid species data for the $\text{K}_2\text{O-Al}_2\text{O}_3$ system
- Table 9. Optimised interaction parameters obtained for the liquid phase of the $\text{K}_2\text{O-Al}_2\text{O}_3$ system
- Table 10. Optimised interaction parameters in the $\text{K}_2\text{O-Na}_2\text{O-SiO}_2$ ternary system
- Table 11. Liquid species data for the $\text{Na}_2\text{O-Al}_2\text{O}_3\text{-SiO}_2$ system
- Table 12. New interaction parameters for the associate liquid in the $\text{Na}_2\text{O-Al}_2\text{O}_3\text{-SiO}_2$ system
- Table 13. Solid solution species data for the nepheline phase
- Table 14. Solid solution species data for the carnegieite phase
- Table 15. Optimised data for the albite
- Table A.1. Basic phase diagram points in the system $\text{Na}_2\text{O-SiO}_2$ taken into account for optimisation.
- Table A.2. Basic phase diagram points in the system $\text{Al}_2\text{O}_3\text{-SiO}_2$ taken into account for optimisation

Lebenslauf

Name	Elena Yazhenskikh
Geburtsdatum, Geburtsort	14. Mai 1978 Dorf Scherkali, Tümen Gebiet, Russische Föderation
Familienstand	Ledig
Staatsangehörigkeit	Russisch
Schulausbildung 1985-1995	Mittelschule im Dorf Scherkali (Tümen Gebiet, Russland), Abschluss mit Auszeichnung (mit der silbernen Medaille)
Studium 1995-2001	Studium an der Ural's Staatlichen Universität, Ekaterinburg (Russland), Chemische Fakultät, Lehrstuhl für Physikalische Chemie, Universitätsabschluss mit Auszeichnung
Februar-März 1999	Praktikum am Institut für Hochtemperaturelektrochemie der Uralabteilung der Russischen Akademie der Wissenschaften. Thema: „Untersuchung der elektrischen Leitfähigkeit im System La-Sr-Ga-Co-O“.
1999	Grad des Bakkalaureus in Chemie, Qualifikationsarbeit: «Untersuchung der Phasengleichgewichte und elektrischen Leitfähigkeit im System La-Sr-Ga-Co-O»
2001	Grad des Magisters in Chemie, Fachrichtung: «Physikalische Chemie». Thema der Dissertationsarbeit: «Phasengleichgewichte im System La-Sr-Co-Ga-O».
Seit Januar 2002	Doktorandin im Forschungszentrum Jülich, Institut für Werkstoffe und Verfahren der Energietechnik IWV-2